REPORT DOCUMENTATION PAGE

Form Approved
OMB No. 0704-0188

1. REPORT DATE *(DD-MM-YYYY)*	**2. REPORT TYPE**	**3. DATES COVERED** *(From - To)*
02/28/2012	Final Report	02/15/2008 - 12/31/2011

4. TITLE AND SUBTITLE

Numerical Simulation of Pulse Detonation Rocket-Induced MHD Ejector (PDRIME) Concepts for Advanced Propulsion Systems

5a. CONTRACT NUMBER

5b. GRANT NUMBER
FA9550-08-1-0048

5c. PROGRAM ELEMENT NUMBER

6. AUTHOR(S)

Ann R. Karagozian

5d. PROJECT NUMBER

5e. TASK NUMBER

5f. WORK UNIT NUMBER

7. PERFORMING ORGANIZATION NAME(S) AND ADDRESS(ES)

University of California, Los Angeles
Mechanical and Aerospace Engineering Department
420 Westwood Plaza
Los Angeles, CA 90095-1597

8. PERFORMING ORGANIZATION REPORT NUMBER

9. SPONSORING / MONITORING AGENCY NAME(S) AND ADDRESS(ES)

AFOSR/PKR2
USAF, AFRL DUNS 143574726
875 N. Randolf Street, Room 3112
Arlington, VA 22203

10. SPONSOR/MONITOR'S ACRONYM(S)

11. SPONSOR/MONITOR'S REPORT NUMBER(S)

12. DISTRIBUTION / AVAILABILITY STATEMENT

Approved for public release: distribution unlimited

13. SUPPLEMENTARY NOTES

14. ABSTRACT

The primary goal of this research project has been to use high resolution numerical methods to explore reactive and magnetohydrodynamic (MHD) flow phenomena as a means of potentially improving the performance of hypersonic propulsion through a range of alternative and innovative combined-cycle concepts, such as the Pulse Detonation Rocket-Induced MHD Ejector (PDRIME) Concept. These studies constitute an assessment of the potential improvements possible through PDRIME concepts via detailed numerical simulations as well as simplified modeling. On the basis of both simplified modeling and highly resolved simulations, an optimization of system level configuration has been explored in detail. .

15. SUBJECT TERMS

16. SECURITY CLASSIFICATION OF:			**17. LIMITATION OF ABSTRACT**	**18. NUMBER OF PAGES**	**19a. NAME OF RESPONSIBLE PERSON**
a. REPORT	**b. ABSTRACT**	**c. THIS PAGE**	SAR		**19b. TELEPHONE NUMBER** *(include area code)*
U	U	U			

Standard Form 298 (Rev. 8-98)
Prescribed by ANSI Std. Z39.18

FINAL REPORT:
AFOSR Grant Number: FA9550-08-1-0048

Numerical Simulation of Pulse Detonation Rocket-Induced MHD Ejector (PDRIME) Concepts for Advanced Propulsion Systems

PI: Prof. Ann R. Karagozian
UCLA Department of Mechanical and Aerospace Engineering
310-825-5653; ark@seas.ucla.edu
AFOSR Program Manager: Dr. Mitat A. Birkan, AFOSR/RSA
mitat.birkan@afosr.af.mil

Abstract

The primary goal of this research project has been to use high resolution numerical methods to explore reactive and magnetohydrodynamic (MHD) flow phenomena as a means of potentially improving the performance of hypersonic propulsion through a range of alternative and innovative combined-cycle concepts, such as the Pulse Detonation Rocket-Induced MHD Ejector (PDRIME) Concept. Such a combined cycle propulsion concept has the potential to achieve improved system performance over conventional rockets or pulse detonation rocket engine (PDRE) concepts in a range of flight conditions, via temporal energy bypass from a pulse detonation rocket to an MHD-augmented component. These studies constitute an assessment of the potential improvements possible through PDRIME concepts via detailed numerical simulations as well as simplified modeling. On the basis of both simplified modeling and highly resolved simulations, an optimization of system level configuration has been explored in detail. Beyond the PDRIME explorations, based on discussions with Dr. Birkan, as part of this grant our research group has also examined fundamental resolution of detonation instabilities with complex reaction kinetics and the potential influence of an applied magnetic field on the reactive flow, in addition to experiments relevant to acoustically-coupled coaxial jet instabilities in rocket chambers.

1. Introduction and Background

Robust propulsion systems for advanced high speed air breathing and rocket vehicles are critical to the future of Air Force missions, including those for global/responsive strike and assured access to space. A novel combined cycle propulsive concept, the Pulse Detonation Rocket-Induced MHD Ejector (PDRIME) proposed by Dr. Jean-Luc Cambier[1] of the Air Force Research Laboratory at Edwards, is one of a number of alternative MHD augmentation ideas that shows promise for application to a wide range of advanced propulsion systems. Taking advantage of the unsteady engine cycle associated with the pulse detonation rocket engine (PDRE), PDRIME involves periodic temporal energy bypass to a seeded airstream, with MHD acceleration of the airstream for thrust enhancement and control. The range of alternative MHD-augmented propulsion configurations that could be employed suggests that the PDRIME type of concept could be applied to hypersonic air-breathing systems, space power production for

directed energy weapons (DEW) and remote sensing systems, electromagnetic countermeasures, and other potential Air Force systems for the mid-to-far term.

A schematic of the PDRIME configuration and associated flow processes is shown in **Figures 1ab**. A PDRE can be designed to have a converging-diverging nozzle such that the initial peak pressure in the combustion chamber results in a pressure at the nozzle exit plane that is well above ambient. Under these circumstances the nozzle exhausts a shock structure (locally oblique) at the nozzle lip, indicated in Fig. 1a. The shock produced at the PDRE's nozzle exit can then enter the bypass channel, traveling upstream. If the air is initially at high Mach number in the channel, this traveling shock brings the air to high temperature, generating a slowly-moving slug of high-temperature air that can be more easily ionized. As the pressure at the nozzle exit drops during blowdown, the shock then slows down, and eventually the ionized air starts to move downstream. At this point, electrical power can be applied to accelerate the air slug, generating thrust (Figure 1b). The procedure can then be repeated at each cycle.

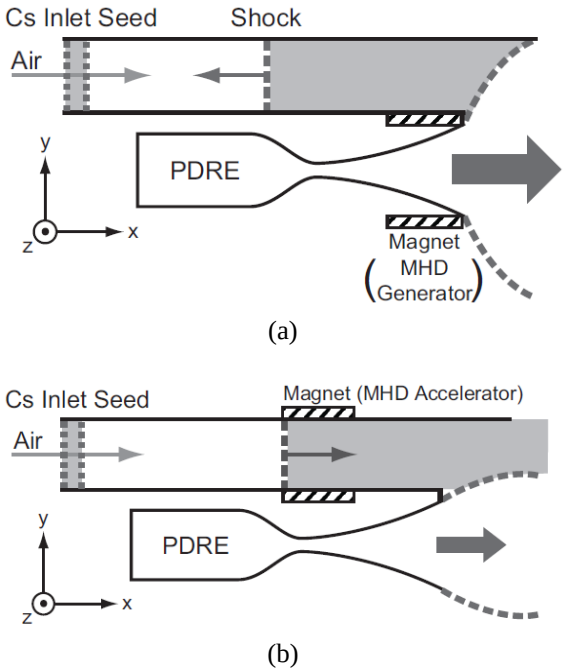

Figure 1. Schematic of the PDRIME concept during (a) the initial portion of the cycle, where over-pressure at the nozzle exit allows an upstream propagating shock (dashed line) to enter the bypass section, and (b) during blowdown, where exhaust of the compressed and heated air from the bypass channel takes place.

Another alternative configuration by which MHD can be used to augment thrust generated by a PDRE is one in which energy extracted by MHD from the high velocity flow in the expansion portion of the nozzle can be applied to the combustion chamber. Creation of a "magnetic piston" in the chamber, as shown in **Figure 2**, can be used to exhaust combustion products from the chamber at an optimal portion of the cycle while allowing a fresh mixture of reactants to fill the available volume. Both the PDRIME with bypass and magnetic piston concepts were explored as a part of this research project.

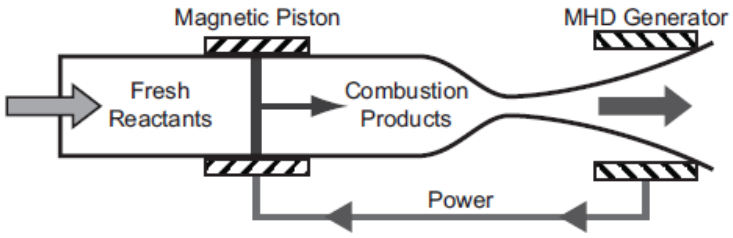

Figure 2. Schematic of the Magnetic Piston Concept. The piston accelerates the combustion products out of the chamber in such a way that, as long as it continuously operates, constant pressure and temperature are maintained at the throat. Fresh reactants are simulatenously drawn in to replace the evacuated products.

2. Methods and Summary of Results on Alternative PDRIME Configurations

Due to the large number of available system parameters in the PDRIME, to accomplish efficient performance calculation and optimization, a rapid simulation technique is required, one that is simpler than a detailed numerical simulation of flow and reactive processes in the PDRE chamber and adjacent flow sections. For the PDRE configuration, after the shock waves have subsided in the combustion chamber, the properties of the fluid within the chamber are mostly uniform, resembling the products of a constant volume reaction. For these reasons a blowdown model was developed by Cambier[2] to predict chamber properties as a function of time after a constant volume reaction; this model was incorporated in the present PDRIME configuration simulations.

The diverging section of the nozzle and the bypass-tube are then divided into cells and fully discretized. The 2D transient equations which govern this flow in conservative form are similar to those used to simulate PDEs as done in He and Karagozian[3,4] but with additional species terms (to simulate air, water vapor exhaust, cesium atoms, and cesium ions), an ionization/recombination source term when we simulate the injection of cesium, and an MHD source term denoting related momentum and energy effects.

Details on the simulation methods and preliminary results for the PDRIME configurations are described in a conference paper[5] (**Appendix A**) while more complete results may be found in a recent journal paper[6] (**Appendix B**) as well as in the Ph.D. thesis of Zeineh[7], the M.S. thesis of Roth[8], and the Ph.D. prospectus of Cole[9]. The student documents are available upon request.

A few of the important observations from the above simulations are included in the body of this report. **Figure 3**, for example, shows temperature contours for the PDRIME geometry (without the presence of a magnetic piston), both for the cases without MHD at all and with only the MHD nozzle generator operating (that is, extracting energy from the nozzle and applying it in the bypass section). Results are shown for an altitude of 25 km and at flight Mach numbers 7, 9, and 11. This is the altitude and flow regime in which MHD augmentation would have the most benefit according to earlier quasi-1D simulations[8,9]. We observe that much greater heating occurs in the bypass section when we activate the nozzle generator because the higher pressure at the nozzle exit allows a stronger shock, traveling at a higher speed, to enter the bypass section. Increasing the

nozzle exit pressure through extraction of the flow's kinetic energy is vital to the heating and ionization of the bypass fluid, which in turn is vital to MHD acceleration for the PDRIME. Unfortunately, although the quasi-1D simulations for the PDRIME suggest improvements with the application of MHD energy in the bypass section, detailed 2D simulations such as those in Figure 3 indicate that there is vorticity generation that alters the transfer of the shock and flow in the bypass section, actually producing a reduction in overall performance of the PDRIME when compared with the baseline PDRE without MHD effects (see the comparisons of total impulse in **Figure 4**).

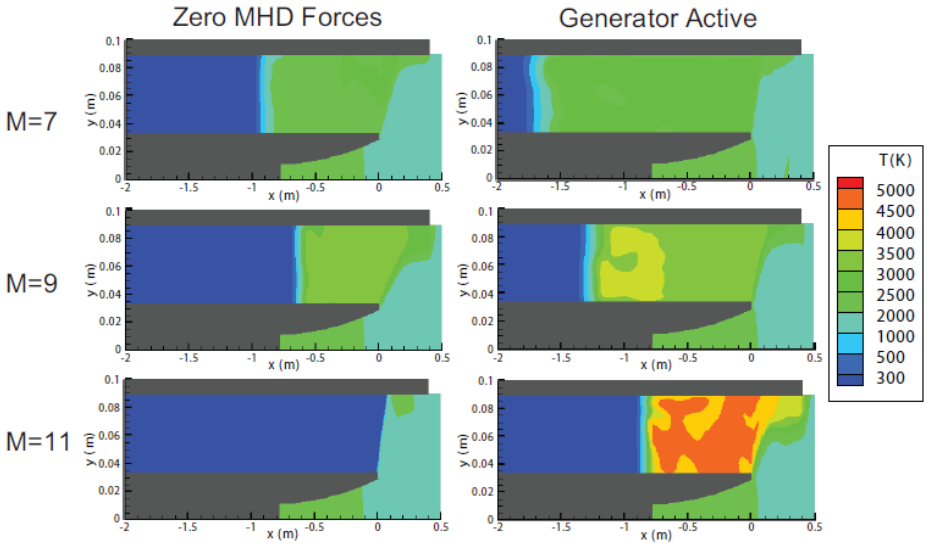

Figure 3. Temperature contours of the PDRIME, with and without the nozzle generator running, at time t=3ms. The altitude of operation is 25 km, with an initial chamber temperature of 3000 K.

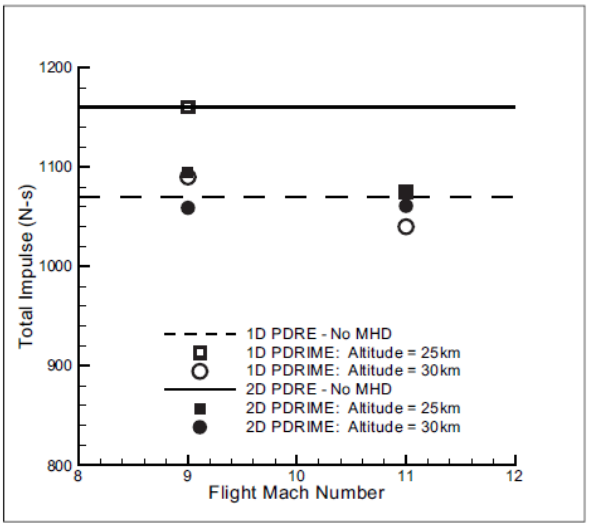

Figure 4. Comparisons between quasi-1D and 2D simulations of the PDRIME in which initial chamber temperature is set to 3000 K and conductivity is constant. The dashed and solid lines indicate the minimum impulse that the bypass must contribute in order to outperform the PDRE without any MHD components for the quasi-1D and 2D simulations, respectively.

Optimization of the operation of the PDRIME with the presence of the magnetic piston and with lower flight Mach numbers can lead to improvements in performance over the baseline, however. As described in detail in Zeineh, et al.[6] and as summarized in **Figure 5**, increasing the size of the bypass section can also produce increases in the impulse per cycle.

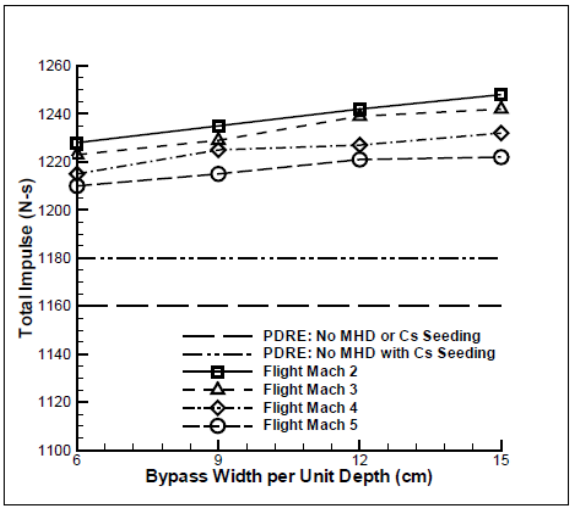

Figure 5. PDRIME total impulse per cycle at 25km varying with flight Mach number and bypass area per unit depth. Initial chamber temperature of 3000K. Bypass length = 4m. Chamber is initially seeded with 0.5% cesium by moles, and the width of the bypass is seeded with 0.1% cesium by moles.

3. Ongoing Studies

Fundamental to the utilization of MHD to augment the performance of pulse detonation rocket engine configurations is the ability for the magnetic field to affect the propagation of detonation waves. As a consequence, one of the graduate students initially supported by this grant, Lord Cole, is continuing his Ph.D. studies at UCLA, in collaboration with Dr. Cambier of AFRL, by examining detailed detonation instabilities with complex reaction and ionization kinetics. Preliminary studies on various characteristics of detonation instabilities are described in a recent paper presented at the ICDERS 2011 conference[10], and subsequent studies are examining the effect of an applied magnetic field on these instabilities.

In addition, separate experimental studies on the response of cryogenic coaxial jet flows to external acoustic disturbances have been and are being completed by another graduate students initially supported by this grant, Sophonias Teshome. These experiments have been conducted at AFRL, and recent results[11] have been analyzed using Proper Orthogonal Decomposition. These studies also are ongoing but we expect completion by March of 2012.

References

[1] J.-L. Cambier, "MHD Augmentation of Pulse Detonation Rocket Engines", 10th Intl. Space Planes Conf., Kyoto, Japan, April 2001, AIAA paper 2001-1782.

[2] Cambier, J.-L., "Preliminary Model of Pulse Detonation Rocket Engines", Proceedings from the 35th AIAA/ASME/SAE/ASEE Joint Propulsion Conference, June 1999, AIAA paper 1999-2659.

[3] He, X. and Karagozian, A. R., "Numerical Simulation of Pulse Detonation Engine Phenomena", **Journal of Scientific Computing,** Vol. 19, Nos. 1-3, pp.201-224, December**,** 2003.

[4] He, X. and Karagozian, A. R., "Pulse Detonation Engine Simulations with Alternative Geometries and Reaction Kinetics", **Journal of Propulsion and Power**, Vol. 22, No. 4, pp. 852-861, 2006.

[5] Cambier, J.-L., Roth, T., Zeineh, C., and Karagozian, A. R., "The Pulse Detonation Rocket Induced MHD Ejector (PDRIME) Concept" Paper AIAA-2008-4688, 44th AIAA/ASME/SAE/ASEE Joint Propulsion Conference and Exhibit, July, 2008.

[6] Zeineh, C. F., Cole, L. K., Roth, T., Karagozian, A. R., and Cambier, J.-L., "Magnetohydrodynamic Augmentation of Pulse Detonation Rocket Engines", **Journal of Propulsion and Power**, Vol. 28, No. 1, pp. 146-159, January 2012.

[7] Zeineh, C., "Numerical Simulation of Magnetohydrodynamic Thrust Augmentation for Pulse Detonation Rocket Engine", Ph.D. thesis, UCLA Department of Mechanical and Aerospace Engineering, 2010.

[8] Roth, T., "Modeling and Numerical Simulations of Pulse Detonation Engines with MHD Thrust Augmentation", M.S. thesis, Department of Mechanical and Aerospace Engineering, UCLA, 2007.

[9] Cole, L., "Combustion and magnetohydrodynamic processes in advanced pulse detonation rocket engines", Ph.D. prospectus, Department of Mechanical and Aerospace Engineering, UCLA, 2010.

[10] Cole, L. K., Karagozian, A. R., and Cambier, J.-L., "Stability of Flame-Shock Coupling in Detonation Waves: 1D Dynamics", Paper 89, 23rd International Colloquium on the Dynamics of Explosions and Reactive Systems (ICDERS), UC Irvine, July 24-29, 2011.

[11] Teshome, S., Leyva, I. A., Talley, D., and Karagozian, A. R., "Cryogenic High-Pressure Shear-Coaxial Jets Exposed to Transverse Acoustic Forcing", presented at the 50th AIAA Aerospace Sciences Meeting, Nashville, TN, January 9-12, 2012.

The Pulse Detonation Rocket Induced MHD Ejector (PDRIME) Concept

Jean-Luc Cambier*
Air Force Research Laboratory, Aerophysics Branch, Edwards AFB, CA 93524

Timothy Roth†, Christopher Zeineh‡, and Ann R. Karagozian§
Department of Mechanical and Aerospace Engineering, UCLA, Los Angeles, CA 90095-1597

Pulse detonation engines (PDEs) have received significant attention due to their potentially superior performance over constant pressure engines. However due to the unsteady chamber pressure, the PDE system will either be over- or under-expanded for the majority of the cycle, with substantial performance loss in atmospheric flight applications. Thrust augmentation, such as PDE-ejector configurations, can potentially alleviate this problem. Here, we study the potential benefits of using Magneto-hydrodynamic (MHD) augmentation by extracting energy from a Pulse Detonation Rocket Engine (PDRE) and applying it to a separate stream. In this PDRE-MHD Ejector (PDRIME) concept, the energy extracted from a generator in the nozzle is applied directly to a by-pass air stream through an MHD accelerator. The air stream is first shocked and raised to high-temperature, allowing thermal ionization to occur after appropriate seeding. The shock-processing of the high-speed air stream is accomplished by using the high initial PDRE nozzle pressures of the under-expanded phase. Thus, energy could be efficiently transferred from one stream to another. The present simulations involve use of a simple blowdown model for PDE behavior, coupled to quasi-1D and 2D numerical simulations of flow and MHD processes in the rest of the PDRIME configuration. Results show potential performance gains but some challenges associated with achieving these gains.

Nomenclature

A	=	Cross-sectional area
B	=	Magnetic field
c	=	Speed of sound
$\vec{E}$	=	Electric field
E, $\hat{E}$	=	Energy
F_L	=	Lorenz force
Re_m	=	Magnetic Reynolds Number
I	=	Impulse
j	=	Current density
$\dot{m}$	=	Mass flux
p	=	Pressure
T	=	Thrust
u	=	Velocity
x,y,z	=	Streamwise, transverse, and axial coordinates
γ	=	Ratio of specific heats
ρ	=	Density
σ	=	Electrical conductivity

* Senior Scientist, AFRL/RZSA
† Graduate Student Researcher; currently Member of the Technical Staff, Northrop-Grumman Electronic Systems
‡ Graduate Student Researcher
§ Professor, AIAA Fellow; corresponding author (ark@seas.ucla.edu)

Introduction

Robust propulsion systems for advanced high speed air breathing and rocket vehicles are critical to the future of Air Force missions, including those for global/responsive strike and assured access to space. A novel combined cycle propulsive concept, the Pulse Detonation Rocket-Induced MHD Ejector (PDRIME) proposed by Cambier[1], is one of a number of alternative magneto-hydrodynamic (MHD) augmentation ideas that could have promise for application to a wide range of advanced propulsion systems. Taking advantage of the periodic engine cycle associated with the pulse detonation rocket engine (PDRE), PDRIME involves periodic temporal energy bypass to a seeded airstream, with MHD acceleration of the airstream for thrust enhancement and control. The range of alternative MHD-augmented propulsion configurations that could be employed suggests that the PDRIME type of concept could be applied to hypersonic air-breathing systems, space power production for directed energy weapons (DEW) and remote sensing systems, electromagnetic countermeasures, and other potential Air Force systems for the mid-to-far term.

Background: Conventional Rocket Systems and PDREs

Chemical rocket engines store both fuel and oxidizer, unlike air-breathing engines which utilize the oxygen in air in the combustion process. Liquid rockets typically employ a constant pressure reaction, where reactants are continually fed at high pressure into the combustion chamber. Rocket engines typically use a converging-diverging (Laval) nozzle to expand the flow and convert the high pressure and temperature of the propellants into thrust. Properties of a nozzle flow depend strongly on the pressure upstream (inside the combustion chamber, P_c), and at ambient (p_a), downstream of the nozzle exit, as well as the exit-to throat area ratio for the nozzle, A_e/A_*. The thrust generated by a rocket is typically expressed as:

$$T = \dot{m} V_e + (p_e - p_a) A_e \tag{1}$$

where $\dot{m}$ is the mass flux of gas exiting the nozzle, V_e is the exhaust velocity, and p_e is the pressure at the exhaust of the nozzle.

The maximum thrust[2] occurs when the propellants are expanded to the point where the pressure at the exit of the nozzle is equal to the ambient pressure. Further expansion of the gas in the nozzle will reduce the thrust, as the ambient pressure will then exceed the exhaust pressure, creating pressure drag. This added drag can outweigh momentum gains arising from the further acceleration of the flow from the nozzle, i.e., the increase in exhaust velocity. Under-expansion in the nozzle will result in lower than optimal thrust as the maximum momentum gains are not realized. Another performance parameter, impulse I, is the thrust integrated over time t:

$$I \equiv \int_0^t T(\tau) d\tau \tag{2}$$

Another common performance parameter, specific impulse I_{sp} ,is the impulse divided by the weight of the reactants or propellants.

One alternative configuration to the traditional rocket engine which has the potential for operating as a constant volume cycle, and hence could be theoretically more efficient, is the pulse detonation engine or PDE (a subset of which is the pulse detonation rocket engine or PDRE). The pulse detonation engine operates in a cycle. Reactants are added to the combustion chamber at low pressure, and are mixed. The mixture is ignited and a detonation wave propagates across the chamber. This detonation raises the propellants to high pressure and temperature, and can be modeled as a constant volume reaction, which is more efficient than a constant pressure reaction. After the detonation wave (or shock wave, after reactants have been consumed) exits the nozzle, an expansion wave is reflected back into the nozzle and eventually propagates into the chamber. The expansion wave thus lowers the overall pressure throughout the chamber, and upon reflection at the thrust wall, the lowered pressure allows reactants to be drawn into the chamber. The reflection of the expansion wave at the nozzle exit results in a reflected compression wave, which is strengthened and becomes a shock. When the shock reflects at the thrust wall, the reactants in the chamber can be ignited, and the ignition of the detonation wave starts the process once again. A number of recent studies have explored the nature and performance characteristics of PDEs of various geometries[3,4,5,6,7,8]. The PDE was even recently tested for the first time in flight on a Scaled Composites Long EZ aircraft[9], with four PDE tubes operating at a cycle frequency of 20 Hz.

In the past, our group at UCLA[10,11] has explored the influence of PDE geometry, reaction kinetics, and flow processes using high order numerical methods. A fifth-order WENO (weighted essentially non-oscillatory[12,13]) scheme was used for spatial integration of the reactive Euler equations, with a 3rd -order Runge-Kutta time integration in the case of simplified reaction kinetics; a stiff ODE solver was used for temporal integration in complex kinetics simulations. While the simulations using complex kinetics provide useful quantitative data, the

simulations with reduced kinetics (a single step reaction) in fact can provide very similar quantitative performance results.

In general, two different methods could be used to generate thrust from PDREs. The first involves a straight or slightly contoured nozzle. The main goal of this configuration is to exploit the thrust generation from the ignition of the detonation wave near the thrust wall and the propagation of the detonation wave through the device, as described above. The second approach is more similar to a constant-pressure rocket. Here the nozzle throat is small enough to prevent the main detonation wave to escape the chamber. This creates multiple reflected compressive waves in the chamber; which homogenize the chamber pressurization, resulting in an approximately constant volume reaction. During the blow-down period the reactants are driven out from the chamber and through the nozzle. Similar to the constant-pressure rocket, the exhaust gases are expanded, increasing the velocity and reducing the pressure. The difference between this type of PDRE and a constant-pressure rocket is that in the PDRE, the chamber pressure is decreasing throughout the blow-down period as mass is ejected from the chamber with no immediate replacement. New reactants are added to the combustion chamber once the pressure has been reduced to a specified value and then the cycle is repeated.

Due to the unsteady nature of the chamber pressure, however, a PDRE nozzle can only be perfectly expanded briefly within a blow-down period. This implies suboptimal use of energy to attain this condition for most of the cycle. At low altitudes, nozzles with large area ratios are subject to large drag forces ($P_a > P_e$), while nozzles with relatively smaller exit areas will be under-expanded for the majority of blow-down.

The PDRIME Concept

Ejectors are often used to transfer energy from one stream to another stream, providing an additional source of thrust, especially for an air-breathing engine. Ejectors have been shown to produce overall thrust gains when energy is being taken from a high velocity flow and transferred to a low energy stream, in the ejector, with a high mass flow rate. In the present application for the PDRE, energy can be extracted from the nozzle when the marginal decreases in thrust are small and added to a bypass air flow, to assist in augmentation of the thrust. Ejectors typically transfer energy between streams through shear stress between separate flow streams. A portion of the main flow is diverted into a channel to mix with the lower velocity flow. The drawback of this method is that the ability to transfer energy is limited by the contact area between the two streams. At large velocities shear layer thicknesses are small, leading to the necessity for large channels for mixing, which add weight.

In contrast, if magnetohydrodynamic (MHD) forces are applied as body forces to the ejector flow, affecting the entire field immediately, there can be substantial benefits[14]. This could reduce the length of the bypass tube and time necessary for complete energy transfer as well as providing the flexibility of energy extraction and application, since the applied fields can be varied.

Our possible configuration attaches a converging-diverging nozzle to the combustion chamber of a PDRE with a bypass tube. A generic configuration for this concept, called the Pulse Detonation Rocket Induced MHD Ejector (PDRIME), is shown in **Figure 1**. For the present applications, a simple Faraday configuration is used in both channels, with magnetic and electric fields in the z and y direction respectively, and normal to the fluid velocities (in the nozzle and bypass-tube, the x-direction). A planar design is used to achieve a spatially uniform magnetic field, only in the z-direction, by placement of magnets above and below each region.

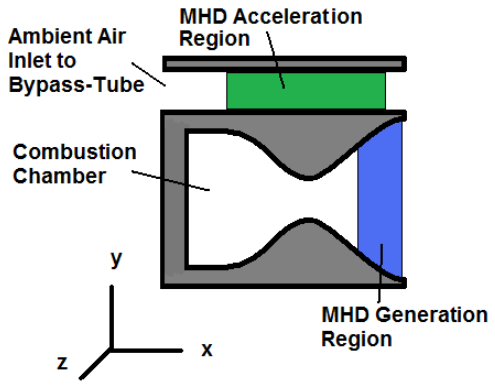

Figure 1: The generic PDRIME configuration, indicating the PDRE combustion chamber and regions in which MHD generation/extraction and flow acceleration in a bypass section take place.

In the expanding (divergent) section of the nozzle the fields are configured as an MHD generator to extract energy from the flow. In the adjacent by-pass channel, ambient air is periodically accelerated by MHD forces, using the energy extracted from the nozzle. A gain in thrust is possible by extracting energy from the high-speed flow[14] in the nozzle, and by applying it to a slower flow. This would require that the air in the by-pass tube be slowed down to velocities below that of the flow in the PDRE nozzle. Typically, this would imply significant drag forces; however, the PDRE operation, with its initially under-expanded phase during blowdown, may provide an elegant solution to this problem, as shown in **Figures 2a and 2b**.

A PDRE can be designed to have a converging-diverging nozzle such that the initial peak pressure in the combustion chamber results in a pressure at the nozzle exit plane that is well above that of the by-pass tube. The initial shock of the rapid pressurization of the PDRE chamber can diffract at the nozzle lip and travel upstream in the by-pass. More importantly, as shown in Fig. 2a, a slowly varying contact discontinuity is generated during the blow-down, and blocks the incoming air flow in the by-pass channel. If the air is initially at high Mach number in the bypass channel, an upstream-propagating shock brings the air to stagnation at high temperature. If the air is initially seeded with an alkaline seed such as Cesium by an upstream injector, the stagnated high-temperature air may be thermally ionized and become sufficiently conductive for efficient MHD coupling. Note that the air is brought to stagnation without requiring channel constriction, i.e. without any drag forces.

As the pressure at the nozzle exit drops during blow-down, the shock then slows down, and eventually the ionized air starts to move downstream. At this point, electrical power can be applied to accelerate the slowly-moving air slug from the bypass tube and thus generating thrust (**Fig. 2b**). The procedure can then be repeated at each cycle. One only needs to design the nozzle such that the flow is under-expanded during the initial part of the blow-down phase. In fact, there may be a self-adjusting process at work, depending on PDRE nozzle design and altitude as outlined by Cambier[1]. While at launch, the nozzle exit pressure is equal to ambient and there is no interaction with the bypass air, as the vehicle accelerates and gains altitude, the nozzle becomes progressively under-expanded, so that eventually a strong shock can be generated for the bypass channel to ionize the seeded air, and the ejector operates. This is one of several configurations in which the PDRIME concept could be used for thrust augmentation in advanced propulsion systems.

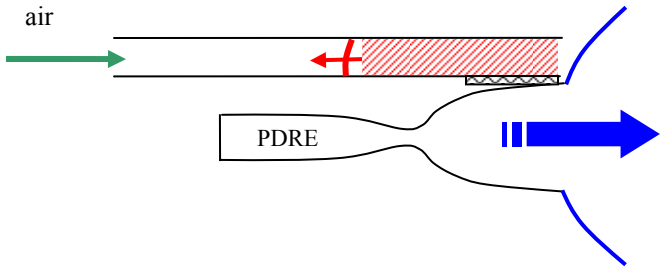

Figure 2a: Schematic of the PDRIME concept during the initial portion of the cycle. Overpressure at the nozzle exit blocks flow in the bypass channel. An upstream propagating shock slows and raises the temperature of the seeded air in the bypass channel.

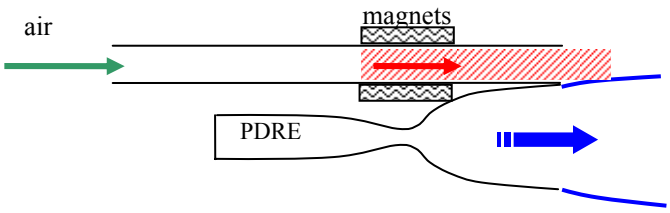

Figure 2b: Schematic of the PDRIME concept during the latter part of the cycle, during blow-down. As the pressure at the nozzle exit drops, exit of the compressed and heated air from the bypass channel takes place. Power is applied during the MHD acceleration of the air slug.

As noted above, the MHD "generator" is located in the diverging section of the nozzle where the velocity is largest, so that the expansion of the fluid counteracts some of the velocity reduction arising from the Lorentz ("drag") force acting in the generator. The ionized flow is characterized by a current density $\vec{j}$ which, using the simplest form of Ohm's law, can be written as:

$$\vec{j} = \sigma(\vec{E} + \vec{u} \times \vec{B}) \tag{3}$$

where σ is the electrical conductivity (with units of Mho/m). It is also assumed that the self-induced magnetic field is negligible, i.e. the magnetic field is given by the applied field. This assumption is equivalent to the limit of small magnetic Reynolds number R_m, defined as:

$$R_m = \mu\sigma u L \tag{4}$$

where μ is the permeability of free space (units of N/A^2), u the velocity and L is a characteristic length scale. The MHD coupling to the flow is described by source terms to the conservation laws, namely the Lorentz force F_L and a Joule energy deposition Q_J:

$$\vec{F}_L = \vec{j} \times \vec{B} \tag{5a}$$

$$Q_J = \vec{j} \cdot \vec{E} = \frac{\vec{j}^2}{\sigma} + \vec{u} \cdot (\vec{j} \times \vec{B}) \tag{5b}$$

The terms on the right-hand-side of (4b) are respectively the ohmic heating (dissipation) and mechanical work of the Lorentz force. For the Faraday configuration used here, the current density has a non-zero component in the y-direction only:

$$j_y = \sigma\left(E_y - u_x \times B_z\right) \tag{6}$$

It is convenient to define a loading factor K_y describing the respective strengths of the applied and induced electric fields,

$$K_y = \frac{E_y}{(u \times B)_y} \tag{7}$$

In a quasi-1D analysis, there is a single component of the velocity and using the loading factor, (3) can be written as:

$$j_y = \sigma u B \cdot (K_y - 1) \tag{8}$$

The Lorentz and Joule terms then become:

$$F_L = \sigma u B^2 (K_y - 1) \tag{9a}$$

$$Q_J = \sigma u^2 B^2 \cdot K_y (K_y - 1) \tag{9b}$$

When $K_y < 1$, the Lorentz force is negative (flow deceleration) and the Joule power is negative (energy extracted from the fluid). In the accelerator (bypass section), a positive Lorentz force and application of energy takes place. Regardless of the loading factor, the Ohmic heating will always be a positive term, since it is proportional to $(K_y - 1)^2$, representing a loss in both cases. Ignoring dissipative effects, we see that the Lorentz force scales with velocity, while the energy associated with both generation and acceleration scales with velocity squared. For this reason, maximum thrust gain is achieved when energy is extracted from high velocity flows, as in the nozzle, and applied to low velocity flows.

It is easily seen[15] that the optimal loading factor for MHD generation is $K_y = 0.5$. In the accelerator section (by-pass tube), the loading factor is generally greater than 1, and is chosen to be $K_y = 1.5$, but if a negative flow is detected in that location in the course of the cycle, $K_y = 0.5$ is assumed in order to assist with flow reversal.

The Magnetic Piston Concept

Another alternative configuration by which MHD can be used to augment thrust generated by a PDRE is one in which energy extracted from the high velocity flow in the expansion portion of the nozzle can be applied to the combustion chamber in order to accelerate combustion products from the chamber while allowing a fresh mixture of reactants to fill the available volume. By effectively creating a "magnetic piston" in the chamber, as outlined in Cambier[1], the combustion products can be pushed out from the chamber while simultaneously allowing a fresh mixture of reactants to fill the available volume. Such a configuration is shown in **Figure 3**. The extraction of

energy from a high velocity stream and delivered to a low velocity stream is one mechanism for thrust augmentation, hence a configuration such as that in **Fig. 3** can theoretically lead to performance gains. As indicated by Cambier[1], the average thrust increases with an increasing fraction of energy extracted from the flow, and with reduction in the filling time. It is noted that, when blow-down and filling processes are allowed to overlap via appropriate application of the magnetic field, filling time is effectively reduced, leading to a large increase in average thrust. The magnetic piston concept, separately as well as in concert with the PDRIME with bypass flow, will be explored here.

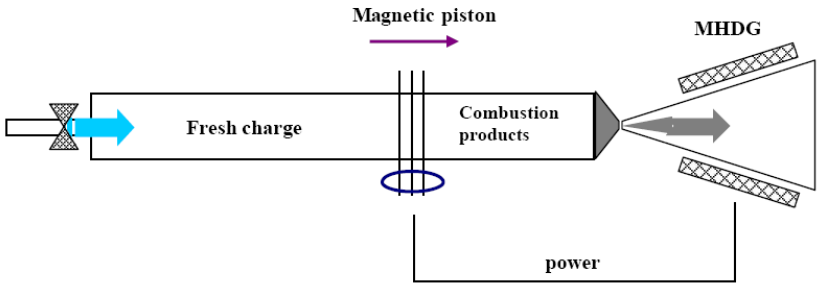

Figure 3: Schematic of the PDRE concept with MHD augmentation via a generator in the nozzle and a magnetic piston in the chamber (from Cambier[1]).

The goal of the present research involves use of a simplified model for the blow-down portion of the PDRE, coupled to a more detailed simulation of the relevant MHD processes in the nozzle and/or adjacent bypass sections, as a means of predicting overall PDRIME and magnetic piston phenomena and performance parameters. The model is validated using detailed numerical simulations of PDRE processes, so that projections for optimal performance and operating conditions may be made.

Description of the PDRIME Model and Simulation Procedure

Model Framework

Due to the large number of available system parameters in the PDRIME, a rapid simulation technique is required, one that is simpler than a detailed numerical simulation of flow and reactive processes in the PDRE and adjacent flow sections. Detonations constitute a major computational cost. The sharp gradients and large sound speeds present in the PDE greatly reduce the time-step and require finer spatial resolution[16,17]. After the shock waves have subsided in the combustion chamber, the properties of the fluid within the combustion chamber are mostly uniform, resembling the products of a constant volume reaction. For these reasons a blow-down model was developed by Cambier[18] to predict chamber properties as a function of time after a constant volume reaction. This blow-down model is in a single cell which represents the entire PDE combustion chamber. The converging section of the nozzle is also represented by a single cell approximation. An adiabatic solution for the throat conditions for every time-step is determined based on the combustion chamber properties and the assumption that the throat is choked. The divergent section, throat to exit, is fully discretized, as is the entire bypass-tube. In order to validate certain aspects of the engine cycle and flow processes, comparisons with full 2D transient numerical simulations are also made.

Description of Blowdown Model

The PDE cycle begins when the combustion chamber is full of reactants. An external spark then sends a detonation wave through the combustion chamber, raising the pressure of the propellants. The pressure difference between the combustion chamber and the ambient air drives the propellants out of the combustion chamber, representing the blow-down process. The presence of a nozzle changes the blow-down profile. Intuitively, a smaller throat, which restricts the mass flow of propellants out of the chamber, will lead to a slower decay, increasing the blow-down period. With small enough throat areas, the constant pressure period following the PDE's detonation becomes negligible and only blow-down needs to be considered for thrust calculations. Here the reaction is approximated as a constant volume reaction.

To predict this pressure decay inside the combustion chamber a simple model developed by Cambier is used. This model starts with the combustion chamber filled with post-constant volume reaction products at high pressure

and temperature. The mass and energy flow rate of the products through the throat are then calculated based on current conditions:

$$\frac{dM}{dt} = -\dot{m} = -\Gamma \rho_o c_o A^* \tag{10a}$$

$$\frac{dE}{dt} = -\dot{m} \cdot h_o = -\dot{m} \cdot C_p T_o \tag{10b}$$

where

$$\Gamma = \left(\frac{2}{\gamma + 1} \right)^{\frac{\gamma+1}{2(\gamma-1)}} \tag{11}$$

and ρ_o is the density of the products, A* is the area of the choked throat, c_o is the sound speed, h_o is the total enthalpy, and C_p is the heat capacity at constant pressure. In (10a-b), $M = \rho_0 \mathsf{V}_c$ and $E = \rho_0 C_\mathrm{v} T_0 \mathsf{V}_c$. The chamber volume V_c is constant, thus the system of equations (10) reduces to a partial differential equation for the stagnation temperature, which can be easily integrated[1]. This blowdown process is assumed to be adiabatic and quasi-steady. For high temperature water vapor (products), γ ~ 1.2 and is held constant. In this approach the entire combustion chamber is represented with a single cell, greatly reducing computational time.

Discretization of Nozzle and Bypass Sections

The diverging section of the nozzle and the bypass-tube are divided into cells. The quasi-1D equations which govern this flow in conservative form are similar to those in He and Karagozian[11] but without the species terms and with the inclusion of momentum and energy source terms corresponding to MHD effects:

$$\frac{\partial (AU)}{\partial t} + \frac{\partial A F_x(U)}{\partial x} = \frac{dA}{dx} H + A S(U) \tag{12}$$

$$U = \begin{pmatrix} \rho \\ \rho u \\ \widehat{E} \end{pmatrix}, \; F_x(U) = \begin{pmatrix} \rho u \\ \rho u^2 + p \\ (\widehat{E} + p) u \end{pmatrix}, \; H = \begin{pmatrix} 0 \\ p \\ 0 \end{pmatrix}, \; S(U) = \begin{pmatrix} 0 \\ j_y B_z \\ j_y E_y \end{pmatrix} \tag{13}$$

$$\widehat{E} = \frac{p}{\gamma - 1} + \frac{\rho u^2}{2} \tag{14}$$

where A(x) is the cross-sectional area as a function of position, and $\widehat{E}$ is the total energy density . To further streamline this rapid simulation, the flow inside the diverging section of the nozzle is modeled using a quasi-steady solution to these equations. This is valid when the characteristic time scale of the flow in the nozzle with the small throat is much shorter than the blow-down time scale of the chamber. First the governing equations are rewritten in primitive form:

$$\frac{1}{\rho}\frac{d\rho}{dx} + \frac{1}{u}\frac{du}{dx} + \frac{1}{A}\frac{dA}{dx} = 0 \tag{15}$$

$$\frac{dp}{dx} + \rho u \frac{du}{dx} = j_y B_z \tag{16}$$

$$\frac{\gamma}{\gamma - 1} \rho u \frac{d}{dx}\left(\frac{p}{\rho} \right) + \rho u^2 \frac{du}{dx} = j_y E_y \tag{17}$$

These equations are then normalized and solved with a forward marching scheme, starting with the throat conditions and marching to the exit. The flow is supersonic everywhere in the diverging section of the nozzle, which allows for the quasi-steady forward-marching scheme to be employed. Since this model is quasi-steady, there is no numerical time integration, though the time-step between applications of the model is still limited by the speed of sound in the combustion chamber.

When the pressure at the exit drops to sufficiently low levels, a shock will propagate into the nozzle. The forward-marching scheme has no way to detect this condition, hence a separate check of the conditions at the exit is performed. When a shock enters the nozzle, it reduces the local exit velocity and raises the pressure at the exit to become equal to the ambient fluid just outside the nozzle.

Transient flow in the bypass-tube involves a shock created by the nozzle exhaust, traveling into the bypass exit and propagating to the left into a high speed right-moving flow. Quasi-steady forward-marching methods are thus not adequate for these regimes, especially since this method has a singularity when the flow Mach number is equal to one. For these reasons, a fully transient numerical scheme must be used to simulate flow in the bypass-tube.

In simulating flow in the bypass-tube, the WENO method[13] is used to approximate spatial derivatives, with a stencil including upstream and downstream cells. WENO is an adaptation of the Essentially Non-Oscillatory (ENO) method[12,,19] which uses the conservation laws for high order accuracy with shock capturing capabilities. Artificial viscosity is added via the Local Lax Friedrich (LLF) scheme to avoid entropy violation and reduce dispersion. Temporal integration is performed by a 3rd order Runge-Kutta method, which uses an internally iterative process to achieve fairly large time-steps without loss of high order accuracy. The time-step is regulated by the Courant-Friedrichs-Levy (CFL) condition, which ensures stability by limiting the time-step to a ratio of the cell lengths and sound speeds.

Integration of PDRIME Model Components

The **c**omputation of flow in the combustion chamber and nozzle constituting the PDE is decoupled from that in the bypass-tube. The PDE system simulation does not require input from the bypass-tube simulation and will be discussed first. No components of the engine system have dependence on past time-steps using Cambier's blow-down model. This cycle starts with the initiation of blow-down and ends when combustion chamber pressure reaches a prescribed value (specified by the refill process). At a given time the combustion chamber properties are calculated by the blow-down model, which is only a function of time and system parameters. The conditions in the throat are then determined based on chamber properties. The flow in the diverging section of the nozzle is then found by marching forward from the throat, where the properties are known, to the exit. The maximum allowable time-step is then calculated; time is increased, and the blow-down model again calculates combustion chamber properties. The cycle continues until the chamber pressure is reduced far enough or until shock conditions are detected.

Each cycle may be simulated for specific ambient conditions dictated by altitude. For the engine system, altitude affects pressure downstream of the nozzle, and changes the thrust calculated by equation (1), via changes in P_a. The PDE code thus stores exit pressure and Mach number as a function of time, as well as total impulse and energy extracted for every altitude and engine system configuration. The bypass-tube is then employed and coupled with a specific engine system simulation. The bypass model is run using the specified altitude to determine inlet conditions. The exit pressure from the PDE system is used as a time dependent boundary condition for the downstream end of the bypass-tube. The energy applied in the bypass-tube to accelerate the air is limited to the energy extracted from the engine system at that time during the cycle. At the end, the net impulse arising from flow in both systems over one cycle is found. The speed at which the vehicle travels is the only independent variable in the bypass-tube and dictates the inlet velocity or Mach number.

Two-Dimensional Transient Simulations

As a means of validating many of the assumptions that enter in to the quasi-1D simulations of the PDRIME configuration, corresponding simulations of two-dimensional flow in the nozzle, bypass tube, and exterior region have been conducted by Zeineh[20]. These simulations employ a simplified representation of the blow-down process as done in the present modeling, but then employ a 5th order WENO scheme for spatial discretization and a 3rd -order Runge-Kutta scheme for time integration, as done in He and Karagozian[10,11], to resolve the detailed evolution of flow beyond the nozzle throat and exterior to the PDRIME. This allows assumptions pertaining to the transmission of the shock from the nozzle to the bypass tube, for example, to be validated.

Model Validation

This section shows the steps taken to ensure that, despite the many simplifications utilized in these simulations, the results reasonably accurately reflect the performance of a PDRIME system. Thrust estimation from flow properties may be derived from the momentum fluxes in the problem. For PDREs, the contributions of the transient term in the momentum conservation equation are observed to be negligible, a result of the blow-down approximation with a small throat area.

As noted previously, to reduce computational costs the present model represents the PDE cycle by a constant volume reaction followed by a blow-down period. The validity of this model depends on the throat cross-sectional area. A large throat area will allow propellants to leave the combustion chamber as the detonation wave propagates through it, hence this will not produce a constant volume reaction. A smaller throat area (compared with the cross-

sectional area of the chamber) can limit the amount of mass which escapes until the reflected waves have brought the products in the combustion chamber to conditions resembling the result of a constant volume reaction. Cambier[17] demonstrated that the aforementioned simple blow-down model (with a constant volume reaction) can produce nearly the same computed impulse for the actual pulse detonation reaction with a nozzle, with chamber-to-throat area ratio of 16. The comparison is accomplished by closing the throat in the PDE computation until the reaction has gone to completion and then allowing the reactants to escape. The full quasi-1D PDE cycle starts with reactants being ignited by a detonation wave, whose evolution is simulated numerically using a 4th order piecewise parabolic method (PPM) . These two different methods show good agreement and have consistent trends, hence the present exploration incorporates the Cambier blow-down model in its PDRIME simulations.

Comparison of the simple blow-down model and a quasi-1D, transient numerical simulation of blow-down is also conducted and also shows good agreement. The adiabatic calculation which approximates the conditions at the nozzle throat, based on the combustion chamber properties, can be validated using the quasi-1D numerical code. **Figure 4** shows consistency between the WENO simulation and the rapid blow-down model, but with a slight time lag. This provides us with confidence in replacing the entire numerical domain for the PDE, from combustion chamber to the nozzle throat, with the simplified blow-down model, which provides similar results at a fraction of the computational cost.

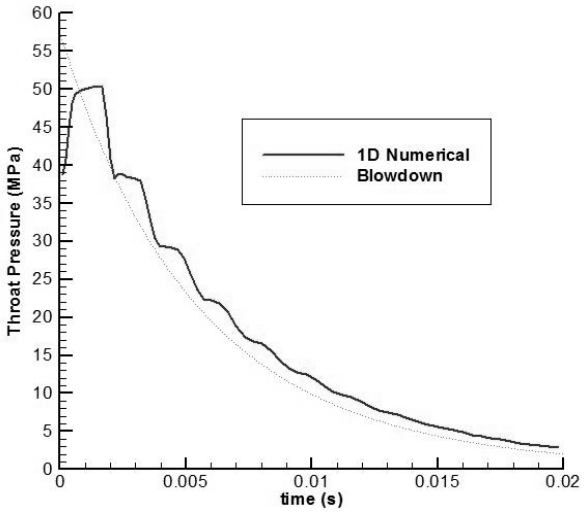

Figure 4: Throat pressure (MPa) as a function of time (s), derived using the numerical, quasi-1D spatially resolved model and the blow-down model.

We finally note that use of a quasi-1D simulation for flow processes associated with a PDE with a nozzle, as compared with results from a fully 2D transient code; yield very similar results for relatively low exit-to-throat nozzle ratios (He and Karagozian[11]). Hence both the blow-down model and quasi-1D portions of the simulation should represent the PDRIME concept quite well.

Results and Performance Evaluation

MHD Energy Generation/Extraction versus Thrust Lost

This section first focuses only on resolving phenomena for the PDE, that is, in the combustion chamber and nozzle. The results of this system are hence independent of the presence of bypass-tube. The impulse and thrust of this system are shown with and without MHD generation to compare the net result of MHD energy extraction from the nozzle on device performance. Extracted energy as well as nozzle exit pressure are quantified as a function of time, to be used as inputs to the bypass-tube computations.

As an example of conditions for PDE operation using the blow-down model, the cycle starts with water vapor products in the combustion chamber at a pressure and temperature of 100atm and 3000K, respectively. The chamber is 0.5m in length and 0.1257m^2 in cross-sectional area with a chamber-to-throat area ratio of 5. The cycle is first assumed to operate at an altitude of 10km and has an exit-to-throat ratio of 35. A magnetic field is uniformly applied (spatially) across the rear half of the diverging section. The strength of the magnetic field is varied with time to maximize energy extraction while keeping the flow at the exit supersonic, at a specified Mach number of 1.2. For this cycle the strength of the applied magnetic field, B as a function of time is shown in **Figure 5**.

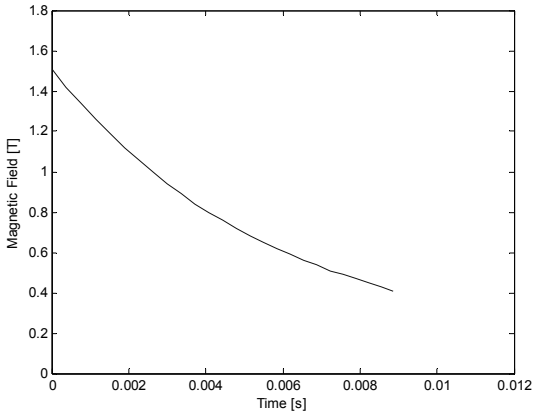

Figure 5: Magnetic field applied across the divergent section, in units of Tesla, as a function of time.

The applied magnetic field must be reduced in time as the chamber pressure decays in order to maintain a constant exit Mach number for the present computation. The applied magnetic field shown in **Figure 5** maximizes the energy extracted while avoiding decelerating the flow to subsonic speeds. **Figure 6** shows the actual Mach number obtained at the nozzle exit on the basis of the applied magnetic field shown in **Fig. 5**.

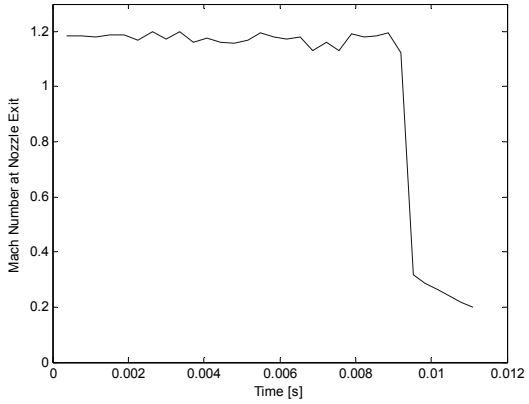

Figure 6: Nozzle exit Mach number as a function of time, computed from the blow-down model for the applied magnetic field shown in **Fig. 5**.

Note that at a time of about 9ms, a shock does enter the nozzle, indicated by the drop in the exit Mach number in **Fig. 6**. This shock is a result of a reduced dynamic pressure at the nozzle exit from the blow-down pressure decay and not a result of MHD application. The magnetic field is turned off when this shock occurs. This particular system operates at a relatively high ambient pressure and with a high exit-to-throat ratio. Both factors contribute to the formation of a shock. This will not occur with most other configurations.

The effect of the MHD generation/extraction on the Mach number within the nozzle flow is shown in **Figure 7**. At time t = 2.3ms, the plot shows Mach number, starting at the throat of the nozzle where the flow is sonic and ends at the nozzle exit. No MHD is applied in the first half of this section to allow the flow to be accelerated, since energy extraction at high velocities is beneficial. A spatially uniform magnetic field is applied to the downstream half of the diverging section, with temporal variation as shown in **Figure 5**. The energy extracted and drag created by the MHD generator lowers the Mach number. Without the MHD generator the flow would be accelerated to Mach ~ 4, but the flow is only Mach 1.2 (by design) with the generation at the nozzle exit. This greatly reduces the impulse for the PDE, as momentum flux is the main component of thrust for this type of configuration. The Lorentz force and joule heating do raise the pressure in this divergent section, and at the exit at the time shown in **Fig. 7**, the exit pressure with MHD generation is 6 times higher than without the MHD. A lower exit Mach number increases the shock angle of the exhaust and increases the PDE's ability to have a shock travel into the bypass-tube.

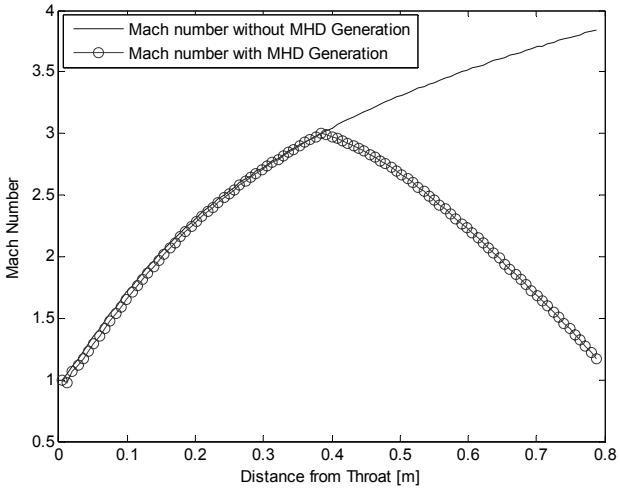

Figure 7: Mach number spatial evolution in the divergent section of the nozzle as a function of distance from the nozzle throat, at time 2.3ms. Results are shown for the PDE (blow-down model) with and without MHD generation in the region between 0.4 and 0.8m from the throat.

The six-fold exit pressure increase due to MHD generation is not enough to overcome the drag imparted on the system by the Lorentz force. **Figure 8** plots the overall impulse versus time with and without the MHD generation, as well as energy extracted (generated). There is a 40% loss of impulse due to the MHD generation in the nozzle for these conditions, but over 3 MJ may be extracted from this process for operation of the PDRIME.

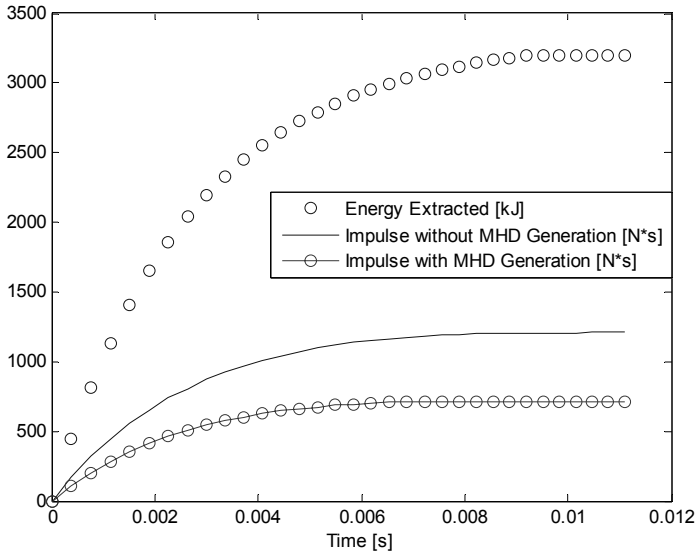

Figure 8: Energy extracted and impulse with and without MHD generation, plotted as a function of time, for the PDE (blow-down model).

The results of the PDE/blow-down model are then input into the bypass-tube model. There it can be determined whether this generated energy can be used to improve the net impulse of the system. This performance will be explored in a later section. At 6.8ms into blow-down, the chamber pressure is $1/10^{th}$ of its initial value. By this time, as seen in **Fig. 8**, nearly 100% of the impulse of this cycle has been produced and 95% of the energy has been generated. This is potentially a time at which the combustion chamber can start to be refilled with reactants.

The chamber pressure after a constant volume reaction is dependent on the pre-reaction pressure and temperature, assuming a fixed mass and volume. To achieve a ten-fold pressure increase during combustion, the initial temperature of the reactants must be 300K. Higher pressure increases are created by lowering the initial

temperature proportionally. The design trade-off is then average thrust versus required filling pressure. The total impulse of each cycle is relatively independent of the filling choice. However, filling at higher chamber pressures allows the filling process to start sooner, increasing the average thrust but requiring more elaborate pumping, something the basic PDE itself is supposed to avoid. At 10.8 ms, the chamber pressure is reduced to $1/30^{th}$ of the initial value. A 30-fold pressure increase can be achieved with reactants filled at 100K. Depending on the application, this 4ms increase in blow-down time may be beneficial.

For every PDE configuration there are four important results to examine in the PDRIME concept. First, the impulse per cycle without MHD augmentation is recorded as a baseline. Next, both impulse per cycle with the MHD generation in the nozzle, as well as the energy generated, are also quantified. Lastly, the pressure at the exit of the nozzle is saved as a function of time.

The effect of the exit-to-throat area ratio and the altitude of operation for the PDRIME system may thus be explored for the PDE itself with a fixed combustion chamber geometry and an initial chamber pressure of 100atm. Cases with alternative initial chamber pressure conditions were run, as were cases with different chamber volumes while holding the initial chamber pressure constant. This latter instance increases the total mass of propellants used per cycle, but it makes little difference in specific impulse results. Initial combustion chamber pressure does have an impact on performance which is not fully explained by the proportional increase in propellant mass per cycle required to achieve it. This will be discussed further below. For the results in this section, the initial chamber pressure is held constant. Chamber pressure does proportionally change the nozzle exit pressure, of course.

Figure 9 plots the impulse per cycle of the PDE itself (via the blow-down model) for different values of the exit-to-throat area ratio and for different altitudes, without MHD generation and without the presence of the bypass tube. It should be noted that the ambient pressure is approximately halved with an altitude increase of 5km. At roughly ground level, where the ambient pressure is highest, the impulse is lowest due to the high drag ($P_a >> P_e$ in equation 1). The optimal exit-to-area ratio for this altitude is five. Similar to constant-pressure rockets, as the ambient pressure is decreased, higher exit-to-throat area ratios are preferred, as the flow can be further expanded so as to equal the ambient pressure. At altitudes in excess of 15km, no maximum is achieved within this area ratio range. Due to the quasi 1-D approximation, momentum losses due to non-streamwise velocities are not accounted for. At large area ratios this will significantly reduce impulse. In addition, heavier nozzles required to achieve larger area ratios will counteract gains. These cycles all use 0.46kg of propellants. Here an impulse I of 1,000N*s corresponds to a specific impulse Isp of 221s.

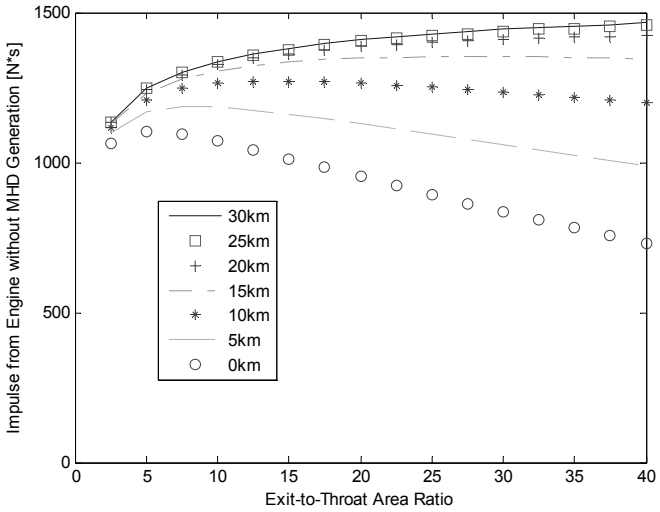

Figure 9: Total impulse as a function of exit-to-throat area ratio for various altitudes, for a single cycle PDE without MHD generation or augmentation.

MHD generation via a Lorentz force exerted on the propellant in the nozzle during energy extraction reduces the impulse of the engine system. **Figure 10** plots the impulse per cycle of the PDE, as a function of exit-to-throat ratio, with MHD generation in the nozzle's divergent section but without accounting for flow in the bypass tube. As seen in the figure, the greatest impulse reductions occur with the larger area ratios, due to the higher velocities and larger areas over which MHD is applied. These factors also lead to a larger amount of energy being extracted from the flow.

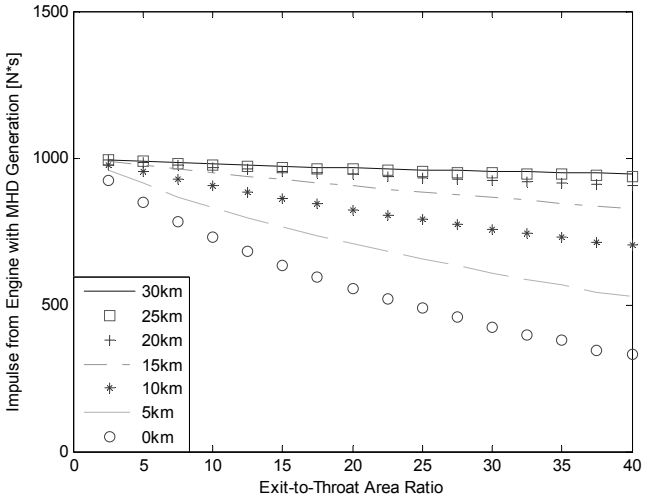

Figure 10: Impulse as a function of exit-to-throat area ratio for various altitudes for a PDE with MHD generation in the nozzle.

Figure 11 plots the energy generated by MHD in the nozzle as a function of nozzle exit-to-throat area ratio. The energy extracted in the nozzle strongly increases with increase exit-to-throat area ratio. Above 5km these are fairly independent of altitude. At lower altitudes the formation of shocks in the nozzle at high area ratios prematurely ends the energy extraction process. A comparison of energy generated per impulse lost, measured as the difference between impulse without and with MHD generation, yields approximately 6.3 [kJ/N*s] for all area ratios and altitudes.

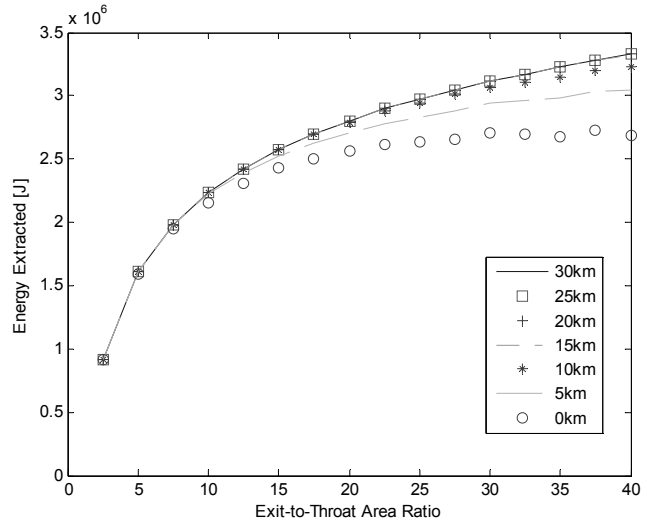

Figure 11: MHD energy generated in the nozzle as a function of exit-to-throat area ratio at different altitudes

At higher altitudes (20 km and above), **Figure 10** shows the impulse per cycle is nearly constant versus given area ratio. More energy is extracted at higher area ratios and this would appear to be the favorable configuration. However, this extra energy cannot be applied because of lower PDE nozzle exit pressures. **Figure 12** plots nozzle exit pressure versus time for different exit-to-throat area ratios at an altitude of 20km. The initial exit pressure for an area ratio of 2.5 is 9 times larger than for the area ratio 22.5 and 5 times greater than for the area ratio 12.5. In order to apply this extracted energy to the bypass-tube section, a shock must be produced to slow the flow in the bypass-tube. Low PDE nozzle exit pressures will not create strong enough (or any) shocks. All altitudes higher than 20km will have identical exit pressure profiles, as the ambient pressure is too low to allow formation of a shock

in the nozzle, which would disrupt blow-down. The results in **Fig. 13** suggest that lower nozzle area ratios could be more appropriate for PDRIME performance improvements.

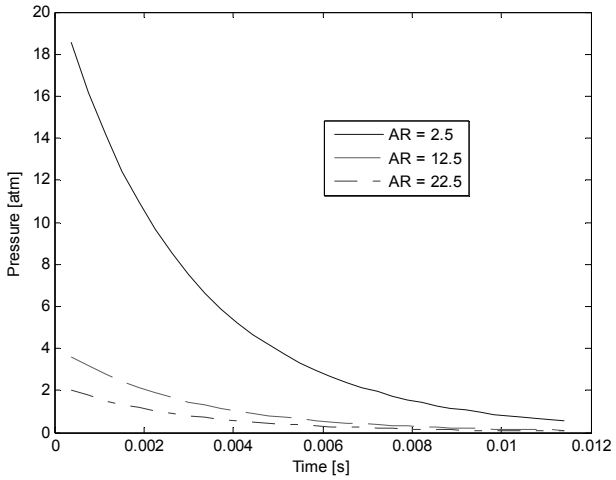

Figure 12. PDE nozzle exit pressure as a function of time for different exit-to-throat area ratios, with MHD generation in the nozzle.

For a given area ratio, the exit pressure can be proportionally increased by increasing the initial chamber pressure. Holding the post-reaction temperature in the chamber constant at 3000K dictates that an increase in initial chamber pressure also increases density proportionally. For all initial chamber pressures where nozzle shocks do not occur, energy extracted behaves identically as a function of area ratio when normalized by initial mass. While PDE impulse per cycle per mass does not behave the same for different initial chamber pressures at the same altitude, the values of specific impulse per cycle, for equal initial chamber to ambient pressure ratios, are equivalent. **Figure 13** plots the specific impulse, Isp, per cycle for initial chamber pressures of 100 and 200 atm at several different altitudes, thus producing different chamber-to-ambient pressure ratios. This result allows quick estimates of extracted energy, impulse per cycle and exit pressure versus time to be obtained for different initial chamber pressures, information that allows computation of PDE impulse.

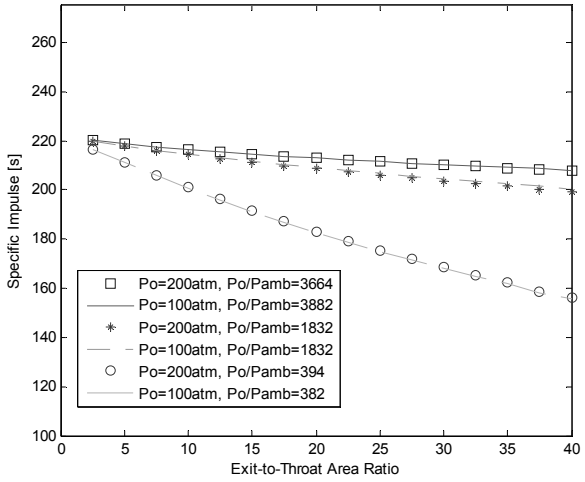

Figure 13. Specific impulse (Isp) per cycle for different initial PDE chamber to ambient pressure ratios.

PDRIME Behavior

To study the overall PDRIME concept, the PDE model results may be used as input for bypass-tube computations. The energy extracted from the PDE is used to power an MHD accelerator in the bypass-tube to create additional thrust. The performance of the whole system is analyzed.

As a 0^{th}-order approximation to this process, the pressure at the downstream end of the bypass-tube is set equal to the recorded PDE exit pressure. In reality the exhaust expands as it exits the PDE nozzle, reducing pressure, thus this 0^{th} order approximation is clearly an over-estimation. The actual phenomena associated with shock transfer from the nozzle to the bypass section are explored separately using 2D transient WENO simulations, discussed later. For now, the best case scenario is assumed. This allows for the validity of this method of augmentation to be shown and important trends to be identified.

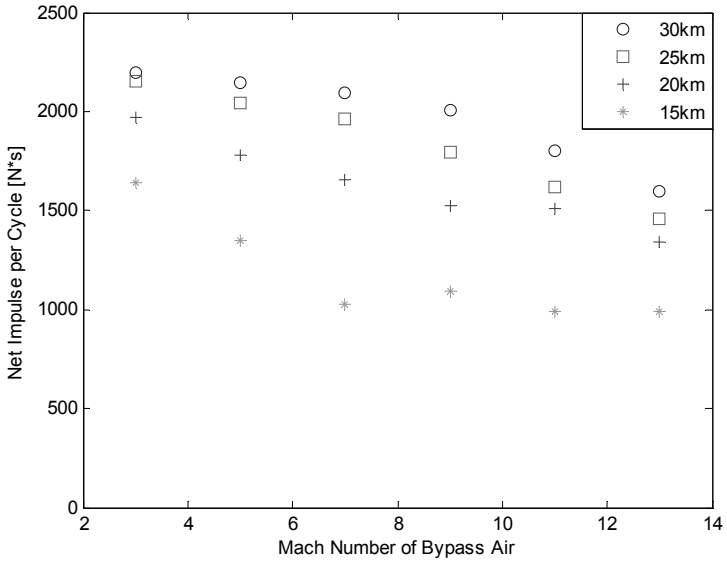

Figure 14: Net impulse of the PDRIME cycle as a function of bypass air Mach number at different altitudes for an exit-to-throat area ratio of 2.5 with a bypass-tube area of $0.09m^2$.

Figure 14 plots the net impulse per cycle of the PDRIME system with an exit-to-throat area ratio of 2.5. Each set of similar marks represent a single PDRIME operating at a fixed altitude at different flight Mach numbers. A net impulse of 2,200N*s is achieved at two different altitudes. One set of operating conditions where this is achieved is at an altitude of 25km where the vehicle is traveling at Mach 3 (the inlet Mach number for the bypass tube). This corresponds to a specific impulse of 489s, more than a 60% increase in impulse over any non-augmented PDE configuration with the same geometry, and shows potential for the PDRIME concept.

There are several factors which contribute to the range of inlet Mach numbers and altitudes for which the PDRIME can be effective. At low flight Mach, the shock in the by-pass tube may not be strong enough to raise the temperature of the air above 3000K in order to be able to achieve thermal ionization of the injected Cesium seed. Yet at large flight Mach numbers (and sufficiently low altitudes) the total pressure of the air stream can become too large, and no shock can enter the bypass-tube. Low altitudes are specially challenging, due to both pressure and temperature jump constraints; at altitudes below 15km the PDRIME system does not appear to be viable, at least for peak PDE chamber pressures of the order of 100 atm.

If the exit pressure of the PDE nozzle is too low, no combination of altitude and Mach number can be successful. Even if a shock can be formed in the bypass section, it will not generate the require temperature gain. **Figure 15,** for example**,** plots the net impulse per cycle of the PDRIME system for only the PDE portion with an exit-to-throat area ratio of 7.5, producing a high Mach number and relatively low pressure at the nozzle exhaust; the resulting impulse is over a factor of two below that for the nozzle with area ratio 2.5, shown in **Fig. 14**. This illustrates the principal difficulty of this system and its need for high nozzle exit pressure. Even when assuming no pressure loss or expansion as the shock travels from the nozzle exit to the downstream end of the bypass section, the net impulse is relatively low; the system is in fact ineffective for exit-to-throat areas exceeding 5.

Weak exit pressures reduce total net impulse in three ways. First, the lower pressures fail to keep the shock in the bypass-tube at higher Mach numbers. Second, the lowered pressure ratio results in less of a temperature jump across the shock entering the bypass section, making seeding difficult. Third, the velocity of the air behind the bypass-tube shock is higher for lower pressures across the entering shock. These higher velocities in the tube require more energy to be applied to produce the same addition impulse.

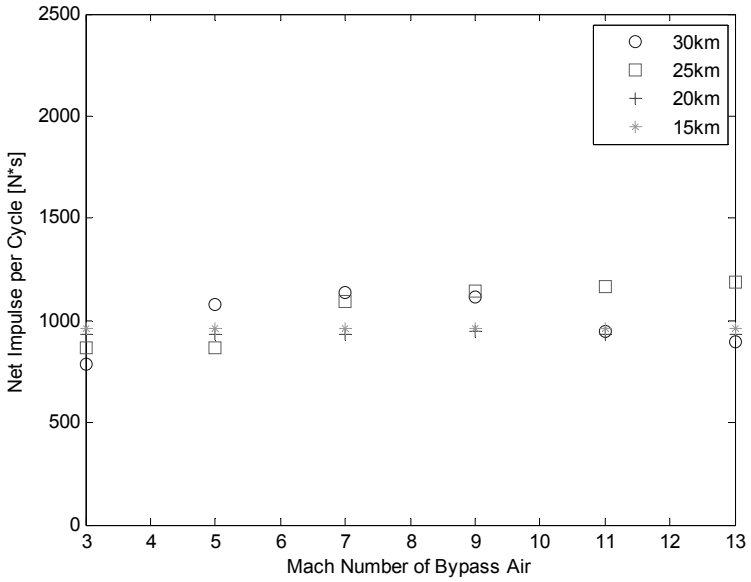

Figure 15: Net impulse of the PDRIME cycle as a function of bypass air Mach number at different altitudes for an exit-to-throat area ratio of 7.5 with a bypass-tube area of 0.09m^2.

The effect of the cross-sectional area of the bypass-tube is now considered. First this will be examined while maintaining the pressure match between the exit of the PDE nozzle and the exit of the bypass-tube. **Figure 16** plots the net impulse of the PDRIME cycles at an altitude of 25km for different cross-sectional areas of the bypass-tube. There is a clear trend indicating that the higher the bypass-tube area, the greater the net impulse of the cycle. Recall that the energy applied is proportional to velocity squared. When MHD acceleration is applied, a Lorentz force is exerted on the air in the nozzle as an equal and opposite force to that which acts on the bypass-tube magnets providing thrust. If the bypass-tube area is large, most of the energy can be applied before the air is accelerated to very high velocities where MHD acceleration becomes inefficient.

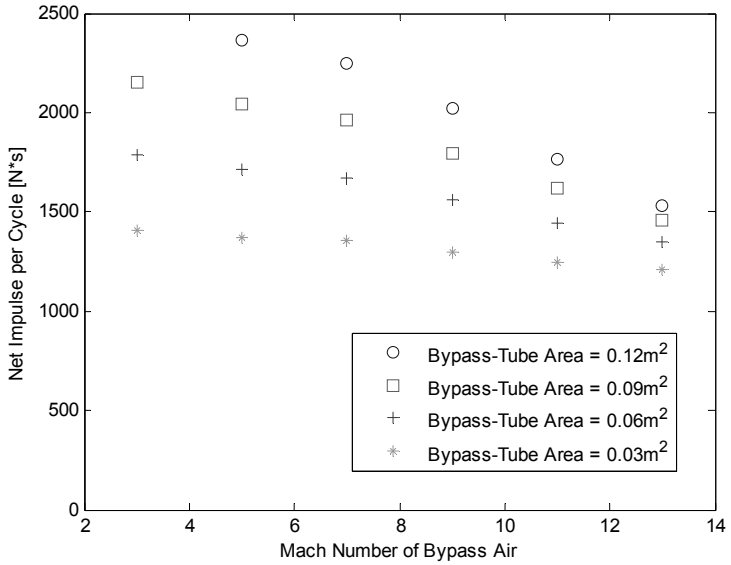

Figure 16: Net impulse of the PDRIME cycle as a function of bypass air Mach number at different bypass-tube areas for an exit-to-throat area ratio of 2.5 at an altitude of 25km, assuming no shock pressure losses associated with flow from the nozzle exit to the bypass exit.

The exit area of the PDE used in **Figure 17** is 0.06m^2. The ability of the nozzle exhaust to send a shock into the bypass-tube will surely be a function of the bypass-tube cross-sectional area. To put a theoretical limit on the bypass-tube area, the energy of the exhaust flow may be quantified. The exit pressure for the quasi-1D simulation represents the entire pressure across the nozzle exit. If this is viewed as a type of energy density, when the exhaust leaves the nozzle and expands vertically across the bypass-tube exit, the maximum pressure that can be present at the bypass-tube exit could be considered to be the "new" energy density, which accounts for this expansion via the relation:

$$p_{by} = \left(\frac{A_e}{A_e + A_{by}} \right) \cdot p_e \tag{18}$$

where p_{by} is the pressure applied to the exit of the bypass-tube accounting for the bypass section's cross-sectional area, A_{by}, and the nozzle exhaust area, A_e. This expression is still an over-estimation of the pressure at the bypass tube exit because it assumes uniform pressure in the transition from the center of the nozzle exit to the top of the bypass-tube. **Figure 17** shows the variation in net impulse for the PDRIME as a function of flight Mach number for different bypass tube cross-sectional areas. In comparison with the more idealized performance shown by the results in **Figure 16**, there is a considerable drop in impulse, in some cases by a factor of two. It is clear that the benefits of larger bypass-tube areas are canceled by the more realistically low average pressure across the tube's exit.

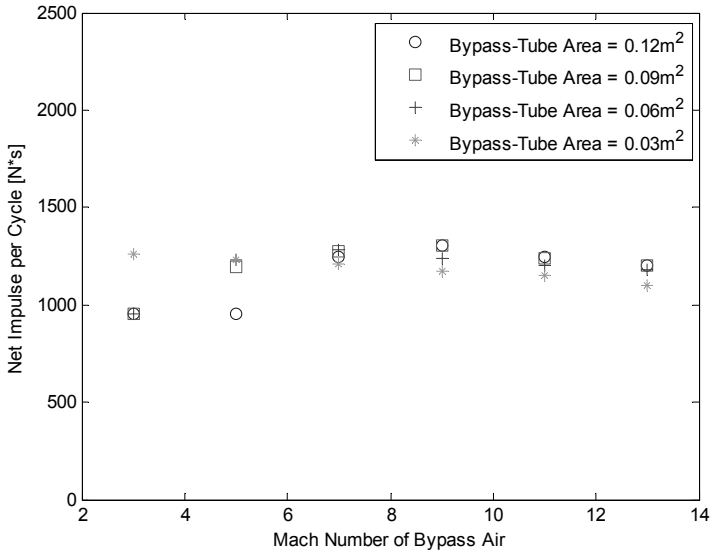

Figure 17: Net impulse of the PDRIME cycle as a function of bypass air Mach number at different bypass-tube areas for an exit-to-throat area ratio of 2.5 at an altitude of 25km, accounting for expansion pressure losses via (18).

As noted previously, a comparison of results from the present simplified blow-down model and quasi-1D nozzle and bypass tube simulations to represent the PDRIME configuration may be made with a more realistic, 2D transient simulation of nozzle, external flow, and bypass tube flow and MHD processes. The transmission of the shock from the nozzle exit to the end of the bypass tube is one obvious phenomenon to explore, given the approximations leading to the differing results in **Figures 16 and 17**. For example, using the 2D transient simulation, it is observed that, for the PDRIME configuration with a nozzle area ratio of 2.5 operating at Mach 10 and at an altitude of 30 km, the shock exiting the nozzle does propagate into the bypass tube and travel upstream. But it is observed in this case that the temperature in the bypass section does not exceed 3000K, a requirement for ionizing seeded Cesium in the tube. Hence a slightly altered PDRIME geometry, one where the upper wall is extended by 0.4 m, is considered in these simulations. This altered system allows the shock to be directed and captured more fully into the bypass tube, and correspondingly allows the temperature there to increase, exceeding 3000K. A comparison of the temperature fields at the same time for both configurations is shown in **Figure 18**. Since the presence of the upper wall would not have an effect in the idealized, inviscid quasi-1D model results, the configuration with the extended upper wall will be used in the 2D simulations for further comparisons.

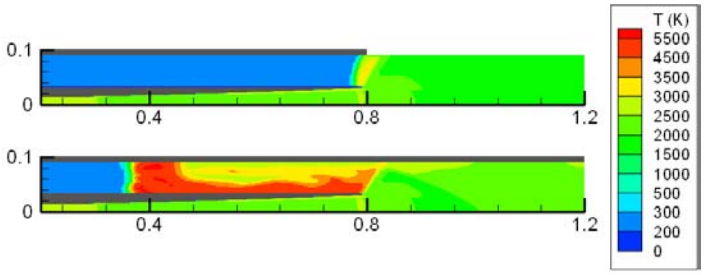

Figure 18: 2D temperature field contours for the upper part of the PDE section and the bypass section, at a time t = 0.6 ms after the start of the blowdown process. Both images show a PDRIME geometry with MHD generation in the nozzle but without energy application in the bypass section, but the lower image has a 0.4 m extension to the upper wall of the bypass section; the upper image does not. The flight Mach number is 10 at altitude 30 km, the nozzle area ratio is 2.5 and the bypass section cross-sectional area is 0.06 m^2.

Figures 19 and 20 show the predicted evolution of the pressure and temperature fields, respectively, for the PDRIME with MHD generation in the nozzle and with energy application in the bypass tube, for a geometry that includes the bypass upper wall extension. A shock structure is observed to transition from the nozzle to the bypass tube before being forced back downstream under the influence of both the Mach 10 inlet flow and the MHD accelerator.

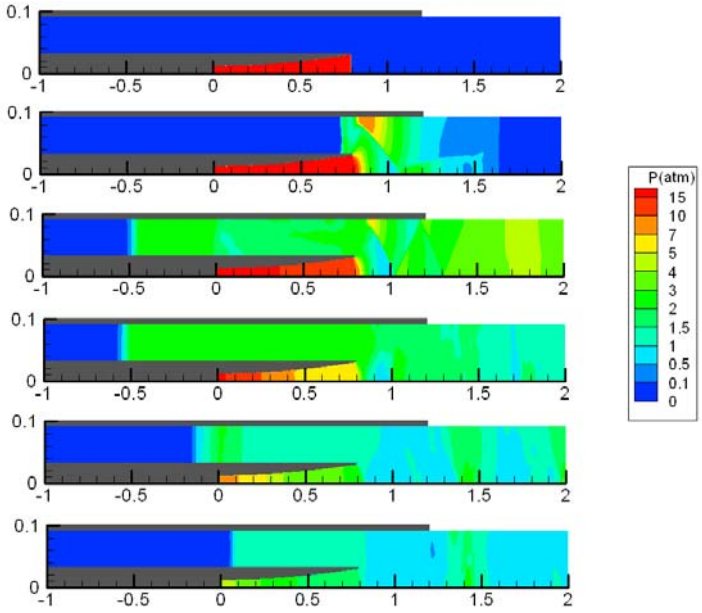

Figure 19: 2D pressure (in atm) field contours for the upper part of the PDE section and the bypass section, at different times after the start of the blowdown process (top to bottom, t = 0.0 ms, 0.2 ms, 2.0 ms, 4.0 ms, 6.0ms, and 8.0 ms). Results are for a PDRIME geometry with MHD generation in the nozzle and with energy application in the bypass section. The flight Mach number is 10 at altitude 30 km, the nozzle area ratio is 2.5 and the bypass section cross-sectional area is 0.06 m^2.

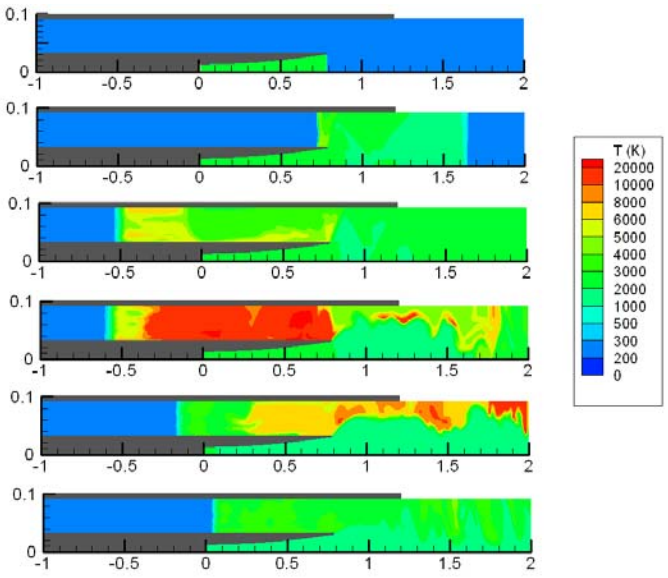

Figure 20: 2D temperature (in K) field contours for the upper part of the PDE section and the bypass section, at different times after the start of the blowdown process (top to bottom, t = 0.0 ms, 0.2 ms, 2.0 ms, 4.0 ms, 6.0ms, and 8.0 ms). Results are for a PDRIME geometry with MHD generation in the nozzle and with energy application in the bypass section. The flight Mach number is 10 at altitude 30 km, the nozzle area ratio is 2.5 and the bypass section cross-sectional area is 0.06 m^2.

The temperature plot in **Fig. 20** illustrates a few sectors of very high-temperature fluid appearing briefly within the bypass tube, a result of the vertical Lorentz forces accelerating the fluid upward and away from the wall, producing a small very low-density region. In reality, viscous forces would likely prevent these regions from forming, while the artificial dissipation inherent to the WENO numerical scheme is likely over-estimating the associated temperature. Since this is an inviscid simulation and since artificial dissipation is necessary for properly capturing shocks, we prevent the temperature from rising to unrealistic degrees by setting the accelerator to induce force on a fluid cell only if its temperature lies below 15000K. The nozzle/bypass exit pressure evolution indicates that after the bypass has begun pushing back the shock, the bypass tube exit pressure p_{by} is roughly half of the nozzle exit pressure, which is consistent with the approximation in eqn. (18). Yet at the earlier stages of the cycle, this loss factor is below the value predicted by eqn. (18).

Magnetic Piston Effects

The Magnetic Piston MHD augmentation concept (see **Fig. 3**) extracts energy in the divergent section of the nozzle and applies a portion of this energy in the combustion chamber to effectively reduce the chamber volume and keep the chamber pressure constant. This avoids the decay in chamber pressure during the blowdown portion of the cycle and thus increases the PDE nozzle exit pressure. This is desired in the PDRIME concept to help keep a shock in the bypass-tube. **Figure 21** plots the PDE nozzle exit pressure as a function of time for a nozzle of area ratio 2.5 operating at an altitude of 25km and compares this exit pressure with that for a PDE operating at similar conditions with a magnetic piston in the chamber. This shows that the PDE exit pressure can be maintained at a constant level instead of decaying. The magnetic piston does shorten the length of the cycle, however (from about 5.5 msec to 3 msec). The higher chamber pressure forces the propellants through the throat faster, and once they are exhausted, the pressure at the exit will rapidly drop to ambient.

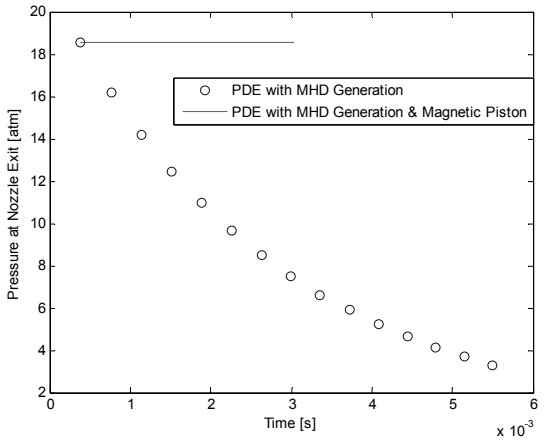

Figure 21 PDE nozzle exit pressure versus time for a with and without magnetic piston operating in the combustion chamber for PDEs with a exit-to-throat area ratio of 2.5.

Figure 22 plots the impulse per cycle of the PDE for a range of exit-to-throat area ratios for several alternative configurations. The square symbols show the results for the PDE itself without bypass and with no MHD generation. The star symbols represent impulse for the PDE with MHD generation in the nozzle but without application of the extracted energy in the bypass tube or for a Magnetic Piston. The solid line shows impulse for the PDE with MHD generation in the nozzle and with partial energy application toward the Magnetic Piston (the remainder is available for application in the bypass tube).

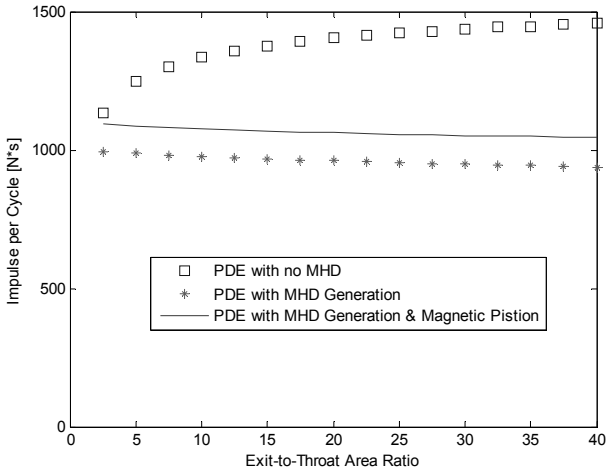

Figure 22: Impulse per cycle at an altitude of 25km of PDEs for a range of exit-to-throat area ratios. Results are shown for the configurations of the PDE with no MHD generation in the nozzle (square symbols), the PDE with MHD generation but without application of the extracted energy in the chamber (star symbols), and MHD generation in the nozzle with partial energy application in the chamber (solid line).

It can be seen from **Figure 22** that in addition to increasing the PDE nozzle exit pressure, the Magnetic Piston does moderately increase the impulse per cycle via energy application in the chamber. When used alone, not in conjunction with a bypass-tube (the PDRIME concept), the Magnetic Piston's main advantage is its shortening the cycle time, thus increasing the PDE's frequency and average thrust. It should be noted that the energy extracted by the MHD generator in the PDE nozzle is affected by application of energy in the Magnetic Piston. At a nozzle to throat area ratio of 2.5, half of the energy extracted in the PDE nozzle is required to power the Magnetic Piston, although less than 10% of the energy extracted is required for an area ratio of 10. While under these conditions the magnetic piston will improve the ability of the PDE nozzle exhaust to shock the bypass-tube air for the PDRIME

concept, the reduction in available energy to accelerate this air reduces the effectiveness of this combined augmentation strategy.

Overall Performance

Although there are clearly differences between the more realistic flow evolution predicted by the 2D PDRIME simulation and the flow predicted the quasi-1D idealized model, the ultimate difference in PDRIME total impulse is not very large. For the PDRIME configuration with MHD generation and acceleration in the bypass section, the differences between the 2D and quasi-1D computed impulses achieved by the end of the cycle are on the order of 10% or lower. The favorable comparisons between relatively inexpensive, quasi-1D simulation results and the more detailed, computationally expensive 2D results suggest that the former model may be quite suitable for quick performance estimates for various PDRIME configurations.

With the more "realistic" 2D flow simulation, there is actually an overall reduction in impulse seen between the case without MHD thrust augmentation and with MHD in the generator/single bypass system, in contrast to the improvement in impulse observed by the quasi-1D simulation. On the other hand, when a second bypass tube is employed in the 2D simulations (not shown here), below the PDE (thus creating a symmetric configuration), there is an approximate 10% improvement in overall impulse observed. Splitting the energy extracted from the PDE nozzle between bypass-tubes above and below the PDE allows the energy to be applied at low velocities, effectively doubling the bypass-tube area without reducing the pressure by its exit. Additional 2D computations described by Zeineh[20] suggest that the added effect of the "magnetic piston" in the chamber, in addition to the PDRIME bypass configuration, can yield further increases in impulse, that is, when energy extraction from the nozzle is used to accelerate flow in the bypass section as well as to accelerate products out of the combustion chamber. Further exploration of these alternative MHD thrust augmentation concepts is ongoing.

Discussion and Conclusions

The present simulations do suggest that the PDRIME system may have some potential for an increase in both impulse and specific impulse, but serious difficulties remain to be resolved . Under idealized, optimal conditions, a possible 60% increase in these performance parameters is observed, but only under the assumption of matching pressure in the nozzle exit and the bypass-tube exit. Under the still idealized energy density conditions assumed via eqn (18) for the area difference between the nozzle exit and the bypass tube, the net improvement is greatly decreased, but comparisons with full 2D simulations suggest that this reduced performance may be a reasonable approximation for actual performance.

The potential benefits of the PDRIME system are mainly seen for low exit-to-throat area ratios, 2.5, due to the reduction in exit pressure from further expansion. Yet the impulse gained by the PDRIME system is strongly dependent on the area of the bypass-tube and the exit pressure applied to its exit. With the idealization of the nozzle exit pressure boundary condition applied to the bypass-tube held constant, larger areas lead to larger impulse improvements, due to the larger amount of energy which can be applied before this acceleration brings the bypass air to high velocities. The bypass-tube area is limited by the decrease in average pressure which occurs as its cross-sectional area is increased. This relationship between average pressure and area makes this concept seem unlikely to create great improvement in net impulse over standard PDEs with larger area ratios. On the other hand, this concept may be able to provide modest impulse gains at high altitudes. At low altitudes the MHD energy transfer mechanisms can be disengaged. Due the low area ratio required for the PDRIME, drag as a result of high ambient pressure could be mitigated. The PDRIME system would thus be best suited for low and high altitude flight.

The PDRIME concept may achieve more of its high potential by inventive methods for increasing the pressure at the exit of the bypass-tube. One method is a extending the top wall of the bypass-tube to trap the exhaust from the nozzle exit, as shown in **Fig. 18** and subsequent images, or by employing a second bypass tube, or by also employing a magnetic piston with the PDRIME, all of which are being explored in greater detail by Zeineh[19]. There are thus a range of alternative configurations to explore in assessing the benefits of MHD thrust augmentation for propulsive devices.

Acknowledgments

The authors wish to acknowledge the technical assistance of Dr. Xing He of the UCLA Department of Radiological Sciences in performing the 2D transient simulations, and by Mr. Lord Cole of the UCLA MAE Department in performing the quasi-1D simulations described in this work. This research has been supported at UCLA by the Air Force Office of Scientific Research under the space power and propulsion program managed by Dr. Mitat Birkan

(Grants FA9550-07-1-0156 and FA9550-07-1-0368). Grant management by Dr. Andrew Ketsdever of the Air Force Research Laboratory at Edwards, CA (AFRL/RZSA) is also gratefully acknowledged.

References

[1] J.-L. Cambier, "MHD Augmentation of Pulse Detonation Rocket Engines", 10th Intl. Space Planes Conf., Kyoto, Japan, April 2001, AIAA paper 2001-1782.
[2] Hill, P. and Peterson, C., **Mechanics and Thermodynamics of Propulsion**, 2nd Edition, Addison-Wesley publishing company, 1992.
[3] Kailasanath, K., and Patnaik, G., "Performance Estimates of Pulse Detonation Engines," ***Proceedings of the Combustion Institute***, Vol. 28, 2000, pp. 595–602.
[4] Cooper, M., and Shepherd, J. E., "The Effect of Nozzles and Extensions on Detonation Tube Performance", AIAA paper 02-3628, 38th AIAA/ASME/SAE/ASEE Joint Propulsion Conference, July, 2002.
[5] Cooper, M. and Shepherd, J. E., "Single Cycle Impulse from Detonation Tubes with Nozzles", ***Journal of Propulsion and Power,*** Vol.24 no.1, 2008, pp. 81-87.
[6] Eidelman, S., Grossmann, W., and Lottati, I., "Review of Propulsion Applications and Numerical Simulations of the Pulse Detonation Engine Concept," ***Journal of Propulsion and Power***, Vol. 7, No. 6, 1991, pp. 857–865.
[7] Wintenberger, E., Austin, J. M., Cooper, M., Jackson, S., and Shepherd, J. E., "An Analytical Model for the Impulse of a Single Cycle Pulse Detonation Engine," ***Journal of Propulsion and Power***, Vol. 19, No. 4, 2003, pp. 22–38; also ***Journal of Propulsion and Power***, Vol. 20, No. 4, 2004, pp. 765–767.
[8] Li, C., and Kailasanath, K., "Partial Fuel Filling in Pulse Detonation Engines," ***Journal of Propulsion and Power***, Vol. 19, No. 5, 2003, pp. 908–916.
[9] Warwick, G., "U.S. AFRL proves pulse-detonation engine can power aircraft", Flight Magazine, March 5, 2008 (online at http://www.flightglobal.com/articles/2008/03/05/222008/us-afrl-proves-pulse-detonation-engine-can-power-aircraft.html).
[10] He, X. and Karagozian, A. R., "Numerical Simulation of Pulse Detonation Engine Phenomena", ***Journal of Scientific Computing***, Vol. 19, Nos. 1-3, pp.201-224, December, 2003.
[11] He, X. and Karagozian, A. R., "Pulse Detonation Engine Simulations with Alternative Geometries and Reaction Kinetics", ***Journal of Propulsion and Power***, Vol. 22, No. 4, pp. 852-861, 2006.
[12] Harten, A., Osher S. J., Engquist, B. E., and Chakravarthy, S. R., "Some Results on Uniformly High-Order Accurate Essentially Nonoscillatory Schemes", ***J. Appl. Numer. Math.***, Vol. 2, pp. 347-377, 1986.
[13] Jiang, G. S. and Shu, C. W., "Efficient Implementation of Weighted ENO Schemes", ***Journal of Computational Physics***, Vol. 126, pp. 202-228, 1996.
[14] Cole, J., Campbell J., Robertson A., "Rocket-Induced Magnetohydrodynamic Ejector – A Single-Stage to Orbit advanced propulsion concept", AIAA Space Programs and Technology Conference, Huntsville, Sept. 1995: AIAA paper 1995-4079.
[15] Cambier, J.-L., "A Thermodynamic Study of MHD Ejectors", 34th AIAA/ASME/SAE/ASEE Joint Propulsion Conference, 1998, AIAA 98-2827.
[16] Hwang, P., Fedkiw, R. P., Merriman, B., Aslam, T. D., Karagozian, A. R., and Osher, S. J., "Numerical Resolution of Pulsating Detonation Waves", ***Combustion Theory and Modelling***, Vol. 4, No. 3, pp. 217-240, September, 2000.
[17] Henrick, A. K., Aslam, T. D., and Powers, J. M., "Mapped Weighted Essentially Non-oscillatory Schemes: Achieving Optimal Order near Critical Points," ***Journal of Computational Physics***, Vol. 207, No. 2, 2005, pp. 542–567.
[18] J.-L. Cambier, "Preliminary Model of Pulse Detonation Rocket Engines", 35th AIAA/ASME/SAE/ASEE Joint Propulsion Conference, Los Angeles, June 1999, AIAA paper 1999-2659.
[19] Shu, C. W., and Osher, S., "Efficient Implementation of Essentially Non-Oscillatory Shock Capturing Schemes II", ***Journal of Computational Physics***, Vol. 83, pp. 32-78, 1989.
[20] Zeineh, C., "Numerical Simulation of Magnetohydrodynamic Thrust Augmentation for Pulse Detonation Rocket Engines", Ph.D. prospectus, UCLA Department of Mechanical and Aerospace Engineering, 2008.

JOURNAL OF PROPULSION AND POWER
Vol. 28, No. 1, January–February 2012

Appendix B

Magnetohydrodynamic Augmentation of Pulse Detonation Rocket Engines

Christopher F. Zeineh,* Lord K. Cole,† Timothy Roth,‡ and Ann R. Karagozian§
University of California, Los Angeles, Los Angeles, California 90095-1597
and
Jean-Luc Cambier¶
U.S. Air Force Research Laboratory, Edwards Air Force Base, California 93524

DOI: 10.2514/1.B34146

Pulse detonation engines are the focus of increasing attention due to their potentially superior performance over constant-pressure cycle engines. Yet, due to its unsteady chamber pressure, the pulse detonation engine system will either be over- or underexpanded for the majority of the cycle, with energy being used without maximum gain. Magnetohydrodynamic augmentation offers the opportunity to extract energy and apply it to a separate stream where the net thrust can be increased. With magnetohydrodynamic augmentation, such as in the pulse detonation rocket-induced magnetohydrodynamic ejector concept, energy could be extracted from the high-speed portion of the system (e.g., through a magnetohydrodynamic generator in the nozzle) and then applied directly to another flow or portion of the flow as a body force. This paper explores flow processes and the potential performance of such propulsion systems via high-resolution numerical simulations. In the pulse detonation rocket-induced magnetohydrodynamic ejector, at the appropriate point in the pulse detonation engine cycle, the magnetohydrodynamic energy extracted from the nozzle is applied in a separate bypass tube by a magnetohydrodynamic accelerator, which acts to accelerate the bypass air and potentially impart an overall net positive thrust to the system. An additional magnetic piston applying energy in the pulse detonation engine chamber can also act in concert with the pulse detonation rocket-induced magnetohydrodynamic ejector for separate or additional thrust augmentation. Results show potential performance gains under many flight and operating conditions (as high as a 6% increase in total impulse per cycle) but with some challenges associated with achieving these gains, suggesting further analysis and optimization are required.

Nomenclature

A	=	cross-sectional area
$\mathbf{B}$	=	magnetic field
c	=	speed of sound
$\mathbf{E}$	=	electric field
E	=	energy
$\mathbf{F}_{\text{body}}$	=	body force
F_L	=	Lorentz force
I	=	impulse
$\mathbf{J}$	=	current density
K_x	=	loading factor (x component)
K_y	=	loading factor (y component)
$\dot{m}$	=	mass flux
p	=	pressure
R_m	=	magnetic Reynolds number
T	=	thrust
$\mathbf{u}$	=	velocity vector
x, y, z	=	streamwise, transverse, and axial coordinates
β	=	Hall parameter
γ	=	ratio of specific heats
ρ	=	density
σ	=	electrical conductivity
$\dot{\Omega}_{Cs}$	=	cesium atom reaction source term
$\dot{\Omega}_{Cs^+}$	=	cesium ion reaction source term

Superscript

$*$	=	throat value

Subscripts

byp	=	bypass
cham	=	chamber value
conv	=	converging section
div	=	diverging section
e	=	exit value
open	=	open area downstream of nozzle exit
uwall	=	upper wall downstream of nozzle exit
0	=	initial value

Received 9 October 2010; revision received 20 April 2011; accepted for publication 23 May 2011.

*Graduate Student Researcher, Department of Mechanical and Aerospace Engineering; currently Technical Staff Member, The Aerospace Corporation, El Segundo, California 90245-4609.
†Graduate Student Researcher.
‡Graduate Student Researcher; currently Technical Staff Member, Northrop Grumman Electronic Systems, Azusa, California 91702.
§Professor; ark@seas.ucla.edu. Fellow AIAA (Corresponding Author).
¶Senior Scientist, Aerophysics Branch.

I. Introduction

ROBUST propulsion systems for advanced high-speed airbreathing and rocket vehicles are critical to the future of military missions, including those for global/responsive strike and assured access to space. A novel combined cycle propulsive concept, the pulse detonation rocket-induced magnetohydrodynamic ejector (PDRIME) proposed by Cambier et al. [1], is one of a number of alternative magnetohydrodynamic (MHD) thrust augmentation ideas that could have promise for application to a wide range of advanced propulsion systems. Taking advantage of the periodic engine cycle associated with the pulse detonation rocket engine (PDRE), the PDRIME involves periodic temporal energy bypass to a seeded airstream, with MHD acceleration of the airstream for thrust enhancement and control. The range of alternative MHD-augmented propulsion configurations that could be employed suggests that the

PDRIME type of concept could be applied to supersonic or hypersonic airbreathing systems, space power production for remote sensing systems, and other potential military systems for the mid- to far terms. This paper explores the fundamental flow processes associated with the PDRIME and modifications thereof via numerical simulation.

Liquid rocket engines typically employ a constant pressure reaction, where reactants are continually fed at high pressure into the combustion chamber and a nozzle expands and exhausts the flow, generating thrust for the vehicle. The general expression for the force or thrust acting on an object takes the form

$$\mathbf{F}_{\text{body}} = \frac{\partial}{\partial t}\iiint_V \rho\mathbf{u}\,\mathrm{d}V + \iint_S (\rho\mathbf{u}\cdot\mathrm{d}\mathbf{S})V + \iint_S p\,\mathrm{d}\mathbf{S} \qquad (1)$$

where ρ is the local density, $\mathbf{u}$ is the local velocity vector, and $\mathbf{F}_{\text{body}}$ is the sum of the thrust and any forces acting from outside the control volume over which the integrals are calculated; in the case of the present studies, $\mathbf{F}_{\text{body}}$ includes MHD forces. The control volume can be constructed either around the rocket's interior walls or around the nozzle exit, encapsulating all fluid therein. The former method calculates MHD forces as body forces, while the latter calculates the changes in momentum resulting from these forces. Both methods, which we call the pressure flux and momentum flux methods, produce the same results [2], and we choose to use the pressure in the present study. For a steady flow rocket engine with a solid back wall, Eq. (1) reduces to the standard expression for rocket thrust:

$$T = \dot{m}u_e + (p_e - p_a)A_e \qquad (2)$$

where $\dot{m}$ is the mass flux of gas exiting the nozzle, u_e is the exhaust velocity, A_e is the nozzle exit cross-sectional area, p_a is the ambient pressure, and p_e is the pressure at the exit plane of the nozzle. The total impulse I over the course of an engine cycle is calculated by integrating thrust over time t. The maximum thrust [3] for an engine occurs when the exhaust gases are expanded to the point where the pressure at the exit of the nozzle is equal to the ambient pressure in Eq. (2). Further expansion of the gas in the nozzle will reduce the thrust, as the ambient pressure will then exceed the exhaust pressure, creating pressure drag. This added drag can outweigh momentum gains arising from the further acceleration of the flow from the nozzle, i.e., the increase in exhaust velocity. Underexpansion in the nozzle will result in lower than optimal thrust as the maximum momentum gains are not realized. MHD augmentation is in part designed to recapture some of these losses through modification of the exhaust pressure.

One alternative and theoretically more efficient configuration to the traditional rocket engine is the pulse detonation engine (PDE), a subset of which is the PDRE. The PDE operates in a cycle wherein reactants are mixed into the combustion chamber at low pressure, the mixture is ignited, and a detonation wave propagates across the chamber, raising the pressure and temperature and creating a constant-volume reaction, which is more efficient than a constant pressure reaction [4]. After the detonation wave (or shock wave, after reactants have been consumed) exits the nozzle, a reflected expansion wave propagates into the chamber, lowering the overall pressure throughout the chamber and, upon reflection at the thrust wall, allows reactants to be drawn into the chamber. The reflection of the expansion wave at the nozzle exit results in a compression wave, which can be strengthened to become a shock, igniting reactants in the chamber as a detonation and starting the process once again. A number of studies have explored the reactive flow and performance characteristics of PDEs of various geometries [4–8]. The PDE was recently tested for the first time in flight on a Scaled Composites Long-EZ aircraft [9], with four PDE tubes operating at a cycle frequency of 20 Hz.

In the past, our group at the University of California, Los Angeles [10,11], has explored the influence of PDE geometry, reaction kinetics, and flow processes using high-order numerical methods. A fifth-order weighted essentially nonoscillatory (WENO) scheme [12,13] is used for spatial integration of the reactive Euler equations, with a third-order Runge–Kutta time integration in the case of simplified reaction kinetics; a stiff ordinary differential equation solver was used for temporal integration in complex kinetics simulations. While the simulations using complex kinetics provide useful quantitative data, the simulations with reduced kinetics (a single-step reaction) can in fact provide very similar quantitative performance results.

In general, two different methods could be used to generate thrust for the PDRE. The first involves a straight or slightly contoured nozzle, as examined for the PDE. The main goal of this configuration is to exploit the thrust generation from the reflection of the wave, the ignition of the detonation near the thrust wall, and its propagation through the device, as described above. The second approach is more similar to a constant-pressure rocket. Here, the nozzle throat area A_t is very small: small enough to prevent the main detonation wave from escaping the chamber. This creates multiple reflected compressive waves in the chamber that homogenize the chamber pressurization, resulting in an approximately constant-volume reaction. During the blowdown period, the reactants are driven out from the chamber and through the nozzle. Similar to the constant-pressure rocket, the exhaust gases are expanded, increasing the velocity and reducing the pressure. The difference between this type of PDRE and a constant-pressure rocket is that in the PDRE, the chamber pressure is decreasing throughout the blowdown period as mass is ejected from the chamber, with no immediate replacement. New reactants are added to the combustion chamber once the pressure has been reduced to a specified value, and then the cycle is repeated.

Because of the unsteady nature of the chamber pressure, however, a PDRE nozzle can only be perfectly expanded briefly within a blowdown period. This implies suboptimal use of energy to attain this condition for most of the cycle. At low altitudes, nozzles with large area ratios are subject to large drag forces [$p_a > p_e$ in Eq. (2)], while nozzles with relatively smaller exit areas will be underexpanded for the majority of blowdown. Whether or not the configuration includes a converging section, the lack of perfect matching conditions essentially negates the benefits of a constant-volume combustion [14].

Ejectors are often used to transfer energy from one stream to another stream, providing an additional source of thrust, especially for an airbreathing engine. Ejectors have been shown to produce overall thrust gains when energy is taken from a high-velocity flow and transferred to a low energy stream (in the ejector) that has a high mass flow rate. In the present application for the PDRE, energy can be extracted from the nozzle when the marginal decreases in thrust are small and added to a bypass airflow that acts as an ejector to assist in augmentation of the thrust. Ejectors typically transfer energy between streams through shear stress between separate flow streams, where a portion of the main flow is diverted into a channel to mix with the lower velocity flow. The drawback of this method is that the ability to transfer energy is limited by the contact area and the slow rate of viscous transport between the two streams. At large velocities, shear layer thicknesses are small, leading to the necessity for large channels and/or large interfacial surfaces such as lobed shapes [15] for mixing, which add weight to the vehicle.

In contrast, if MHD forces are applied as body forces to the ejector flow, affecting the entire flowfield immediately, there can be benefits. This could reduce the length of the bypass tube and time necessary for complete energy transfer as well as providing the flexibility of energy extraction and application, since the applied fields can be varied [16]. One possible configuration attaches a converging–diverging nozzle to the combustion chamber of a PDRE with a bypass tube. Just as the AJAX concept [17] proposes to divert energy from an inlet flow by an MHD generator before reapplying it after the combustor via an MHD accelerator, this energy bypass concept could also be applied to the PDRE [16].

A generic configuration for this concept, the PRDIME, is shown in Figs. 1a and 1b , where the interaction between a magnetic field and an electrically conducting fluid flow (MHD) takes place. For the present applications, magnetic and electric fields are both applied normal to each other in the z and y directions, respectively, and

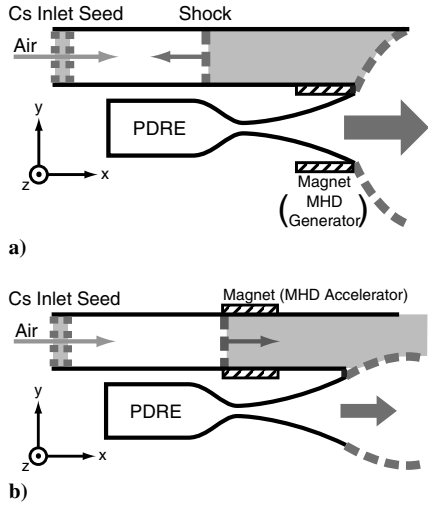

Fig. 1 Schematics of the PDRIME concept: a) During the initial portion of the cycle. Overpressure at the nozzle exit allows an upstream propagating shock (dashed line) to enter the bypass section. This shock slows and raises the temperature of the seeded air in the bypass channel, shown in the shaded portion of the figure. A magnet adjacent to the nozzle extracts energy from the flow. b) In the latter part of the cycle, during blowdown. As the pressure at the nozzle exit drops, exhaust of the compressed and heated air from the bypass channel takes place. Power is applied via the magnets shown, resulting in the MHD acceleration of the air slug in the bypass channel.

normal to the fluid velocities (which are, in the nozzle and bypass tube, in the x direction). In the expanding (divergent) section of the nozzle, magnetic and electric fields are applied to extract energy from this portion of the flow. A bypass tube sits adjacent to the engine. Ambient air enters this tube and is accelerated by an MHD accelerator powered by the energy extracted from the nozzle. A gain in thrust is realized by extracting energy from the nozzle, which would otherwise be used inefficiently, and by applying the energy to the air in the bypass tube. A planar design is used here to achieve a spatially uniform magnetic field, only in the z direction, by placement of magnets above and below each region.

The evolution of the flow cycle for the PDRIME is shown in Figs. 1a and 1b. Because a PDRE can be designed to have a converging–diverging nozzle such that the initial peak pressure in the combustion chamber results in pressure at the nozzle exit plane that is well above ambient, a contact surface originates at the nozzle lip and extends to the upper wall of the bypass tube, creating conditions for an unsteady shock with propagates into the bypass channel, as shown in Fig. 1a. If the air in the bypass channel is initially at high Mach number, this traveling shock brings the air to a high temperature. If a species such as cesium can be added to the flow, high conductivity can be attained by thermal ionization. The cesium seeded into the nozzle is assumed to be premixed with the reactants in the chamber, while the cesium for the bypass is assumed to be seeded uniformly across the width of the tube. The ionization potential of cesium is approximately 3.6 eV, which is low enough to provide sufficient conductivity to operate the MHD components operating within the 2000 K range. Hence, the shock generates a slowly moving slug of high-temperature air, shown as the shaded section in Fig. 1a, that can be more easily ionized. This approach eliminates the need for nonequilibrium ionization, as in the AJAX concept.

As the pressure at the nozzle exit drops during blowdown, the shock then slows down, and eventually, the ionized air in the bypass section starts to move downstream. At this point, electrical power can be applied via an MHD accelerator to eject the air slug from the bypass tube, and thus generate thrust (Fig. 1b). In the present simulations, approximately 3000 J are required to accelerate each gram of air trapped within the bypass section. The procedure can then be repeated at each cycle. One only needs to design the nozzle such that the flow is underexpanded during the initial part of the blowdown phase. In fact, there may be a self-adjusting process at work, depending on PDRE nozzle design and altitude, as outlined by Cambier [14]. While at launch, the nozzle exit pressure is equal to ambient and there is no interaction with the bypass air; as the vehicle accelerates and gains altitude, the nozzle becomes progressively underexpanded, so that eventually a strong shock can be generated for the bypass channel to ionize the seeded air, and the ejector operates. This is one of several configurations in which the PDRIME concept could be used for thrust augmentation in advanced propulsion systems.

As noted above, the MHD generator is located in the diverging section of the nozzle where the velocity is largest, so that the expansion of the fluid counteracts some of the velocity reduction arising from the Lorentz (drag) force acting in the generator. The Lorentz force acts on the conducting fluid carrying a current of density $\mathbf{J}$ in a magnetic field of strength $\mathbf{B}$. This force is given in general by

$$\mathbf{F}_L = \mathbf{J} \times \mathbf{B} \tag{3a}$$

or for the orientation of vectors in Fig. 1 by

$$F_{L,x} = J_y B_z \tag{3b}$$

The current density $\mathbf{J}$ is an important property of the MHD flow system that is related to electric and magnetic fields, $\mathbf{E}$ and $\mathbf{B}$, respectively, and the velocity vector $\mathbf{u}$ via Ohm's law:

$$\mathbf{J} = \sigma(\mathbf{E} + \mathbf{u} \times \mathbf{B}) \tag{4}$$

where σ is the electrical conductivity (with units of reciprocal ohms per meter). For the PDRIME orientation described in Fig. 1, this reduces to a current density with a component in the y direction only:

$$J_y = \sigma(E_y - uB_z) \tag{5}$$

where E_y is the electric field acting in the y direction, and B_z is the magnetic field acting in the z direction. The magnetic field is assumed constant, which implies a low rate of field convection compared with field diffusion. As an analogy to hydrodynamics, the ratio of these two rates is given by the magnetic Reynolds number R_m:

$$R_m = \mu\sigma uL \tag{6}$$

where μ is the permeability of free space (units of newtons per squared cross-sectional area), u is the velocity magnitude, and L is a characteristic length scale. The motion of the electrically conducting fluid induces an additional magnetic field, but for low magnetic Reynolds numbers, this is negligible and the magnetic field may be considered constant. A low magnetic Reynolds number approximation is assumed for our MHD applications. The maximum R_m for the PDRIME configuration is in the vicinity of the nozzle exit, where the fluid velocity is largest in the presence of active magnetic fields; in this region, we estimate R_m to be approximately 0.16.

Note that, with a constant and positive magnetic field, the direction of the current density, and thus of the Lorentz force, depends on the relative magnitudes of E_y and uB_z from Eq. (5). We employ Cambier's definition of a loading factor K to compare these strengths [14]:

$$K_x = \frac{E_x}{\beta u B_z} \qquad K_y = \frac{E_y}{uB_z} \tag{7}$$

where β is the Hall parameter, defined as the ratio of the cyclotron frequency to the total elastic collision frequency of the electrons. When $K_x = 0$, the generator is of the Faraday type, and when $K_y = 0$, it is of the Hall type. For the present study, we consider only Faraday generators; thus, we set E_x and, in turn, K_x to zero. We likewise assume no induced electromagnetic fields are present and no magnetization, so the Hall effect is absent.

For a Faraday configuration, $\mathbf{E}$ and $\mathbf{u} \times \mathbf{B}$ are defined such that they are antiparallel and that K_y is always positive. In all cases

presented in this study, B_z is assumed positive in the z direction throughout all MHD component domains, if not necessarily uniform. Presuming $u > 0$, then E_y and K_y are both positive. If $u < 0$, as can occur within the bypass flow, then $\mathbf{u} \times \mathbf{B} = -uB_y > 0$, so E_y becomes negative while K_y remains positive.

If $u > 0$ and $0 < K_y < 1$, then the current density in the y direction is negative. According to Eq. (3b), this results in a Lorentz force opposing the fluid motion, reflecting the behavior we expect of the nozzle generator. If $u > 0$ and $K_y > 1$, then the current density is positive and the resulting Lorentz force accelerates the fluid, which we require in the bypass accelerator. However, if the shock-induced stagnation of the bypass flow results in local velocities flowing upstream, we would prefer to locally decelerate rather than accelerate this flow. Thus, within these limited domains where $u < 0$, we define $0 < K_y < 1$ such that the local bypass MHD components temporarily act as generators.

For all MHD application, energy effects are governed by the current density multiplied by the electric field. This energy source term can be decomposed as follows:

$$\mathbf{J} \cdot \mathbf{E} = \frac{\mathbf{J}^2}{\sigma} + \mathbf{u} \cdot (\mathbf{J} \times \mathbf{B}) \tag{8}$$

where the terms on the right-hand side represent the dissipative heating and mechanical power, respectively. When $u > 0$ and $0 < K_y < 1$, the mechanical power is negative because energy is being extracted from the fluid. Thus, in the PDRIME configuration, for MHD generation in the nozzle operating under such parameters, energy is extracted from the fluid with a negative Lorentz force. In the accelerator (bypass section), a positive Lorentz force and application of energy takes place (Fig. 1a), with $K_y > 1$. Regardless of the loading factor, the ohmic heating will always be a positive term, representing a loss in both cases. Ignoring dissipative effects, we see that the Lorentz force scales with velocity, while the energy associated with both generation and acceleration scales with velocity squared. For this reason, maximum thrust gain is achieved when energy is extracted from high-velocity flows, as in the nozzle, and applied to low-velocity flows [16].

For $0 < K_y < 1$, the goal is to extract maximum power (K_y) with minimal dissipation (K_y^2). The optimal loading factor magnitude K_y for MHD generation has been demonstrated [14] to be 0.5. The energy generated in the nozzle is then applied in the bypass tube by an MHD accelerator. Any value $K_y > 1$ will accelerate the flow. We arbitrarily choose $K_y = 1.5$ to balance efficiency and effectiveness. However, if a negative flow is detected in that location in the course of the cycle, $K_y = 0.5$ in the accelerator mode, is assumed in the present study in order to help decelerate it.

Another alternative configuration by which MHD can be used to augment thrust generated by a PDRE is one in which energy extracted by MHD from the high-velocity flow in the expansion portion of the nozzle can be applied to the combustion chamber in order to accelerate combustion products from the chamber while allowing a fresh mixture of reactants to fill the available volume. Creation of this magnetic piston in the chamber, as outlined in Cambier [14], can be used to push combustion products from the chamber while allowing a fresh mixture of reactants to fill the available volume. Such a configuration is shown in Fig. 2. As noted above, extraction of energy from a high-velocity stream and delivered to a low-velocity stream is one mechanism for thrust augmentation; hence, a configuration such as that in Fig. 2 can theoretically lead to performance gains. As indicated by Cambier [14], thrust increases with an increasing fraction of energy extracted from the flow and with reduction in the filling time. When blowdown and filling processes are allowed to overlap via appropriate application of the magnetic field, filling time is effectively reduced, leading to a large increase in average thrust. The magnetic piston concept, separately as well as in concert with the PDRIME with bypass flow, will be explored here.

The goal of the present research involves use of a simplified model for the blowdown portion of the PDRE, coupled to a more detailed simulation of the relevant MHD processes in the nozzle and/or adjacent bypass sections, as a means of predicting overall PDRIME and magnetic piston phenomena and performance parameters. The model has been validated using detailed numerical simulations of PDRE processes [2,11] so that projections for optimal performance and operating conditions may be made.

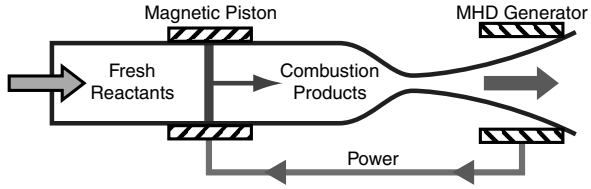

Fig. 2 Schematic of the magnetic piston concept. The piston accelerates the combustion products out of the chamber in such a way that constant pressure and temperature are maintained at the throat. Fresh reactants are simultaneously drawn in to replace the evacuated products.

II. Description of the Pulse Detonation Rocket-Induced Magnetohydrodynamic Ejector Model and Simulation Procedure

A. Framework and Blowdown Model

Because of the large number of available system parameters in the PDRIME, a rapid simulation technique is required: one that is simpler than a detailed numerical simulation of flow and reactive processes in the PDRE and adjacent flow sections. Resolution of detonations constitutes a major computational cost; the sharp gradients and large sound speeds present in the PDE greatly reduce the time step and require finer spatial resolution [18,19]. For the PDRE configuration, after the shock waves have subsided in the chamber, the properties of the fluid within the combustion chamber are mostly uniform, resembling the products of a constant-volume reaction. For these reasons, a blowdown model was developed by Cambier [20] to predict chamber properties as a function of time after a constant-volume reaction. Intuitively, a small throat also restricts the mass flow of propellants out of the chamber, which leads to a slow decay of chamber pressure, increasing the blowdown period.

Cambier's model [20] uses a single computational cell to represent a combustion chamber filled with postconstant volume reaction products at high pressure and temperature. The converging section of the nozzle is also represented by a single-cell approximation. An adiabatic solution for the throat conditions for every time step is determined based on the combustion chamber properties and the assumption that the throat is choked. The divergent section, throat to exit, is fully discretized to account for the MHD coupling, as is the entire bypass tube. To validate certain aspects of the engine cycle and flow processes, comparisons between the blowdown model and full two-dimensional (2-D) transient numerical simulations are made.

The blowdown evolutions of the stagnation variables in the chamber are calculated as functions of specific heat ratio and time [14]:

$$p_0 = \hat{p}_0[f(t)]^{\gamma/(\gamma-1)} \tag{9a}$$

$$\rho_0 = \hat{\rho}_0[f(t)]^{1/(\gamma-1)} \tag{9b}$$

$$T_0 = \hat{T}_0[f(t)] \tag{9c}$$

where the caret (^) indicates the value at time $t = 0$, and the subscript 0 indicates chamber stagnation conditions. The function $f(t)$ has an analytic solution which takes the form

$$f(t) = \frac{1}{(1 + \nu t)^2} \tag{10a}$$

where

$$\nu = \frac{(\gamma-1)\Gamma c_0}{2L_{\text{cham}}}\frac{A^*}{A_{\text{cham}}} \tag{10b}$$

and

$$\Gamma = \left(\frac{2}{\gamma+1}\right)^{(\gamma+1)/[2(\gamma-1)]} \tag{10c}$$

and where c_0 is the chamber fluid's speed of sound, γ is the specific heat ratio, L_{cham} is the chamber length, A^* is the cross-sectional area at the nozzle throat, and A_{cham} is the cross-sectional area of the chamber. All simulations in the present study use sufficiently small time steps such that, within a given time step, we assume the values of γ and Γ in the chamber to be constant, in accordance with the Cambier blowdown model [20]. Between time steps, γ and Γ are updated as new chamber properties are calculated to account for variation over the extended temperature range observed throughout the engine cycle. The caret variables in Eqs. (9a), (9c), and (9c) become the values at current time level t^n, and t becomes the time step at the next time level $\mathrm{d}t = t^{n+1} - t^n$.

B. Discretization of Nozzle and Bypass Sections

The diverging section of the nozzle and the bypass tube are divided into cells. The 2-D transient equations that govern this flow in conservative form are similar to those in He and Karagozian [10,11] but with additional species terms (to simulate air, water vapor exhaust, cesium atoms, and cesium ions), an ionization/recombination source term $S(\mathbf{U})$ when we simulate the injection of cesium, and an MHD source term $M(\mathbf{U})$ denoting related momentum and energy effects:

$$\mathbf{U}_t + \mathbf{F}(\mathbf{U})_x + \mathbf{G}(\mathbf{U})_y = \mathbf{S}(\mathbf{U}) + \mathbf{M}(\mathbf{U}) \tag{11}$$

$$\mathbf{U} = \begin{pmatrix} \rho \\ \rho u \\ \rho v \\ E \\ \rho Y_{Cs} \\ \rho Y_{Cs^+} \\ \rho Y_{\mathrm{H_2O}} \end{pmatrix} \qquad \mathbf{F}(\mathbf{U}) = \begin{pmatrix} \rho u \\ \rho u^2 + p \\ \rho uv \\ (E+p)u \\ \rho u Y_{Cs} \\ \rho u Y_{Cs^+} \\ \rho u Y_{\mathrm{H_2O}} \end{pmatrix}$$

$$\mathbf{G}(\mathbf{U}) = \begin{pmatrix} \rho v \\ \rho uv \\ \rho v^2 + p \\ (E+p)v \\ \rho v Y_{Cs} \\ \rho v Y_{Cs^+} \\ \rho v Y_{\mathrm{H_2O}} \end{pmatrix} \tag{12}$$

$$S(\mathbf{U}) = \begin{pmatrix} 0 \\ 0 \\ 0 \\ 0 \\ \dot{\Omega}_{Cs} \\ \dot{\Omega}_{Cs^+} \\ 0 \end{pmatrix} \qquad M(\mathbf{U}) = \begin{pmatrix} 0 \\ (\mathbf{J}\times\mathbf{B})_x \\ (\mathbf{J}\times\mathbf{B})_y \\ \mathbf{J}\cdot\mathbf{E} \\ 0 \\ 0 \\ 0 \end{pmatrix} \tag{13}$$

where $\dot{\Omega}_{Cs}$ and $\dot{\Omega}_{Cs^+}$ are the cesium reaction source terms for cesium atoms and ions, respectively, which take the Arrhenius form

$$\begin{pmatrix} \dot{\Omega}_{Cs} \\ \dot{\Omega}_{Cs^+} \end{pmatrix} = \frac{\mathrm{d}}{\mathrm{d}t}\begin{pmatrix} [Cs] \\ [Cs^+] \end{pmatrix} = \begin{pmatrix} -k_f[Cs][M] + k_r[Cs^+][M][e^-] \\ k_f[Cs][M] - k_r[Cs^+][M][e^-] \end{pmatrix} \tag{14}$$

where k_f and k_r are the forward the reverse reaction rates; and $[Cs]$, $[Cs^+]$, $[Cs^+]$, $[M]$, and $[e^-]$ are the molar concentrations of cesium atoms, cesium ions, third bodies, and electrons, respectively. Since this is a weakly ionized flow, we also assume that $[e^-] \approx [Cs^+]$. The total energy term E is given by

$$E = \frac{p}{\gamma-1} + \frac{\rho(u^2+v^2)}{2} + \rho q Y_{Cs^+} \tag{15}$$

where the heat release per unit mass $q = 2.827 \times 10^6$ J/k (or 375.7 kJ/mol, the first ionization energy of cesium) and is affixed to the mass fraction of cesium ions since ionization is endothermic and no other reactions take place. As in previous studies, the current simulations assume inviscid flow; at the high-speed conditions at which the PDRIME operates, boundary layers are very thin compared with the dimensions of the PDRIME. For MHD flows, the inviscid assumption is somewhat more approximate, especially for accelerator operation, in that joule heating in the boundary layers is a key contributor to poor MHD accelerator efficiency. Nevertheless, given that the boundary layers are of the order of 3% of the bypass tube width, the inviscid approximation is reasonable for the present performance calculations.

Transient flow in the bypass tube involves a shock created by the nozzle exhaust, traveling into the bypass exit and propagating upstream into a high-speed flow (see Fig. 1a). Quasi-steady forward-marching methods are thus not adequate for these regimes, especially since this method has a singularity when the flow Mach number is equal to 1. For these reasons, a fully transient numerical scheme must be used to simulate flow in the bypass tube.

In simulating flow in the bypass tube, the WENO method [12] is used to approximate spatial derivatives, with a stencil including upstream and downstream cells. WENO is an adaptation of the essentially nonoscillatory method [13] that uses the conservation laws for high-order accuracy with shock capturing capabilities. Artificial viscosity is added via the local Lax–Friedrichs scheme [10] to avoid entropy violation and reduce dispersion while introducing dissipation. Temporal integration is performed by a third-order Runge–Kutta method, which uses a multistep process to achieve fairly large time steps without loss of high-order accuracy. The time step is regulated by the Courant–Friedrichs–Levy condition, which ensures stability in temporal integration by ensuring that information does not propagate completely through any one computational cell in a given time step.

The ionization/recombination source terms in Eq. (13) are discretized using an implicit scheme via operator splitting, and this can introduce some stiffness in nonequilibrium regions such as those exhibiting shocks or large amounts of applied joule heating. We test the degree to which the scheme affects accuracy via single-cell simulations, wherein a molar mixture of 96% water vapor and 4% cesium ions at $P = 10$ atm and $T = 2000$ K is allowed to reach equilibrium over the course of 10^{-2} s, roughly the timescale of the PDRIME cycle in the current study. The size of the time steps for the implicit simulation varies from 10^{-2} s (i.e., a single step) to 10^{-8} s, and the results are compared with the analytical solution. We see in Fig. 3 that, for all time-step magnitudes at or below 10^{-4} s, the results are extremely precise. Since the experiments conducted in this study use time steps below 10^{-6} s within similar pressure and temperature domains, we determine that no significant errors result from the source terms.

C. Geometries and Grid Generation

In quasi-one-dimensional (quasi-1-D) simulations of a PDRIME configuration, as described in recent studies [1,21,22], the computation of quasi-1-D flow in the supersonic nozzle flow must be decoupled from that in the bypass tube, with no resolution

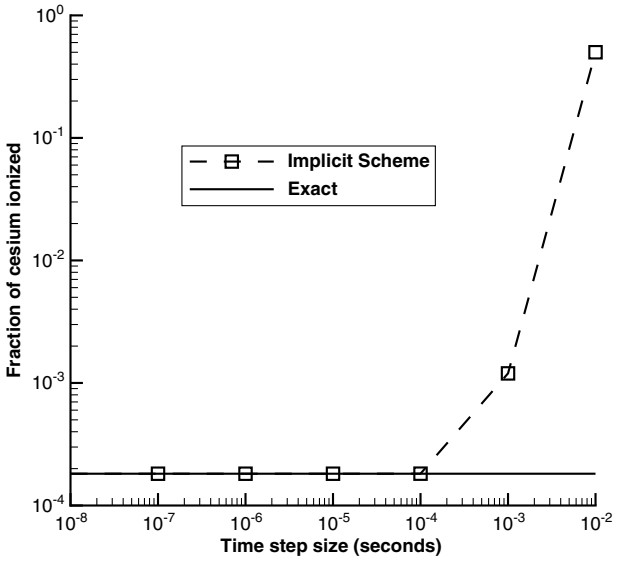

Fig. 3 Single computational cell results for a mixture of water vapor and cesium ions, the latter consisting of 4% of the mixture by moles. Pressure is initialized at 10 atm, temperature to 2000 K, and the mixture is allowed 10 ms to reach equilibrium. Time-step sizes below 0.1 ms are shown to result in sufficient accuracy.

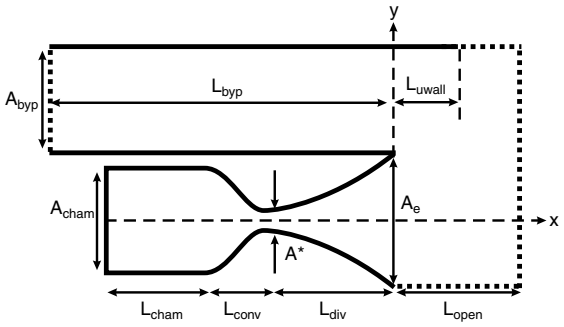

Fig. 4 General configuration of a planar PDRIME of unit depth. The parabolic contour of the nozzle wall and the extension of the upper bypass wall assist in the transfer of high-pressure products from the nozzle exit to the bypass exit.

of the transfer of fluid from the nozzle to the bypass section. These quasi-1-D models thus prescribed the bypass exit boundary conditions as a function of the nozzle exit conditions, which themselves are a function of time. The 2-D simulations conducted in the present study will explore the full 2-D flowfield and will mimic the conditions under which the quasi-1-D tests operated to determine whether the quasi-1-D boundary condition functions accurately reflect 2-D PDRIME behavior.

In the present study, the 2-D configuration for the general form of the planar PDRIME is shown in Fig. 4. A_{cham}, A^*, A_e, and A_{byp} are the areas of the chamber, throat, nozzle exit, and bypass, respectively, and L_{cham}, L_{conv}, L_{div}, L_{byp}, L_{uwall}, and L_{open} indicate the lengths of the chamber, converging nozzle, diverging nozzle, bypass tube, upper wall of the bypass extending beyond the nozzle lip, and outflow area from the nozzle lip, respectively. The expanding nozzle between the throat and the exit is parabolic so that the curved lip of the nozzle allows shocks to more easily follow the contour of the wall to enter the bypass.

The bypass tube runs straight along the top of the PDE, and although the lower bypass wall ends at the tip of the nozzle, the upper wall can extend further. This extension can help maximize impulse by "catching" the outgoing shock from the nozzle and diverting into the bypass tube to be used by the MHD accelerator. The bypass tube should not be excessively wide or else the shock migrating into the tube ceases to be uniform, creating inefficiencies in the MHD accelerator. It must also not be too narrow, lest not enough fluid becomes available to accelerate. The geometrical parameters used in the present calculations are given in Table 1.

The grid used for the present 2-D calculations consists of a grid of cells measuring n_x cells horizontally by n_y cells vertically, flanked on all four sides by a layer of three ghost cells for spatial interpolation (i.e., boundary conditions) along both axes. The grid for these simulations is shown in Fig. 5, representing the PDRIME as well as a downstream area where one can observe the region where the flow from the nozzle into the bypass takes place. Symmetry across the nozzle's centerline enables the 2-D grid to simulate only the upper half of the cross section of the PDRE, and the centerline is treated as a solid wall boundary. The top of the grid indicates the top of the bypass tube, and thus uses a reflective boundary condition along the length of the bypass upper wall. An open-air outflow boundary condition is used for the remaining section downstream of the PDRIME. To minimize the thickness of the nozzle wall, we use a block grid, in which our larger grid is effectively split into two regions: the nozzle with its exhaust downstream and the bypass with its outflow downstream, as illustrated in Fig. 5. This way, the upper nozzle wall and lower bypass wall can meet at a point of zero thickness while the ghost cells needed to simulate either side can be prescribed without hindering each other in a single grid. The nozzle section has as its left boundary condition at the nozzle throat the inlet prescribed by the Cambier blowdown model [20], as described in Sec. II.A.

Since the simulations in this study will use the blowdown model prescribed by Cambier [14], resolution requirements would depend upon the numerical scheme's ability to handle only shocks rather than more tasking detonation waves. The most significant shocks we will observe will be those within the PDRE chamber at the beginning of the blowdown cycle, when the chamber is filled with high-pressure products. We set up a straight 1.0 m shock tube filled with water vapor (i.e., H_2-O_2 reaction products) and initialize the 0.1 m section nearest the wall to $P_0 = 100$ atm, $T_0 = 3000$ K, while the rest of the tube is initialized to $P_0 = 1$ atm, $T_0 = 300$ K. When one simulates this with the quasi-1-D WENO code for which the pressure profiles are shown in Fig. 6a, we see that a horizontal resolution of 100 cells/m sufficiently captures the peak pressure of the shock.

When we conduct 2-D simulations of the PDRIME, we will observe shocks not only through a single species but also across multiple species, as between the water vapor in the nozzle exhaust and the air in the bypass tube. We set up another quasi-1-D shock test using a straight tube, this time measuring 0.6 m and filled with two different species initialized to temperatures and pressures we expect to observe near the nozzle and bypass exits during the PDRIME's operation. The left side is filled with stagnant water vapor at $P_0 = 10$ atm and $T_0 = 3000$ K, while the right side is filled with stagnant air at conditions observed at 25 km: $P_0 = 0.02573$ atm and $T_0 = 216$ K. The resulting waves at $t = 0.1$ ms, as shown in Fig. 6b, illustrate that a resolution of 100 cells per meter (cpm) once again sufficiently captures the peak pressure of the shock, while further resolution produces only marginally improved results.

Table 1 Dimensions of the PDRIME in meters and meters squared for lengths and areas, respectively

Parameter	Value
A_{cham}	0.1256
A^*	0.02513
A_e	0.06283
A_{byp}	0.06
L_{cham}	0.50
L_{conv}	0.02
L_{div}	0.80
L_{byp}	3.00
L_{uwall}	0.40
L_{open}	1.60

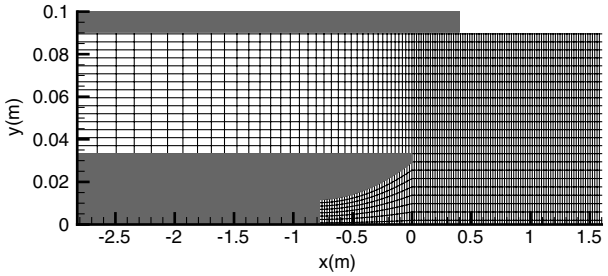

Fig. 5 2-D planar PDRIME domain of real cells.

Thus, our quasi-1-D simulations will use a resolution of 100 cells/m, while the 2-D simulations will use this resolution in both the x and y axes. This is the resolution shown in Fig. 5 in order to accurately capture shocks being transferred from the nozzle into the bypass section.

D. Magnetohydrodynamic Application

The MHD generator in the PDRIME configuration should be active only at the divergent section of the nozzle, where it will most benefit performance during the blowdown phase of the cycle. Thus, the generator source terms will be added to the governing equations for only those grid cells lying in the PDRIME between the nozzle throat and the exit, in particular, the downstream half of the diverging region where they use a loading factor of K_y will be 0.5. In the bypass section, the MHD components must act as a generator in places where the average flow travels upstream and as an accelerator when the local flow travels downstream, thus further accelerating the fluid. When acting as a generator, the loading factor K_y is 0.5, and when acting as an accelerator, K_y is 1.5, as noted previously. This can be accomplished by assuming that the capacitors imposing the electric fields are segmented such that they can be independently and simultaneously activated: some as generators and others as accelerators (obviously an idealized configuration).

A magnetic piston modeled in the chamber operates in the same manner as an MHD accelerator, except that the magnitude of the magnetic field changes in time such that the throat pressure remains constant until the chamber is emptied of products. If we instead model only the diverging nozzle and assign values to the throat inlet based off a blowdown model, we can alternatively use the numerical magnetic piston model to determine its rate of energy consumption while maintaining constant inlet conditions at the throat. Both approaches are explored here.

In all of these cases, the ability of the MHD components to manipulate the flow depends upon the fluid's conductivity, which in turn depends upon the density of cesium ions. Introducing such ions will be accomplished by seeding both the chamber and bypass flows with cesium atoms, which have a low enough ionization energy to be practical for this purpose. The current study simulates the flow of cesium atoms and ions within the PDRIME, calculating conductivity directly, but it also examines an approximation used in earlier research by Roth [21], whereby any fluid in the bypass for which the temperature exceeds 3000 K is assumed to be ionized while any fluid below this threshold is not. The nozzle flow is under no such restriction since the chamber fluid is assumed to be ionized to equilibrium after the initial detonation has left the PDRE and the convection timescale is much less than the chemical timescale, allowing us to assume frozen flow conditions.

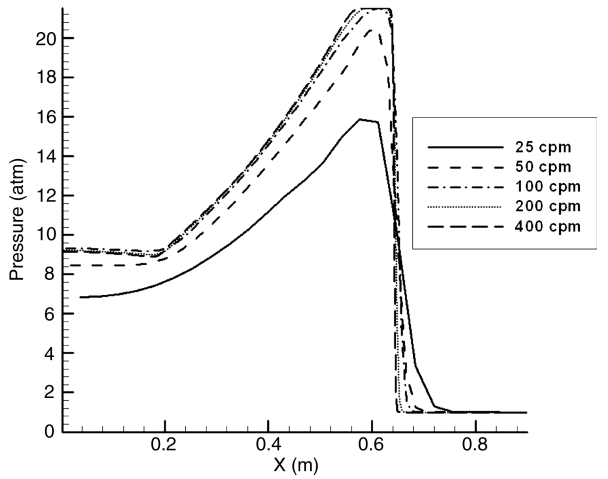

a) Nozzle blowdown resolution test

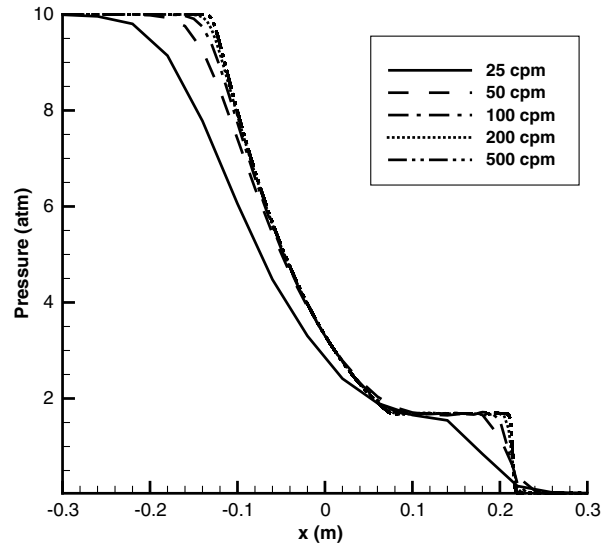

b) Dual species resolution test

Fig. 6 Quasi-1-D shock tube tests with different resolutions in cells per meter: initialized as a) $P_0 = 100$ atm, $T_0 = 3000$ K (left) and $P_0 = 1$ atm, $T_0 = 300$ K (right); and b) water vapor at $P_0 = 10$ atm, $T_0 = 3000$ K (left); $P_0 = 0.02573$ atm, $T_0 = 216$ K (right). All pressure profiles shown at $t = 0.1$ ms.

III. Results and Performance Evaluation

A. Blowdown Validation

Validity of the blowdown model in representing detonation and shock reflections in a PDRE combustion chamber may be ascertained by comparing the behavior of the modeled blowdown process with actual PDRE blowdown as represented via a detailed quasi-1-D or 2-D WENO simulation. The starting conditions of the Cambier model [20] assume that the detonation wave has already left the combustion chamber and that the remaining compression wave has reflected within the chamber sufficiently for the fluid within to become more or less stagnant. Since the chamber pressure and temperature in the wake of the repeatedly reflecting compression wave depend directly upon the reactants' pressure and temperature before the detonation, we must establish a set of assumptions to correspond to a set of initial conditions.

For the purposes of this study, we assume the reactants to be a stoichiometric mixture of hydrogen and oxygen, leaving behind pure water vapor in the chamber, and that the water vapor at the start of the blowdown cycle is pressurized to 100 atm and heated to either 3000 or 4000 K. The fluid in the nozzle is filled with products such that the fluid at the throat is sonic and the fluid in the converging and diverging sections corresponds to a quasi-steady isentropic compression and expansion. Both quasi-1-D and 2-D simulations of this blowdown process will be explored in this validation. For 2-D simulations, the fluid directly downstream of the nozzle will match the fluid at the nozzle exit, while all fluid outside of the nozzle and above the nozzle exhaust will consist of air at the appropriate altitude. The results will be compared with the ignition and propagation of a detonation and relevant reflection of shocks computed for a quasi-1-D PDRE configuration.

The flow and performance characteristics of the quasi-1-D PDRE chamber simulation and the quasi-1-D and 2-D blowdown models

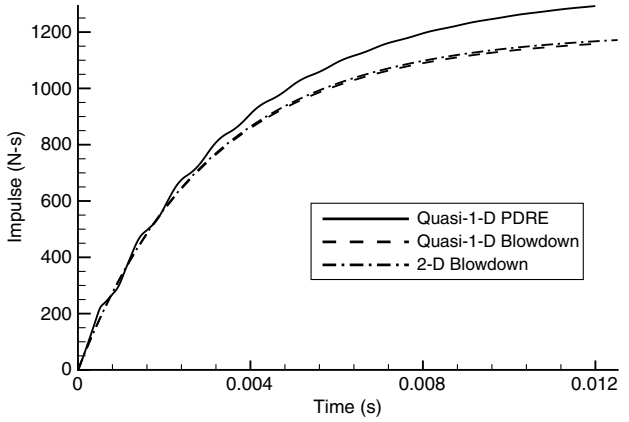

a)Total impulse (N-s)

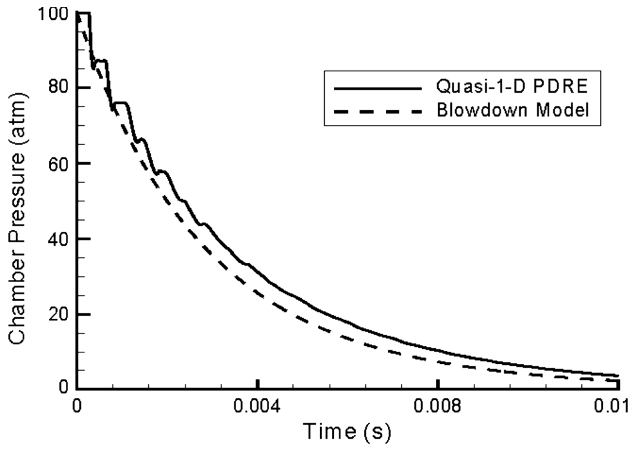

b) Chamber pressure (atm)

Fig. 7 Comparisons among the quasi-1-D PDRE simulation, the quasi-1-D blowdown nozzle simulation, and the 2-D blowdown nozzle simulation, showing a) impulse and b) chamber pressure as a function of time. The chamber pressure blowdown model in Fig. 7b is identical in both quasi-1-D and 2-D simulations.

are shown in Figs. 7a and 7b. We examine the impulse and chamber pressure using the same base case among the alternative cases. The impulse and pressure plots match up very closely with one another, aside from the fact that we assume the initial flow to be stagnant in the PDRE case. The reflecting shock waves observed in the PDRE chamber also expectedly make the corresponding results less smooth than those from the blowdown method, but any oscillations are also shown to become smooth with time, indicating that our substitution of throat model inlet conditions in place of the combustion chamber is appropriate. On this basis, in order to reduce computational costs in performing PDRIME and other MHD-augmentation concepts, we will use Cambier's blowdown model [20] to provide "input" to a detailed simulation of transient flow processes beyond the nozzle throat and, if present, within the PDRIME bypass section.

B. Baseline Pulse Detonation Rocket Engine with and Without Nozzle Generator

The first simulations will use the baseline PDRE geometry with only the diverging nozzle and no bypass tube or active MHD components therein. Cambier's blowdown model [20] is used for the throat inlet conditions. Initial chamber pressure is set to 100 atm, and simulations will be conducted for the initial chamber temperatures set to both 3000 and 4000 K. In both cases, we assume that the blowdown phase of the PDRE cycle ends when the chamber pressure reaches 2% of its original value (i.e., 2 atm). When we keep the initial chamber pressure constant but increase the temperature by 1000 K, the impulse per cycle drops from 1150 to 1025 $\mathrm{N}\cdot\mathrm{s}$ because the initial chamber density has been reduced, thus also reducing the mass available to be expelled from the nozzle.

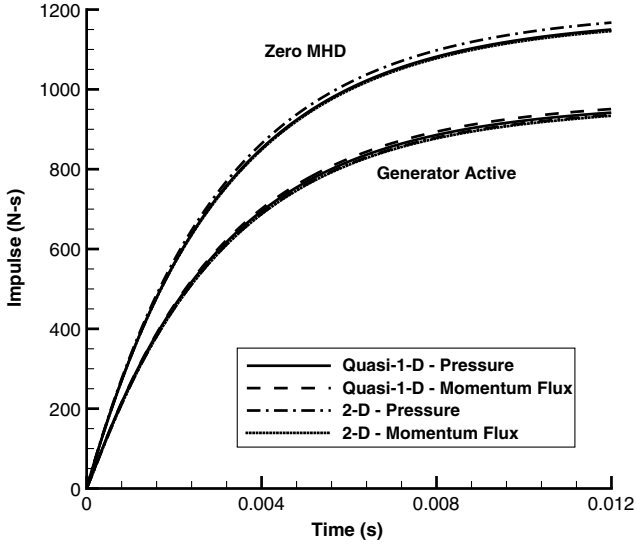

Fig. 8 Impulse calculation test comparing quasi-1-D and 2-D simulations of a PDRE with $AR = 2.5$. Pressure- and momentum-based methods employ wall pressure and momentum flux integrations. Results with and without the MHD generator active in the nozzle are shown for both quasi-1-D and 2-D simulations.

This calculation is compared with the same PDRE but with the nozzle generator activated, indicated in Fig. 8. Quasi-1-D quasi-steady simulations by Roth [21] using the same PDRE design iteratively calculated the magnetic field strength B at each time step such that the nozzle exit Mach number would be 1.2 throughout the blowdown cycle [14]. These data were used to produce a curve fit for the evolution of the magnetic field strength with time that is used in the transient quasi-1-D and 2-D simulations with the nozzle generator. The generator's domain of operation runs between the midpoint and exit of the diverging nozzle section, and it activates as soon as the blowdown commences. The electrical conductivity σ in this entire region is assumed to hold constant at 1000 $\mathrm{mho/m}$.

Both the quasi-1-D and 2-D results for these simulations illustrate how activating the nozzle generator produces energy but at a cost of reduced impulse due to drag. Figure 8 shows that, for a chamber temperature of $T_{0,\mathrm{cham}} = 3000$ K, the reduction in impulse for the PDRE with the nozzle generator is about 120 $\mathrm{N}\cdot\mathrm{s}$ at the end of the cycle. About 420 kJ in available energy is generated during this process; this can be used either in the bypass section or in the magnetic chamber piston, as described previously. As expected, calculating impulse using either the pressure method or momentum flux method produces the similar results; subsequent calculation of impulse uses the pressure method. No substantive differences are observed between quasi-1-D and 2-D results.

The benefits of the nozzle generator in affecting flow from the nozzle to the bypass section may also be explored. The presence of the nozzle generator alone can affect how much of the bypass fluid is blocked by the nozzle exhaust and whether a shock traverses upstream to heat the flow. Figure 9 shows temperature contours for the PDRIME geometry, both for the cases without MHD at all and with only the MHD nozzle generator operating for an altitude of 25 km and at flight Mach numbers 7, 9, and 11. This is the altitude and flow regime in which MHD augmentation would have the most benefit according to earlier quasi-1-D simulations [21,22]. We observe that much greater heating occurs in the bypass section when we activate the nozzle generator because the higher pressure at the nozzle exit allows a stronger shock, traveling at a higher speed, to enter the bypass section. Increasing the nozzle exit pressure through extraction of the flow's kinetic energy is vital to the heating and ionization of the bypass fluid, which in turn is vital to MHD acceleration for the PDRIME.

Unlike in an idealized quasi-1-D simulation of the bypass tube, however, the high-pressure nozzle exhaust does not block the bypass air in such a way that it is brought to a complete halt or even simply

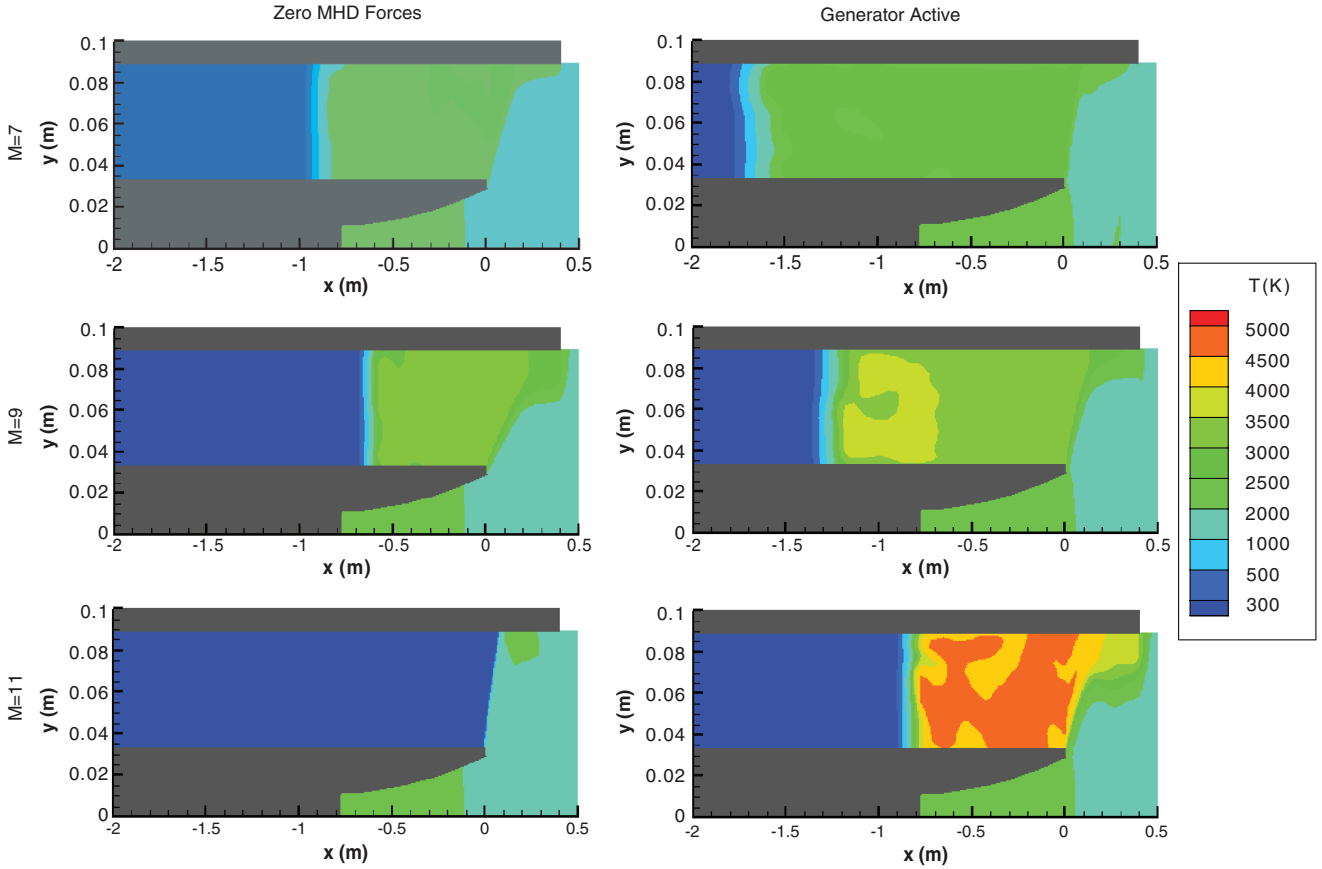

Fig. 9 Temperature contours of the PDRIME, with and without the nozzle generator running, at time $t = 3$ ms. The altitude of operation is 25 km, with an initial chamber temperature of 3000 K.

decelerates. The contact surface between nozzle exhaust and bypass outflow is not always a vertical wall but lies at an angle that grows more shallow as the Mach number increases [1]. Some air creeps over this contact surface, but the rest circulates back and upstream into the bypass tube, partially inducing numerical mixing with the water vapor from the nozzle and creating exit conditions considerably different from those assumed for quasi-1-D PDRIME simulations in earlier research by Roth [21] and Cole [22].

C. Pulse Detonation Rocket-Induced Magnetohydrodynamic Ejector with Nozzle Generator and Chamber Piston

As noted above, energy generated from the nozzle can be reintroduced within the PDRE's chamber, allowing operation of a magnetic chamber piston. Running the piston and the generator at the same time would be counterproductive, so we activate them in series, where the nozzle generator runs until the chamber pressure reaches a fixed percentage of its initial value (called either the generator shutoff pressure or the chamber activation pressure). Immediately after this point, the magnetic chamber piston uses this energy to blow down the remainder of the products. In some cases, not enough energy is available to evacuate all of the remaining products with the piston, in which case normal blowdown resumes after the piston runs out of energy to complete the cycle. Activation pressures that bring about this scenario are said to fall into the "mass-rich" domain. In other cases, the piston is able to evacuate all of the products and still have energy to spare; we call this the "energy-rich" domain. We define the critical pressure to be the activation pressure for which the piston finishes evacuating the chamber with exactly no energy remaining.

Figure 10 shows the effects of varying the activation pressure on the PDRE with the nozzle generator and magnetic chamber piston operating, in contrast to the same configuration but with zero MHD (no generator or chamber piston operational). Results are shown for the impulse at the end of a cycle (Fig. 10a) and the amount of energy that can be generated and consumed for different chamber temperatures (Fig. 10b). The activation pressure at which the energy generated is equal to that consumed by the chamber piston is the critical pressure, which is shown here to be approximately 45 atm.

We note that all of the results for the MHD generator and piston operation shown in Fig. 10a produce impulse per cycle totals that are below those using no MHD application at all. This is expected for the energy-rich simulations where kinetic energy is extracted from the flow and not completely reallocated (i.e., activation pressure is below the critical pressure), but we also see it in the mass-rich simulations where all available extracted energy is completely reallocated (i.e., activation pressure is greater than the critical pressure). This tells us that, while the generator/piston combination can reduce the cycle time, and thus possibly improve impulse per unit time at the cost of extra fuel, it does not improve impulse or operative efficiency. Since our goal is to improve efficiency, the piston should be used only in conjunction with the bypass accelerator. Ideally, this would mean that energy should not be redirected toward the chamber piston unless the bypass accelerator is unable to use all of the energy provided by the generator. If the generator must extract more energy than the bypass accelerator can consume in order to ensure sufficient bypass heating, then the chamber piston can consume the remainder and perhaps be used efficiently. This operation is explored in the PDRIME simulations below.

D. Pulse Detonation Rocket-Induced Magnetohydrodynamic Ejector Simulations with Constant Conductivity

While the results at flight Mach 7 (Fig. 9) produced some heating in the bypass, tests [2] with the 2-D PDRIME simulation reveal that not enough of the flow can be maintained at a temperature above 3000 K to facilitate nonnegligible MHD acceleration. In contrast, our simulations at Mach 9 and 11 heat up just enough of the bypass fluid to be considered useful, so further 2-D simulations with the full PDRIME are conducted only at Mach 9 and Mach 11. Any higher flight speeds at altitudes of 25 or 30 km cause the heated bypass fluid

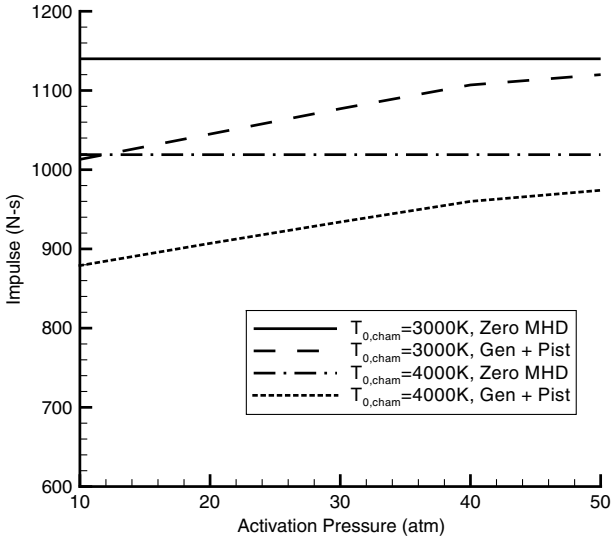

a) Shutdown/activation pressure test - impulse

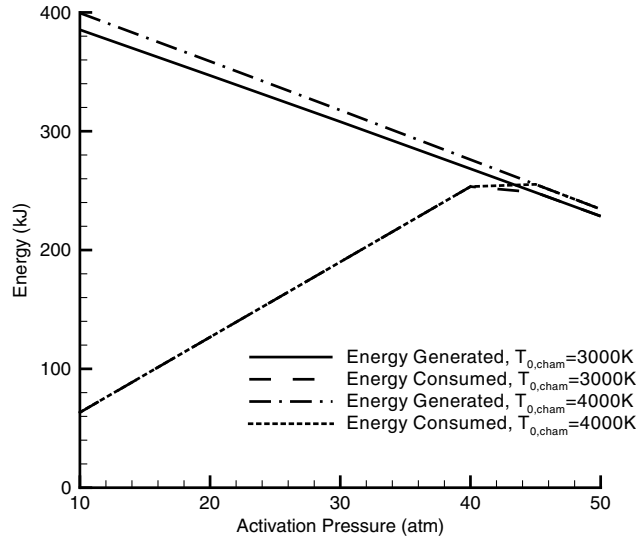

b) Shutdown/activation pressure test - energy

Fig. 10 PDRE operation using the MHD generator in series with the magnetic chamber piston. The MHD generator operates from the beginning of the cycle, and the time at which the generator deactivates and the piston activates is determined by the chamber activation pressure. Simulations are run for initial chamber temperatures of 3000 and 4000 K. (Gen denotes generator; Pist denotes piston.)

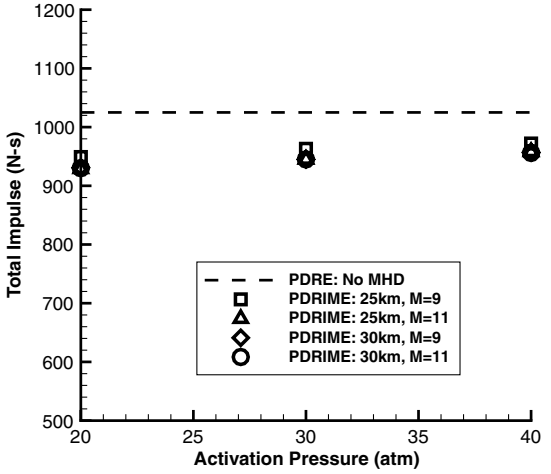

Fig. 11 Total impulse for several constant-conductivity PDRE simulations in which initial chamber temperature is set to 4000 K. The dashed line indicates the minimum impulse that the bypass must contribute in order to outperform the PDRE without any MHD components.

to be too small to use the accelerator. Any slower, and the fluid that is heated will not be hot enough for ionization. First, we calculate flow evolution and performance assuming a constant electric conductivity in the flow.

At altitudes of both 25 and 30 km, and for both flight Mach numbers 9 and 11, the MHD generator heats up the bypass flow enough that the bypass accelerators can reintroduce all available energy into the bypass section at higher activation pressures, meaning that the chamber piston is not actually needed at times. Results for the total impulse as a function of activation pressure for a chamber temperature of 4000 K, for example, are shown in Fig. 11 for different flight Mach numbers and altitudes. In these cases, we activate only the nozzle generator and the bypass accelerator, leaving the chamber piston inactive. The bypass accelerator, however, does not activate until 3.5 ms after the blowdown cycle commences so as to give the nozzle-driven shock sufficient time to propagate and heat the bypass flow. For these simulations in Fig. 11, the conductivity in the nozzle is set to 1000 mho/m, and the conductivity in the bypass is set arbitrarily to 500 mho/m in regions where the average temperature across a given cross section exceeds 3000 K; σ is equal to 0 mho/m elsewhere. The magnetic field strength in the nozzle varies according to the quasi-1-D quasi-steady evolutions determined earlier, while the magnetic field strength in the bypass section is uniformly 3 T, which is used throughout this study unless otherwise noted. While electromagnets in the 2–3 T range introduce considerable weight, such components are still compact enough for large flight vehicles. The simulations are for activation pressures of 20, 30, and 40 atm, as these were deemed the most promising from the chamber piston tests for their residing in the energy-rich domain.

What we discover in Fig. 11 is that, no matter which activation pressure we use for the generator, we are never able to produce enough impulse in the bypass to replace the impulse lost by the nozzle generator. Furthermore, the bypass accelerator is able to provide more impulse at an altitude of 25 km than at 30 km, despite the latter case resulting in greater heating of the bypass tube. At both altitudes, worse performance results are observed when more energy is made available to the bypass accelerator, which evidently cannot use it as efficiently as it was generated.

These results lie in contrast to those observed in quasi-1-D simulations, where at Mach 9 conditions the bypass was able to fully use all available energy to positive effect without either shutting off the generator early or activating the chamber piston. Such results are shown, for example, in Fig. 12. Comparisons between this quasi-1-D simulation and the 2-D simulation are difficult due to the varying nature of the MHD component operation (i.e., the 2-D results correspond to the nozzle generator being shut off at a chamber pressure of 30 atm, while no such shutoff occurs in the quasi-1-D simulations). Moreover, the quasi-1-D results use constant specific heat ratios, while the 2-D results use variable specific heat ratios. As a consequence, even the baseline PDRE results vary between the two simulations, shown in Fig. 13. Despite such differences, it is apparent that the quasi-1-D PDRIME simulations predict performance enhancement, while the 2-D simulations do not, as seen in the figure.

The disparity between MHD effects in Fig. 13 is largely explained by the significant 2-D effects occurring at the contact surface between the bypass outflow and nozzle exhaust. A sample of the 2-D time evolution of temperature for the Mach 9 condition at 25 km, including streamlines, is shown in Fig. 14. Vortical structures are observed to arise due to baroclinic vorticity generation as the shock migrates about the lip of the nozzle into the bypass section. While the quasi-1-D simulation assumes a bypass exit boundary condition consisting of a vertical wall of stagnant high-pressure fluid, in reality, the contact surface between the bypass and nozzle outflows is at a variable angle. The bypass flow travels up the contact surface before circling back along the extended bypass upper wall, creating significant vortical structures that the quasi-1-D simulations cannot resolve, leading to different conditions under which the bypass

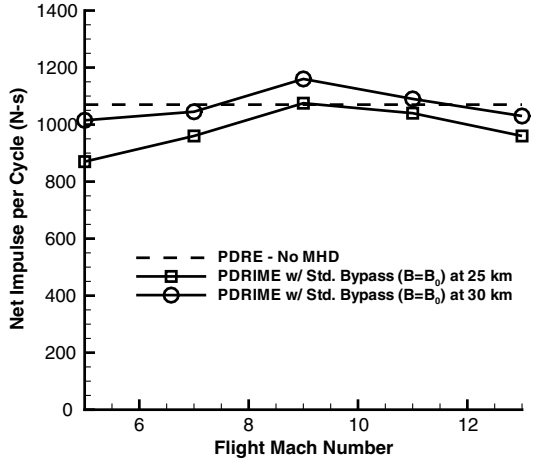

Fig. 12 Total impulse for quasi-1-D constant-conductivity PDRIME simulations in which initial chamber temperature is set to 3000 K. The dashed line indicates the minimum impulse that the bypass must contribute in order to outperform the PDRE without any MHD components.

accelerator operates. While the temperature field appears to be roughly 1-D in the bypass section, the substantial vorticity generation alters the flow from that assumed in quasi-1-D simulations.

E. Pulse Detonation Rocket-Induced Magnetohydrodynamic Ejector Simulations with Cesium Ionization

We now represent the more realistic effects of the seeding, ionization, recombination, and transport of cesium in the nozzle and bypass in the 2-D simulations and calculate the conductivity directly to see how this influences performance. The initial conditions, flight conditions, magnetic field strengths, and PDRIME dimensions are the same. To the chamber, we add a mixture of cesium atoms and ions at equilibrium, amounting to 0.5% of chamber's initial contents on a molar basis. We assume the converging section of the nozzle to be short enough that the level of recombination occurring between the chamber and the nozzle is negligible. To the bypass inlet, we add 0.1% cesium atoms on a molar basis. Overall, cesium amounts to roughly 4% of the propellant weight in the most optimized case studied.

PDRE simulations of cesium ionization with the nozzle generator active can produce conductivity in the nozzle at 1000 mho/m, as prescribed in the simplified simulations, but only if the initial

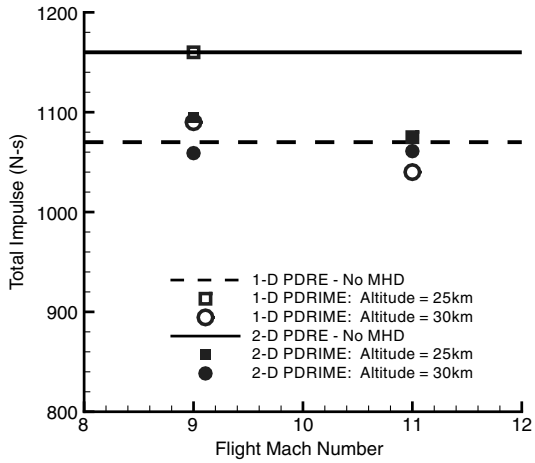

Fig. 13 Comparisons between quasi-1-D and 2-D simulations of the PDRIME in which initial chamber temperature is set to 3000 K and conductivity is constant. Dashed and solid lines indicate the minimum impulse that the bypass must contribute in order to outperform the PDRE without any MHD components for the quasi-1-D and 2-D simulations, respectively.

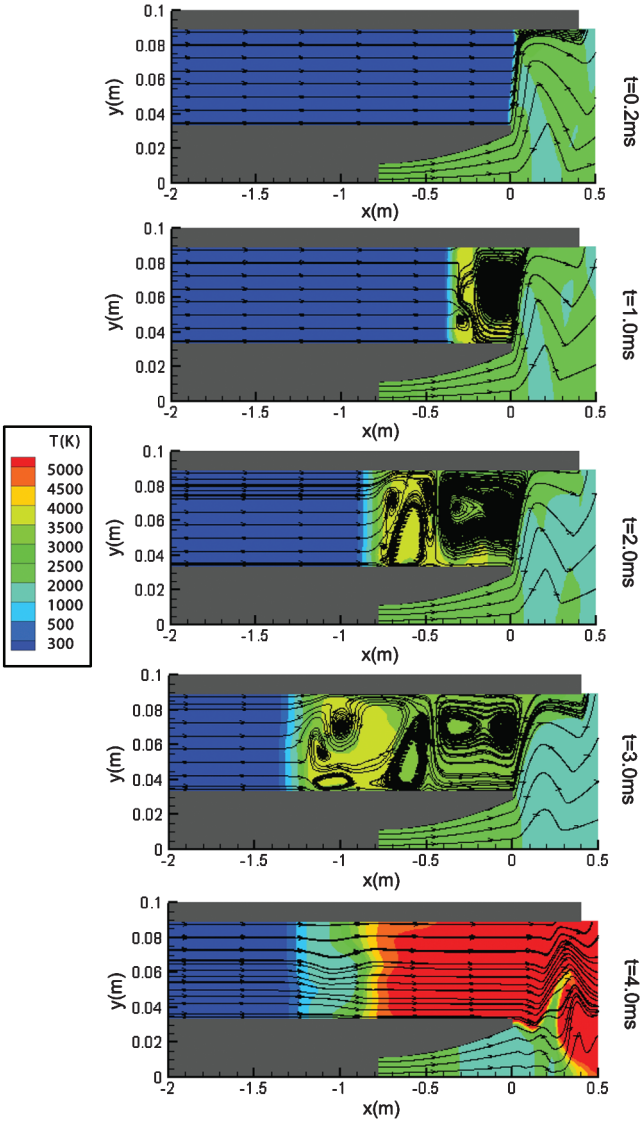

Fig. 14 Temperature contours of the PDRIME with the nozzle generator, superimposed with streamlines to illustrate fragmented vortical structures. Altitude is 25 km, initial chamber temperature is 3000 K, and Mach number is 9.

chamber temperature is set to 4000 K rather than 3000 K. Thus, for this next set of simulations, only a 4000 K chamber pressure initialization will be used. Matching conductivity levels for the 3000 K initialization would require increasing the molar percentage of cesium in the nozzle inlet to 2% of the fluid by moles, or 14% by mass, at which point any performance benefits from MHD augmentation are dwarfed by the momentum imparted by the mass addition of cesium, rendering the MHD components moot.

Running similar test cases as before, with results in Fig. 15, reveals that we are once again unable to obtain significant impulse improvements over the baseline total of 1000 N · s per cycle. Variances between the results in Fig. 11 and those in Fig. 15 arise from the fact that the nozzle fluid conductivity profiles in the former are constant at 1000 mho/m, while those in the latter are transient, despite staying near 1000 mho/m for the majority of the cycle. Furthermore, while the bypass fluid conductivity had previously been assumed to hold constant at 500 mho/m, results with cesium ionization result in conductivities within the bypass varying between 500 and 2500 mho/m.

F. Optimization of Engine Operation

In the foregoing PDRIME configuration, the bypass accelerator is able to use only a small fraction of the energy provided by the nozzle

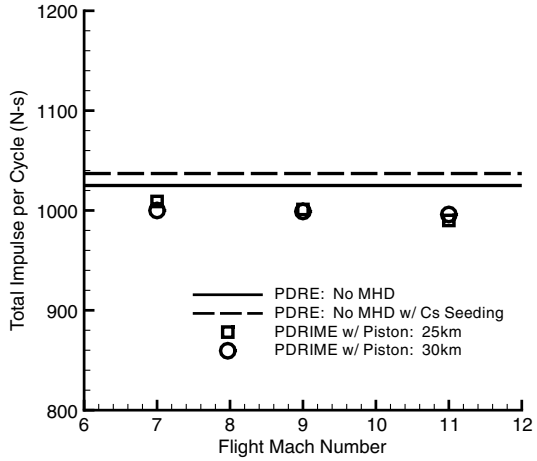

Fig. 15 Maximum total impulse for several 2-D simulations with cesium ionization and recombination. Chamber temperature is initialized to 4000 K. The solid line indicates the total impulse of the PDRE without any MHD components or seeding of cesium. The dashed line indicates the total PDRE impulse with no MHD components but with the additional mass of cesium added. The dashed line also indicates the minimum impulse that the bypass must contribute in order to outperform the PDRE without any MHD components.

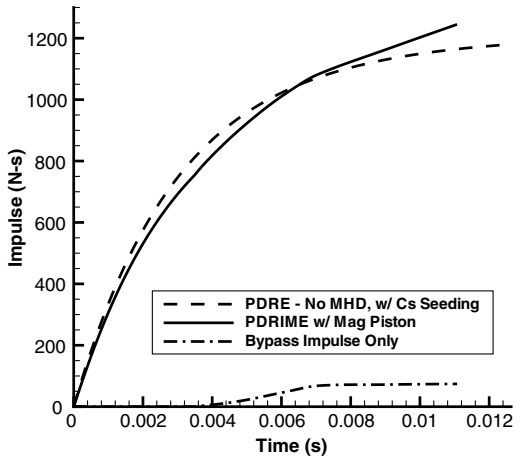

Fig. 16 PDRIME performance at 20 km and flight Mach 2 with initial chamber temperature of 3000 K. Impulse evolution is plotted for both a baseline PDRE seeded with cesium but with no MHD activation and a PDRIME with the nozzle generator, bypass accelerator, and magnetic (Mag) piston activated. An additional impulse plot illustrates the contribution from the bypass accelerator during the PDRIME simulation. Chamber-to-throat $AR = 5.0$, exit-to-throat $AR = 2.5$, and bypass width = 15 cm. Chamber is initially seeded with 0.5% cesium by moles, and the width of the bypass is seeded with 0.1% cesium by moles.

generator, per the results shown in Fig. 10. To prevent unnecessary drag, the remainder of this energy is sent to the chamber piston for consumption (e.g., as in Fig. 11), but this not only introduces significant impulse losses (due to alteration of nozzle exit conditions) but also hastens the end of the cycle and thus allows even less time for the bypass section to conduct its work.

One solution is to generate less energy in the first place by reducing either the nozzle flow conductivity or the MHD generator magnetic field strength. This approach would result in a reduced nozzle exit pressure, higher exit Mach number, and reduced heating in the bypass section; but here, the bypass accelerator would not eject the fluid as quickly as before, and it might be able to consume a greater percent of the total available energy, leaving less for the magnetic piston and lowered impulse losses.

Hence, rather than focus on heating the bypass fluid to as high a temperature as possible, an alternative objective is to provide the bypass with as much ionized low-velocity fluid as possible, even if the fluid is relatively weakly ionized. The air mass in the bypass can be increased by either reducing the altitude to increase its density or by widening the bypass tube to increase its volume. Both of these methods have the drawback of inhibiting propagation of the nozzle-driven shock upstream in the bypass tube, but this can be compensated by reducing the flight Mach number. All of these changes will result in a weaker shock, and thus reduced conductivity, on the order of 300–400 mho/m in the nozzle and 100–200 mho/m in the bypass, so ejecting the increased shock will take more time. If the piston is activated too early, it might consume energy that the bypass accelerator would have used had the cycle been allowed to run longer. Thus, this change to the PDRIME operating conditions will be to desynchronize the generator from the chamber piston, setting the latter to activate at some time after the former shuts off and allowing more time for the bypass accelerator to function.

The next set of results uses all of these suggested improvements at once. The PDRE chamber is initially set to 100 atm and 3000 K, the bypass width is increased to 15 cm, the flight Mach number is reduced to 2, and the altitude is reduced to 20 km so that the bypass inlet pressure and temperature are 5529 Pa and 216 K, respectively. The bypass accelerator continues to run with a uniform magnetic field of 3 T and activates only on fluids that travel slower than 1000 m/s and temperatures above 300 K so that the simulation does not mistake the trace ionization in the unheated bypass fluid as viable ejection material. The bypass length remains at 3 m, and the nozzle dimensions remain the same as in previous tests.

The results in Fig. 16 show that this new PDRIME configuration is much more effective than prior configurations. In contrast with the baseline PDRE (but with cesium seeding to replicate PDRIME mass addition), the PDRIME with the bypass alone has an increase in cycle impulse of 80 N · s, and since the chamber piston uses very little energy, it also costs very little in impulse losses, netting the PDRIME a 60 N · s impulse improvement over the baseline. Figure 17 illustrates how the energy consumption by the magnetic piston and the bypass accelerator is slow and steady, occurring right up until the end of the cycle at roughly 0.012 s.

We run similar tests for a variety of flight Mach numbers and bypass widths, in all of which the generator shuts off when the chamber pressure reaches 30 atm. The time at which the piston activates varies according to that which produces the most efficient performance under the flight conditions. In these cases, the chamber pressure at which the piston activates lies between 8 atm for the lower flight Mach numbers and 18 atm for the higher Mach numbers. Figure 18 demonstrates that, for these calculations, there is

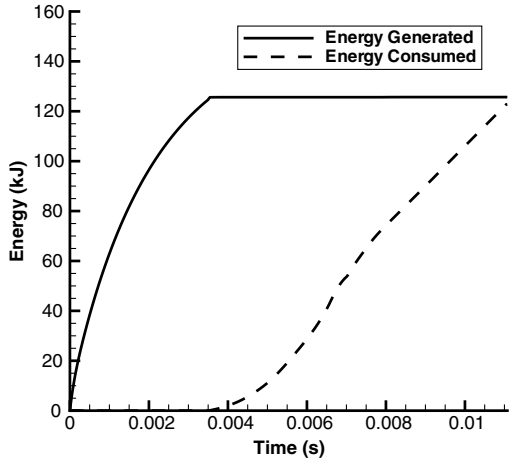

Fig. 17 PDRIME energy generation and consumption at 20 km and flight Mach 2 with initial chamber temperature of 3000 K. The solid line illustrates the initial activation of the nozzle generator and its shutoff at roughly 0.0035 s. At this time, the dashed line illustrates the chamber piston activating, followed by a gradual consumption of energy from the bypass accelerator. Chamber-to-throat $AR = 5.0$, exit-to-throat $AR = 2.5$, and bypass width = 15 cm. Chamber is initially seeded with 0.5% cesium by moles, and the width of the bypass is seeded with 0.1% cesium by moles.

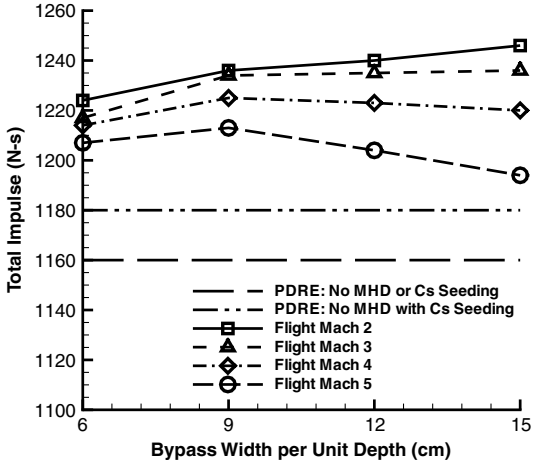

Fig. 18 PDRIME total impulse per cycle at 20 km varying with flight Mach number and bypass area per unit depth. Initial chamber temperature of 3000 K. Bypass length = 3 m. Chamber is initially seeded with 0.5% cesium by moles, and the width of the bypass is seeded with 0.1% cesium by moles.

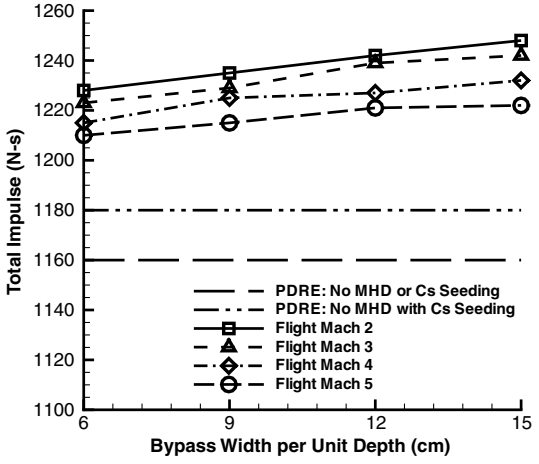

Fig. 20 PDRIME total impulse per cycle at 30 km varying with flight Mach number and bypass area per unit depth. Initial chamber temperature of 3000 K, and bypass length = 6 m. Chamber is initially seeded with 0.5% cesium by moles, and the width of the bypass is seeded with 0.1% cesium by moles.

increasing impulse improvement with a reduced flight Mach number. At lower Mach numbers, increasing the bypass width also increases performance by facilitating the ionization of additional fluid, but as the flight Mach number increases, increasing bypass width produces diminishing returns as the extra inlet mass starts expelling the upstream shock before the bypass accelerator has a chance to operate effectively on the ionized gas. Less energy is redirected into the bypass flow this way, thus necessitating earlier chamber piston activation to make certain that all stored energy is reintroduced. Accounting for cesium seeding in the baseline and PDRIME configurations, Fig. 18 shows up to a 70 N · s increase in impulse for Mach 2 operation.

Running the same experiments at altitudes of 25 and 30 km requires an adjustment to the PDRIME, since in some cases the reduced inlet bypass pressure results in the upstream shock's escaping the tube and taking useful heat energy with it. Thus, at 25 and 30 km, we run the same tests with a bypass of length 4 and 6 m, respectively. Figures 19 and 20 illustrate how we are able to obtain similar results at these altitudes as we did at 20 km (Fig. 18) for the same ranges of flight Mach numbers and bypass widths. In these cases, the shock waves propagate further up the bypass tube and heat the air to higher temperatures, but these are compensated by the reduced air density and greater distances over which the fluid must be accelerated.

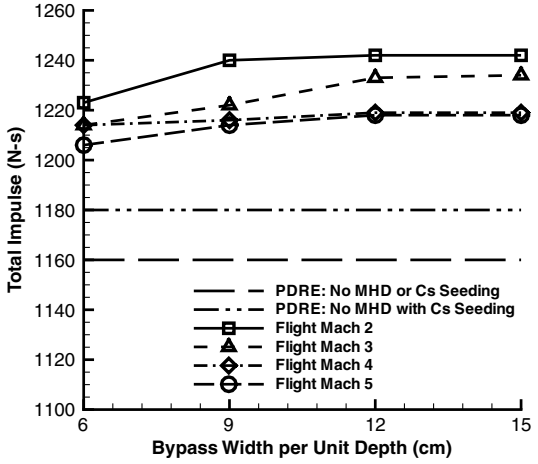

Fig. 19 PDRIME total impulse per cycle at 25 km varying with flight Mach number and bypass area per unit depth. Initial chamber temperature of 3000 K, and bypass length = 4 m. Chamber is initially seeded with 0.5% cesium by moles, and the width of the bypass is seeded with 0.1% cesium by moles.

Despite the similar impulse results per cycle, one significant drawback to operating at higher altitudes is that longer bypass tubes are required to accelerate the extra volume of less dense air, necessitating a heavier PDRIME device with additional electromagnetic components such as magnets. Bypass lengths in excess of 3 m are not required for the higher flight Mach numbers tested, but the best impulse improvement is observed at the lowest flight Mach numbers, thereby rendering 20 km to be the optimal altitude at which to operate this PDRIME configuration.

IV. Conclusions

A range of alternative PDRIME configurations and operating conditions have been explored in the present studies. It has been observed that performance enhancement under the given simulations conditions can be accomplished mainly by the bypass accelerator, and even then only under the condition that it be prevented from accelerating fluid that is already above a given velocity. While the magnetic chamber piston can be used early in the cycle to maintain higher nozzle exit pressure and can aid in causing the shock to propagate up the bypass tube, the piston can also hasten the end of the cycle too quickly for the accelerator to completely eject the heated fluid. This suggests that the piston should be activated later, only as a measure of consuming any energy that would otherwise go unused.

The primary method of performance improvement observed in this study is configuring the PDRIME to heat and ionize a large mass of low-velocity bypass flow just enough for the accelerator to efficiently reintroduce as much available energy as possible before the end of the cycle. This configuration is observed to function most efficiently at low flight Mach numbers and at low altitudes, where the inlet air is slow enough to be efficiently accelerated and dense enough to consume sufficient amounts of energy during acceleration. Improved performance can also be observed at higher altitudes, provided that the bypass tube is extended to prevent the nozzle-driven shock from escaping, but the additional weight of the tube and of the electromagnetic components affixed to it would increase the performance requirements of the PDRIME.

Further studies into the breadth of application of the PDRIME could include alternate chamber and nozzle configurations and determining the corresponding optimal operating and flight conditions. Although the present studies were conducted with a low magnetic Reynolds number approximation, future computations would have to account for induced fields. Future simulations might also operate the bypass ejector in such a way that its cycle period is much longer than that of the chamber detonations, a configuration which cannot be simulated using only the blowdown model, as done in the present studies. All of these simulations eventually require full

coupling of the electric and magnetic fields as well as more detailed analysis of cesium ionization, beyond a single reversible reaction, to determine the complete feasibility.

Acknowledgments

This research has been supported at University of California, Los Angeles, by the U.S. Air Force Office of Scientific Research under the Space Power and Propulsion program managed by Mitat Birkan (grants FA9550-07-1-0156 and FA9550-07-1-0368). The authors wish to acknowledge the technical assistance of Xing He of HyperComp, Inc., in the early stages of this work.

References

[1] Cambier, J.-L., Roth, T., Zeineh, C., and Karagozian, A. R., "The Pulse Detonation Rocket Induced MHD Ejector (PDRIME) Concept," 44th AIAA/ASME/SAE/ASEE Joint Propulsion Conference, AIAA Paper 2008-4688, July 2008.

[2] Zeineh, C., "Numerical Simulation of Magnetohydrodynamic Thrust Augmentation for Pulse Detonation Rocket Engines," Ph.D. Thesis, Dept. of Mechanical and Aerospace Engineering, Univ. of California, Los Angeles, 2010.

[3] Hill, P., and Peterson, C., "Mechanics and Thermodynamics of Propulsion," 2nd ed., Addison Wesley, Reading, MA, 1992.

[4] Eidelman, S., Grossmann, W., and Lottati, I., "Review of Propulsion Applications and Numerical Simulations of the Pulse Detonation Engine Concept," *Journal of Propulsion and Power*, Vol. 7, No. 6, 1991, pp. 857–865. doi:10.2514/3.23402

[5] Kailasanath, K., and Patnaik, G., "Performance Estimates of Pulse Detonation Engines," *Proceedings of the Combustion Institute*, Vol. 28, 2000, pp. 595–602. doi:10.1016/S0082-0784(00)80259-3

[6] Cooper, M., and Shepherd, J. E., "Single Cycle Impulse from Detonation Tubes with Nozzles," *Journal of Propulsion and Power*, Vol. 24, No. 1, 2008, pp. 81–87. doi:10.2514/1.30192

[7] Wintenberger, E., Austin, J. M., Cooper, M., Jackson, S., and Shepherd, J. E., "Analytical Model for the Impulse of a Single Cycle Pulse Detonation Engine," *Journal of Propulsion and Power*, Vol. 19, No. 1, 2003, pp. 22–38. doi:10.2514/2.6099; also erratum, Vol. 20, No. 4, 2004, pp. 765–767. doi:10.2514/1.9442

[8] Li, C., and Kailasanath, K., "Partial Fuel Filling in Pulse Detonation Engines," *Journal of Propulsion and Power*, Vol. 19, No. 5, 2003, pp. 908–916. doi:10.2514/2.6183

[9] Warwick, G., "U.S. AFRL Proves Pulse-Detonation Engine Can Power Aircraft," *Flight Magazine*, March 2008 [online] http://www.flightglobal.com/articles/2008/03/05/222008/us-afrl-proves-pulse-detonation-engine-can-power-aircraft.html [retrieved 2011].

[10] He, X., and Karagozian, A. R., "Numerical Simulation of Pulse Detonation Engine Phenomena," *Journal of Scientific Computing*, Vol. 19, Nos. 1–3, Dec. 2003, pp. 201–224. doi:10.1023/A:1025351924837

[11] He, X., and Karagozian, A. R., "Pulse Detonation Engine Simulations with Alternative Geometries and Reaction Kinetics," *Journal of Propulsion and Power*, Vol. 22, No. 4, 2006, pp. 852–861. doi:10.2514/1.17847

[12] Harten, A., Osher, S. J., Engquist, B. E., and Chakravarthy, S. R., "Some Results on Uniformly High-Order Accurate Essentially Nonoscillatory Schemes," *Applied Numerical Mathematics*, Vol. 2, 1986, pp. 347–377. doi:10.1016/0168-9274(86)90039-5

[13] Jiang, G. S., and Shu, C. W., "Ecient Implementation of Weighted ENO Schemes," *Journal of Computational Physics*, Vol. 126, 1996, pp. 202–228. doi:10.1006/jcph.1996.0130

[14] Cambier, J.-L., "MHD Augmentation of Pulse Detonation Rocket Engines," 10th International Space Planes Conference, Kyoto, Japan, AIAA Paper 2001-1782, April 2001.

[15] O'Sullivan, M. N., Krasnodebski, J. K., Waitz, I. A., Gretizer, E. M., and Tan, C. S., "Computational Study of Viscous Effects on Lobed Mixer Flow Features and Performance," *Journal of Propulsion and Power*, Vol. 12, No. 3, 1996, pp. 449–456. doi:10.2514/3.24056

[16] Cambier, J.-L., "A Thermodynamic Study of MHD Ejectors," 34th AIAA/ASME/SAE/ASEE Joint Propulsion Conference, AIAA Paper 1998-2827, July 1998.

[17] Gurijanov, E. P., and Harsha, P. T., "AJAX: New directions in hypersonic technology," 7th International Space Planes Conference, AIAA Paper 1996-4609, 1996.

[18] Hwang, P., Fedkiw, R. P., Merriman, B., Aslam, T. D., Karagozian, A. R., and Osher, S. J., "Numerical Resolution of Pulsating Detonation Waves," *Combustion Theory and Modelling*, Vol. 4, No. 3, Sept. 2000, pp. 217–240. doi:10.1088/1364-7830/4/3/301

[19] Henrick, A. K., Aslam, T. D., and Powers, J. M., "Mapped Weighted Essentially Non-Oscillatory Schemes: Achieving Optimal Order Near Critical Points," *Journal of Computational Physics*, Vol. 207, No. 2, 2005, pp. 542–567. doi:10.1016/j.jcp.2005.01.023

[20] Cambier, J.-L., "Preliminary Model of Pulse Detonation Rocket Engines," 35th AIAA/ASME/SAE/ASEE Joint Propulsion Conference, AIAA Paper 1999-2659, June 1999.

[21] Roth, T., "Modeling and Numerical Simulations of Pulse Detonation Engines with MHD Thrust Augmentation," M.S. Thesis, Department of Mechanical and Aerospace Engineering, Univ. of California, Los Angeles, 2007.

[22] Cole, L., "Combustion and Magnetohydrodynamic Processes in Advanced Pulse Detonation Rocket Engines," Ph.D. Prospectus, Department of Mechanical and Aerospace Engineering, Univ. of California, Los Angeles, 2010.

J. Powers
Associate Editor

FINAL REPORT:
AFOSR Grant Number: FA9550-08-1-0048

Numerical Simulation of Pulse Detonation Rocket-Induced MHD Ejector (PDRIME) Concepts for Advanced Propulsion Systems

PI: Prof. Ann R. Karagozian
UCLA Department of Mechanical and Aerospace Engineering
310-825-5653; ark@seas.ucla.edu
AFOSR Program Manager: Dr. Mitat A. Birkan, AFOSR/RSA
mitat.birkan@afosr.af.mil

Abstract

The primary goal of this research project has been to use high resolution numerical methods to explore reactive and magnetohydrodynamic (MHD) flow phenomena as a means of potentially improving the performance of hypersonic propulsion through a range of alternative and innovative combined-cycle concepts, such as the Pulse Detonation Rocket-Induced MHD Ejector (PDRIME) Concept. Such a combined cycle propulsion concept has the potential to achieve improved system performance over conventional rockets or pulse detonation rocket engine (PDRE) concepts in a range of flight conditions, via temporal energy bypass from a pulse detonation rocket to an MHD-augmented component. These studies constitute an assessment of the potential improvements possible through PDRIME concepts via detailed numerical simulations as well as simplified modeling. On the basis of both simplified modeling and highly resolved simulations, an optimization of system level configuration has been explored in detail. Beyond the PDRIME explorations, based on discussions with Dr. Birkan, as part of this grant our research group has also examined fundamental resolution of detonation instabilities with complex reaction kinetics and the potential influence of an applied magnetic field on the reactive flow, in addition to experiments relevant to acoustically-coupled coaxial jet instabilities in rocket chambers.

1. Introduction and Background

Robust propulsion systems for advanced high speed air breathing and rocket vehicles are critical to the future of Air Force missions, including those for global/responsive strike and assured access to space. A novel combined cycle propulsive concept, the Pulse Detonation Rocket-Induced MHD Ejector (PDRIME) proposed by Dr. Jean-Luc Cambier[1] of the Air Force Research Laboratory at Edwards, is one of a number of alternative MHD augmentation ideas that shows promise for application to a wide range of advanced propulsion systems. Taking advantage of the unsteady engine cycle associated with the pulse detonation rocket engine (PDRE), PDRIME involves periodic temporal energy bypass to a seeded airstream, with MHD acceleration of the airstream for thrust enhancement and control. The range of alternative MHD-augmented propulsion configurations that could be employed suggests that the PDRIME type of concept could be applied to hypersonic air-breathing systems, space power production for

directed energy weapons (DEW) and remote sensing systems, electromagnetic countermeasures, and other potential Air Force systems for the mid-to-far term.

A schematic of the PDRIME configuration and associated flow processes is shown in **Figures 1ab**. A PDRE can be designed to have a converging-diverging nozzle such that the initial peak pressure in the combustion chamber results in a pressure at the nozzle exit plane that is well above ambient. Under these circumstances the nozzle exhausts a shock structure (locally oblique) at the nozzle lip, indicated in Fig. 1a. The shock produced at the PDRE's nozzle exit can then enter the bypass channel, traveling upstream. If the air is initially at high Mach number in the channel, this traveling shock brings the air to high temperature, generating a slowly-moving slug of high-temperature air that can be more easily ionized. As the pressure at the nozzle exit drops during blowdown, the shock then slows down, and eventually the ionized air starts to move downstream. At this point, electrical power can be applied to accelerate the air slug, generating thrust (Figure 1b). The procedure can then be repeated at each cycle.

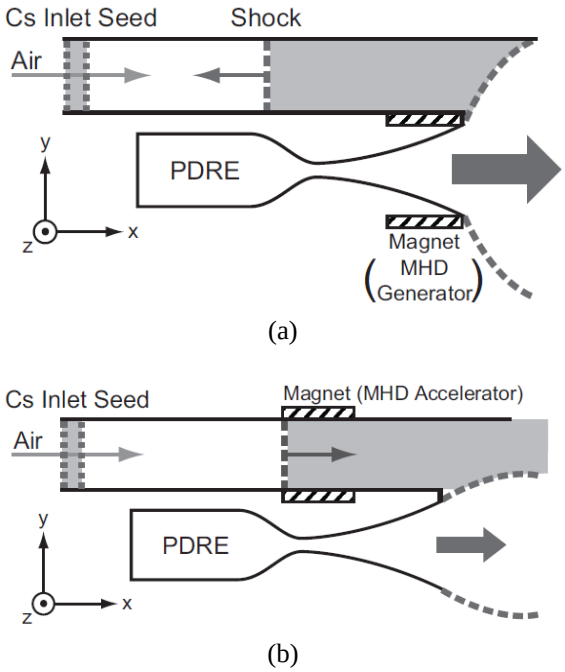

Figure 1. Schematic of the PDRIME concept during (a) the initial portion of the cycle, where over-pressure at the nozzle exit allows an upstream propagating shock (dashed line) to enter the bypass section, and (b) during blowdown, where exhaust of the compressed and heated air from the bypass channel takes place.

Another alternative configuration by which MHD can be used to augment thrust generated by a PDRE is one in which energy extracted by MHD from the high velocity flow in the expansion portion of the nozzle can be applied to the combustion chamber. Creation of a "magnetic piston" in the chamber, as shown in **Figure 2**, can be used to exhaust combustion products from the chamber at an optimal portion of the cycle while allowing a fresh mixture of reactants to fill the available volume. Both the PDRIME with bypass and magnetic piston concepts were explored as a part of this research project.

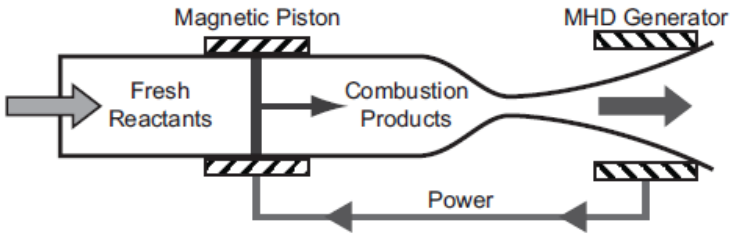

Figure 2. Schematic of the Magnetic Piston Concept. The piston accelerates the combustion products out of the chamber in such a way that, as long as it continuously operates, constant pressure and temperature are maintained at the throat. Fresh reactants are simulatenously drawn in to replace the evacuated products.

2. Methods and Summary of Results on Alternative PDRIME Configurations

Due to the large number of available system parameters in the PDRIME, to accomplish efficient performance calculation and optimization, a rapid simulation technique is required, one that is simpler than a detailed numerical simulation of flow and reactive processes in the PDRE chamber and adjacent flow sections. For the PDRE configuration, after the shock waves have subsided in the combustion chamber, the properties of the fluid within the chamber are mostly uniform, resembling the products of a constant volume reaction. For these reasons a blowdown model was developed by Cambier[2] to predict chamber properties as a function of time after a constant volume reaction; this model was incorporated in the present PDRIME configuration simulations.

The diverging section of the nozzle and the bypass-tube are then divided into cells and fully discretized. The 2D transient equations which govern this flow in conservative form are similar to those used to simulate PDEs as done in He and Karagozian[3,4] but with additional species terms (to simulate air, water vapor exhaust, cesium atoms, and cesium ions), an ionization/recombination source term when we simulate the injection of cesium, and an MHD source term denoting related momentum and energy effects.

Details on the simulation methods and preliminary results for the PDRIME configurations are described in a conference paper[5] (**Appendix A**) while more complete results may be found in a recent journal paper[6] (**Appendix B**) as well as in the Ph.D. thesis of Zeineh[7], the M.S. thesis of Roth[8], and the Ph.D. prospectus of Cole[9]. The student documents are available upon request.

A few of the important observations from the above simulations are included in the body of this report. **Figure 3**, for example, shows temperature contours for the PDRIME geometry (without the presence of a magnetic piston), both for the cases without MHD at all and with only the MHD nozzle generator operating (that is, extracting energy from the nozzle and applying it in the bypass section). Results are shown for an altitude of 25 km and at flight Mach numbers 7, 9, and 11. This is the altitude and flow regime in which MHD augmentation would have the most benefit according to earlier quasi-1D simulations[8,9]. We observe that much greater heating occurs in the bypass section when we activate the nozzle generator because the higher pressure at the nozzle exit allows a stronger shock, traveling at a higher speed, to enter the bypass section. Increasing the

nozzle exit pressure through extraction of the flow's kinetic energy is vital to the heating and ionization of the bypass fluid, which in turn is vital to MHD acceleration for the PDRIME. Unfortunately, although the quasi-1D simulations for the PDRIME suggest improvements with the application of MHD energy in the bypass section, detailed 2D simulations such as those in Figure 3 indicate that there is vorticity generation that alters the transfer of the shock and flow in the bypass section, actually producing a reduction in overall performance of the PDRIME when compared with the baseline PDRE without MHD effects (see the comparisons of total impulse in **Figure 4**).

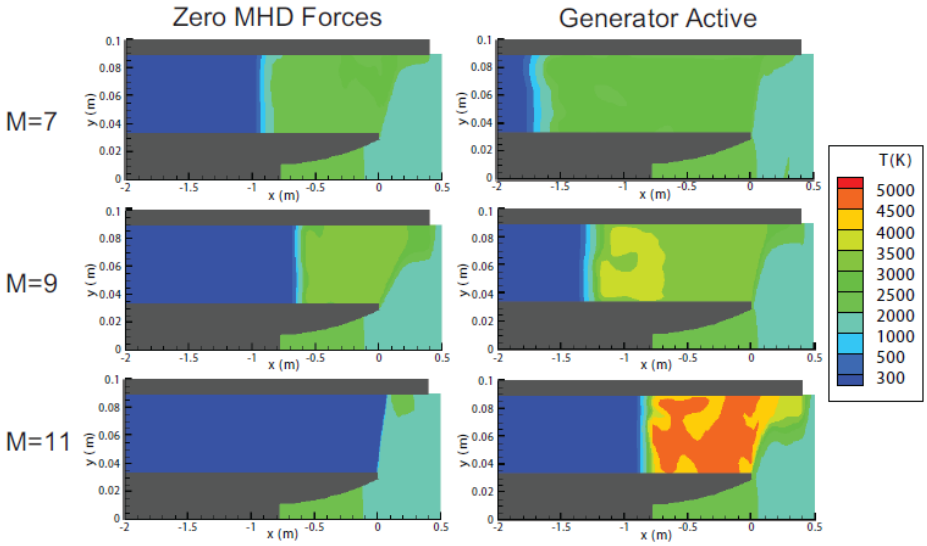

Figure 3. Temperature contours of the PDRIME, with and without the nozzle generator running, at time t=3ms. The altitude of operation is 25 km, with an initial chamber temperature of 3000 K.

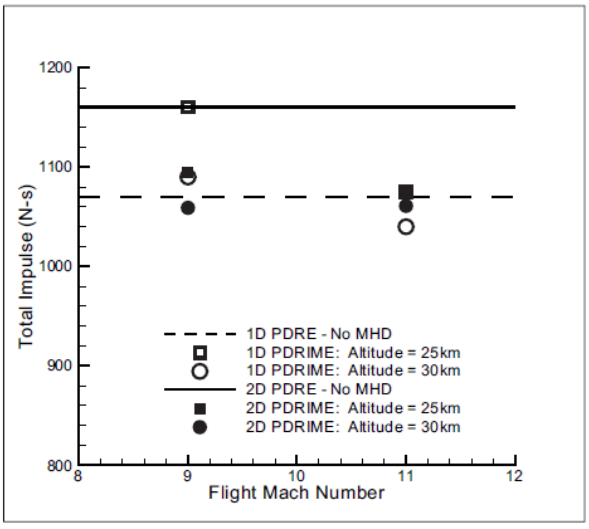

Figure 4. Comparisons between quasi-1D and 2D simulations of the PDRIME in which initial chamber temperature is set to 3000 K and conductivity is constant. The dashed and solid lines indicate the minimum impulse that the bypass must contribute in order to outperform the PDRE without any MHD components for the quasi-1D and 2D simulations, respectively.

Optimization of the operation of the PDRIME with the presence of the magnetic piston and with lower flight Mach numbers can lead to improvements in performance over the baseline, however. As described in detail in Zeineh, et al.[6] and as summarized in **Figure 5**, increasing the size of the bypass section can also produce increases in the impulse per cycle.

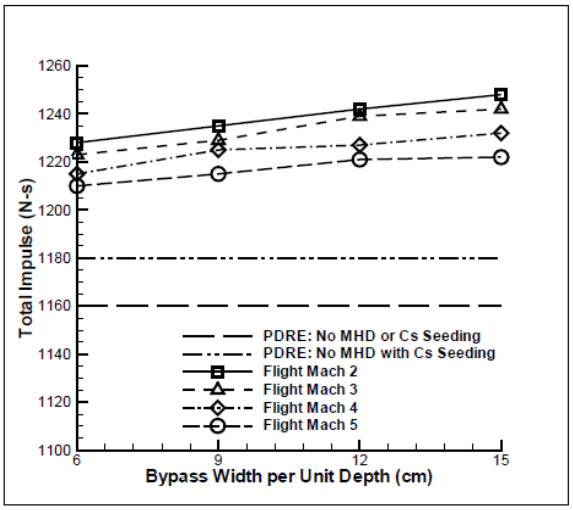

Figure 5. PDRIME total impulse per cycle at 25km varying with flight Mach number and bypass area per unit depth. Initial chamber temperature of 3000K. Bypass length = 4m. Chamber is initially seeded with 0.5% cesium by moles, and the width of the bypass is seeded with 0.1% cesium by moles.

3. Ongoing Studies

Fundamental to the utilization of MHD to augment the performance of pulse detonation rocket engine configurations is the ability for the magnetic field to affect the propagation of detonation waves. As a consequence, one of the graduate students initially supported by this grant, Lord Cole, is continuing his Ph.D. studies at UCLA, in collaboration with Dr. Cambier of AFRL, by examining detailed detonation instabilities with complex reaction and ionization kinetics. Preliminary studies on various characteristics of detonation instabilities are described in a recent paper presented at the ICDERS 2011 conference[10], and subsequent studies are examining the effect of an applied magnetic field on these instabilities.

In addition, separate experimental studies on the response of cryogenic coaxial jet flows to external acoustic disturbances have been and are being completed by another graduate students initially supported by this grant, Sophonias Teshome. These experiments have been conducted at AFRL, and recent results[11] have been analyzed using Proper Orthogonal Decomposition. These studies also are ongoing but we expect completion by March of 2012.

References

[1] J.-L. Cambier, "MHD Augmentation of Pulse Detonation Rocket Engines", 10th Intl. Space Planes Conf., Kyoto, Japan, April 2001, AIAA paper 2001-1782.

[2] Cambier, J.-L., "Preliminary Model of Pulse Detonation Rocket Engines", Proceedings from the 35th AIAA/ASME/SAE/ASEE Joint Propulsion Conference, June 1999, AIAA paper 1999-2659.

[3] He, X. and Karagozian, A. R., "Numerical Simulation of Pulse Detonation Engine Phenomena", **Journal of Scientific Computing,** Vol. 19, Nos. 1-3, pp.201-224, December**,** 2003.

[4] He, X. and Karagozian, A. R., "Pulse Detonation Engine Simulations with Alternative Geometries and Reaction Kinetics", **Journal of Propulsion and Power**, Vol. 22, No. 4, pp. 852-861, 2006.

[5] Cambier, J.-L., Roth, T., Zeineh, C., and Karagozian, A. R., "The Pulse Detonation Rocket Induced MHD Ejector (PDRIME) Concept" Paper AIAA-2008-4688, 44th AIAA/ASME/SAE/ASEE Joint Propulsion Conference and Exhibit, July, 2008.

[6] Zeineh, C. F., Cole, L. K., Roth, T., Karagozian, A. R., and Cambier, J.-L., "Magnetohydrodynamic Augmentation of Pulse Detonation Rocket Engines", **Journal of Propulsion and Power**, Vol. 28, No. 1, pp. 146-159, January 2012.

[7] Zeineh, C., "Numerical Simulation of Magnetohydrodynamic Thrust Augmentation for Pulse Detonation Rocket Engine", Ph.D. thesis, UCLA Department of Mechanical and Aerospace Engineering, 2010.

[8] Roth, T., "Modeling and Numerical Simulations of Pulse Detonation Engines with MHD Thrust Augmentation", M.S. thesis, Department of Mechanical and Aerospace Engineering, UCLA, 2007.

[9] Cole, L., "Combustion and magnetohydrodynamic processes in advanced pulse detonation rocket engines", Ph.D. prospectus, Department of Mechanical and Aerospace Engineering, UCLA, 2010.

[10] Cole, L. K., Karagozian, A. R., and Cambier, J.-L., "Stability of Flame-Shock Coupling in Detonation Waves: 1D Dynamics", Paper 89, 23rd International Colloquium on the Dynamics of Explosions and Reactive Systems (ICDERS), UC Irvine, July 24-29, 2011.

[11] Teshome, S., Leyva, I. A., Talley, D., and Karagozian, A. R., "Cryogenic High-Pressure Shear-Coaxial Jets Exposed to Transverse Acoustic Forcing", presented at the 50th AIAA Aerospace Sciences Meeting, Nashville, TN, January 9-12, 2012.

The Pulse Detonation Rocket Induced MHD Ejector (PDRIME) Concept

Jean-Luc Cambier*
Air Force Research Laboratory, Aerophysics Branch, Edwards AFB, CA 93524

Timothy Roth†, Christopher Zeineh‡, and Ann R. Karagozian§
Department of Mechanical and Aerospace Engineering, UCLA, Los Angeles, CA 90095-1597

Pulse detonation engines (PDEs) have received significant attention due to their potentially superior performance over constant pressure engines. However due to the unsteady chamber pressure, the PDE system will either be over- or under-expanded for the majority of the cycle, with substantial performance loss in atmospheric flight applications. Thrust augmentation, such as PDE-ejector configurations, can potentially alleviate this problem. Here, we study the potential benefits of using Magneto-hydrodynamic (MHD) augmentation by extracting energy from a Pulse Detonation Rocket Engine (PDRE) and applying it to a separate stream. In this PDRE-MHD Ejector (PDRIME) concept, the energy extracted from a generator in the nozzle is applied directly to a by-pass air stream through an MHD accelerator. The air stream is first shocked and raised to high-temperature, allowing thermal ionization to occur after appropriate seeding. The shock-processing of the high-speed air stream is accomplished by using the high initial PDRE nozzle pressures of the under-expanded phase. Thus, energy could be efficiently transferred from one stream to another. The present simulations involve use of a simple blowdown model for PDE behavior, coupled to quasi-1D and 2D numerical simulations of flow and MHD processes in the rest of the PDRIME configuration. Results show potential performance gains but some challenges associated with achieving these gains.

Nomenclature

A	=	Cross-sectional area
B	=	Magnetic field
c	=	Speed of sound
$\vec{E}$	=	Electric field
E, $\hat{E}$	=	Energy
F_L	=	Lorenz force
Re_m	=	Magnetic Reynolds Number
I	=	Impulse
j	=	Current density
$\dot{m}$	=	Mass flux
p	=	Pressure
T	=	Thrust
u	=	Velocity
x,y,z	=	Streamwise, transverse, and axial coordinates
γ	=	Ratio of specific heats
ρ	=	Density
σ	=	Electrical conductivity

* Senior Scientist, AFRL/RZSA
† Graduate Student Researcher; currently Member of the Technical Staff, Northrop-Grumman Electronic Systems
‡ Graduate Student Researcher
§ Professor, AIAA Fellow; corresponding author (ark@seas.ucla.edu)

Introduction

Robust propulsion systems for advanced high speed air breathing and rocket vehicles are critical to the future of Air Force missions, including those for global/responsive strike and assured access to space. A novel combined cycle propulsive concept, the Pulse Detonation Rocket-Induced MHD Ejector (PDRIME) proposed by Cambier[1], is one of a number of alternative magneto-hydrodynamic (MHD) augmentation ideas that could have promise for application to a wide range of advanced propulsion systems. Taking advantage of the periodic engine cycle associated with the pulse detonation rocket engine (PDRE), PDRIME involves periodic temporal energy bypass to a seeded airstream, with MHD acceleration of the airstream for thrust enhancement and control. The range of alternative MHD-augmented propulsion configurations that could be employed suggests that the PDRIME type of concept could be applied to hypersonic air-breathing systems, space power production for directed energy weapons (DEW) and remote sensing systems, electromagnetic countermeasures, and other potential Air Force systems for the mid-to-far term.

Background: Conventional Rocket Systems and PDREs

Chemical rocket engines store both fuel and oxidizer, unlike air-breathing engines which utilize the oxygen in air in the combustion process. Liquid rockets typically employ a constant pressure reaction, where reactants are continually fed at high pressure into the combustion chamber. Rocket engines typically use a converging-diverging (Laval) nozzle to expand the flow and convert the high pressure and temperature of the propellants into thrust. Properties of a nozzle flow depend strongly on the pressure upstream (inside the combustion chamber, P_c), and at ambient (p_a), downstream of the nozzle exit, as well as the exit-to throat area ratio for the nozzle, A_e/A_*. The thrust generated by a rocket is typically expressed as:

$$T = \dot{m} V_e + (p_e - p_a) A_e \tag{1}$$

where $\dot{m}$ is the mass flux of gas exiting the nozzle, V_e is the exhaust velocity, and p_e is the pressure at the exhaust of the nozzle.

The maximum thrust[2] occurs when the propellants are expanded to the point where the pressure at the exit of the nozzle is equal to the ambient pressure. Further expansion of the gas in the nozzle will reduce the thrust, as the ambient pressure will then exceed the exhaust pressure, creating pressure drag. This added drag can outweigh momentum gains arising from the further acceleration of the flow from the nozzle, i.e., the increase in exhaust velocity. Under-expansion in the nozzle will result in lower than optimal thrust as the maximum momentum gains are not realized. Another performance parameter, impulse I, is the thrust integrated over time t:

$$I \equiv \int_0^t T(\tau) d\tau \tag{2}$$

Another common performance parameter, specific impulse I_{sp} ,is the impulse divided by the weight of the reactants or propellants.

One alternative configuration to the traditional rocket engine which has the potential for operating as a constant volume cycle, and hence could be theoretically more efficient, is the pulse detonation engine or PDE (a subset of which is the pulse detonation rocket engine or PDRE). The pulse detonation engine operates in a cycle. Reactants are added to the combustion chamber at low pressure, and are mixed. The mixture is ignited and a detonation wave propagates across the chamber. This detonation raises the propellants to high pressure and temperature, and can be modeled as a constant volume reaction, which is more efficient than a constant pressure reaction. After the detonation wave (or shock wave, after reactants have been consumed) exits the nozzle, an expansion wave is reflected back into the nozzle and eventually propagates into the chamber. The expansion wave thus lowers the overall pressure throughout the chamber, and upon reflection at the thrust wall, the lowered pressure allows reactants to be drawn into the chamber. The reflection of the expansion wave at the nozzle exit results in a reflected compression wave, which is strengthened and becomes a shock. When the shock reflects at the thrust wall, the reactants in the chamber can be ignited, and the ignition of the detonation wave starts the process once again. A number of recent studies have explored the nature and performance characteristics of PDEs of various geometries[3,4,5,6,7,8]. The PDE was even recently tested for the first time in flight on a Scaled Composites Long EZ aircraft[9], with four PDE tubes operating at a cycle frequency of 20 Hz.

In the past, our group at UCLA[10,11] has explored the influence of PDE geometry, reaction kinetics, and flow processes using high order numerical methods. A fifth-order WENO (weighted essentially non-oscillatory[12,13]) scheme was used for spatial integration of the reactive Euler equations, with a 3rd -order Runge-Kutta time integration in the case of simplified reaction kinetics; a stiff ODE solver was used for temporal integration in complex kinetics simulations. While the simulations using complex kinetics provide useful quantitative data, the

simulations with reduced kinetics (a single step reaction) in fact can provide very similar quantitative performance results.

In general, two different methods could be used to generate thrust from PDREs. The first involves a straight or slightly contoured nozzle. The main goal of this configuration is to exploit the thrust generation from the ignition of the detonation wave near the thrust wall and the propagation of the detonation wave through the device, as described above. The second approach is more similar to a constant-pressure rocket. Here the nozzle throat is small enough to prevent the main detonation wave to escape the chamber. This creates multiple reflected compressive waves in the chamber; which homogenize the chamber pressurization, resulting in an approximately constant volume reaction. During the blow-down period the reactants are driven out from the chamber and through the nozzle. Similar to the constant-pressure rocket, the exhaust gases are expanded, increasing the velocity and reducing the pressure. The difference between this type of PDRE and a constant-pressure rocket is that in the PDRE, the chamber pressure is decreasing throughout the blow-down period as mass is ejected from the chamber with no immediate replacement. New reactants are added to the combustion chamber once the pressure has been reduced to a specified value and then the cycle is repeated.

Due to the unsteady nature of the chamber pressure, however, a PDRE nozzle can only be perfectly expanded briefly within a blow-down period. This implies suboptimal use of energy to attain this condition for most of the cycle. At low altitudes, nozzles with large area ratios are subject to large drag forces ($P_a > P_e$), while nozzles with relatively smaller exit areas will be under-expanded for the majority of blow-down.

The PDRIME Concept

Ejectors are often used to transfer energy from one stream to another stream, providing an additional source of thrust, especially for an air-breathing engine. Ejectors have been shown to produce overall thrust gains when energy is being taken from a high velocity flow and transferred to a low energy stream, in the ejector, with a high mass flow rate. In the present application for the PDRE, energy can be extracted from the nozzle when the marginal decreases in thrust are small and added to a bypass air flow, to assist in augmentation of the thrust. Ejectors typically transfer energy between streams through shear stress between separate flow streams. A portion of the main flow is diverted into a channel to mix with the lower velocity flow. The drawback of this method is that the ability to transfer energy is limited by the contact area between the two streams. At large velocities shear layer thicknesses are small, leading to the necessity for large channels for mixing, which add weight.

In contrast, if magnetohydrodynamic (MHD) forces are applied as body forces to the ejector flow, affecting the entire field immediately, there can be substantial benefits[14]. This could reduce the length of the bypass tube and time necessary for complete energy transfer as well as providing the flexibility of energy extraction and application, since the applied fields can be varied.

Our possible configuration attaches a converging-diverging nozzle to the combustion chamber of a PDRE with a bypass tube. A generic configuration for this concept, called the Pulse Detonation Rocket Induced MHD Ejector (PDRIME), is shown in **Figure 1**. For the present applications, a simple Faraday configuration is used in both channels, with magnetic and electric fields in the z and y direction respectively, and normal to the fluid velocities (in the nozzle and bypass-tube, the x-direction). A planar design is used to achieve a spatially uniform magnetic field, only in the z-direction, by placement of magnets above and below each region.

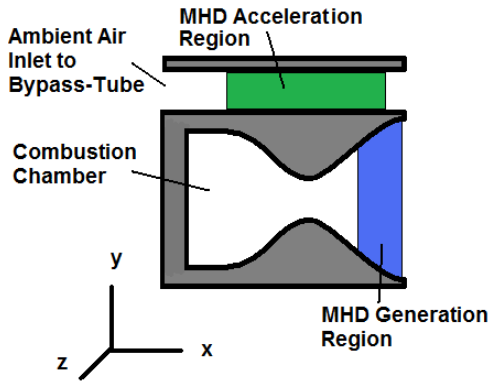

Figure 1: The generic PDRIME configuration, indicating the PDRE combustion chamber and regions in which MHD generation/extraction and flow acceleration in a bypass section take place.

In the expanding (divergent) section of the nozzle the fields are configured as an MHD generator to extract energy from the flow. In the adjacent by-pass channel, ambient air is periodically accelerated by MHD forces, using the energy extracted from the nozzle. A gain in thrust is possible by extracting energy from the high-speed flow[14] in the nozzle, and by applying it to a slower flow. This would require that the air in the by-pass tube be slowed down to velocities below that of the flow in the PDRE nozzle. Typically, this would imply significant drag forces; however, the PDRE operation, with its initially under-expanded phase during blowdown, may provide an elegant solution to this problem, as shown in **Figures 2a and 2b**.

A PDRE can be designed to have a converging-diverging nozzle such that the initial peak pressure in the combustion chamber results in a pressure at the nozzle exit plane that is well above that of the by-pass tube. The initial shock of the rapid pressurization of the PDRE chamber can diffract at the nozzle lip and travel upstream in the by-pass. More importantly, as shown in Fig. 2a, a slowly varying contact discontinuity is generated during the blow-down, and blocks the incoming air flow in the by-pass channel. If the air is initially at high Mach number in the bypass channel, an upstream-propagating shock brings the air to stagnation at high temperature. If the air is initially seeded with an alkaline seed such as Cesium by an upstream injector, the stagnated high-temperature air may be thermally ionized and become sufficiently conductive for efficient MHD coupling. Note that the air is brought to stagnation without requiring channel constriction, i.e. without any drag forces.

As the pressure at the nozzle exit drops during blow-down, the shock then slows down, and eventually the ionized air starts to move downstream. At this point, electrical power can be applied to accelerate the slowly-moving air slug from the bypass tube and thus generating thrust (**Fig. 2b**). The procedure can then be repeated at each cycle. One only needs to design the nozzle such that the flow is under-expanded during the initial part of the blow-down phase. In fact, there may be a self-adjusting process at work, depending on PDRE nozzle design and altitude as outlined by Cambier[1]. While at launch, the nozzle exit pressure is equal to ambient and there is no interaction with the bypass air, as the vehicle accelerates and gains altitude, the nozzle becomes progressively under-expanded, so that eventually a strong shock can be generated for the bypass channel to ionize the seeded air, and the ejector operates. This is one of several configurations in which the PDRIME concept could be used for thrust augmentation in advanced propulsion systems.

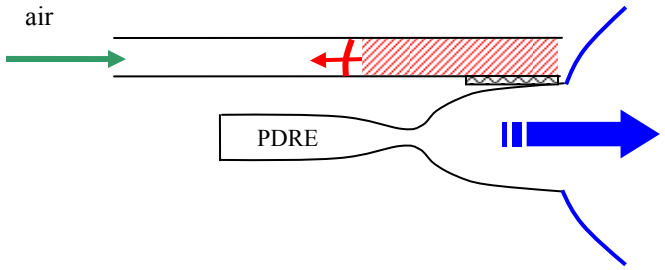

Figure 2a: Schematic of the PDRIME concept during the initial portion of the cycle. Overpressure at the nozzle exit blocks flow in the bypass channel. An upstream propagating shock slows and raises the temperature of the seeded air in the bypass channel.

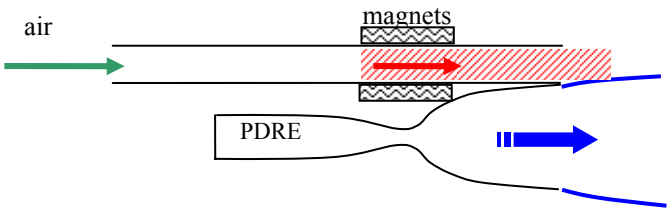

Figure 2b: Schematic of the PDRIME concept during the latter part of the cycle, during blow-down. As the pressure at the nozzle exit drops, exit of the compressed and heated air from the bypass channel takes place. Power is applied during the MHD acceleration of the air slug.

As noted above, the MHD "generator" is located in the diverging section of the nozzle where the velocity is largest, so that the expansion of the fluid counteracts some of the velocity reduction arising from the Lorentz ("drag") force acting in the generator. The ionized flow is characterized by a current density $\vec{j}$ which, using the simplest form of Ohm's law, can be written as:

$$\vec{j} = \sigma(\vec{E} + \vec{u} \times \vec{B}) \tag{3}$$

where σ is the electrical conductivity (with units of Mho/m). It is also assumed that the self-induced magnetic field is negligible, i.e. the magnetic field is given by the applied field. This assumption is equivalent to the limit of small magnetic Reynolds number R_m, defined as:

$$R_m = \mu\sigma u L \tag{4}$$

where μ is the permeability of free space (units of N/A^2), u the velocity and L is a characteristic length scale. The MHD coupling to the flow is described by source terms to the conservation laws, namely the Lorentz force F_L and a Joule energy deposition Q_J:

$$\vec{F}_L = \vec{j} \times \vec{B} \tag{5a}$$

$$Q_J = \vec{j} \cdot \vec{E} = \frac{\vec{j}^2}{\sigma} + \vec{u} \cdot (\vec{j} \times \vec{B}) \tag{5b}$$

The terms on the right-hand-side of (4b) are respectively the ohmic heating (dissipation) and mechanical work of the Lorentz force. For the Faraday configuration used here, the current density has a non-zero component in the y-direction only:

$$j_y = \sigma\left(E_y - u_x \times B_z\right) \tag{6}$$

It is convenient to define a loading factor K_y describing the respective strengths of the applied and induced electric fields,

$$K_y = \frac{E_y}{(u \times B)_y} \tag{7}$$

In a quasi-1D analysis, there is a single component of the velocity and using the loading factor, (3) can be written as:

$$j_y = \sigma u B \cdot (K_y - 1) \tag{8}$$

The Lorentz and Joule terms then become:

$$F_L = \sigma u B^2 (K_y - 1) \tag{9a}$$

$$Q_J = \sigma u^2 B^2 \cdot K_y (K_y - 1) \tag{9b}$$

When $K_y < 1$, the Lorentz force is negative (flow deceleration) and the Joule power is negative (energy extracted from the fluid). In the accelerator (bypass section), a positive Lorentz force and application of energy takes place. Regardless of the loading factor, the Ohmic heating will always be a positive term, since it is proportional to $(K_y - 1)^2$, representing a loss in both cases. Ignoring dissipative effects, we see that the Lorentz force scales with velocity, while the energy associated with both generation and acceleration scales with velocity squared. For this reason, maximum thrust gain is achieved when energy is extracted from high velocity flows, as in the nozzle, and applied to low velocity flows.

It is easily seen[15] that the optimal loading factor for MHD generation is $K_y = 0.5$. In the accelerator section (by-pass tube), the loading factor is generally greater than 1, and is chosen to be $K_y = 1.5$, but if a negative flow is detected in that location in the course of the cycle, $K_y = 0.5$ is assumed in order to assist with flow reversal.

The Magnetic Piston Concept

Another alternative configuration by which MHD can be used to augment thrust generated by a PDRE is one in which energy extracted from the high velocity flow in the expansion portion of the nozzle can be applied to the combustion chamber in order to accelerate combustion products from the chamber while allowing a fresh mixture of reactants to fill the available volume. By effectively creating a "magnetic piston" in the chamber, as outlined in Cambier[1], the combustion products can be pushed out from the chamber while simultaneously allowing a fresh mixture of reactants to fill the available volume. Such a configuration is shown in **Figure 3**. The extraction of

energy from a high velocity stream and delivered to a low velocity stream is one mechanism for thrust augmentation, hence a configuration such as that in **Fig. 3** can theoretically lead to performance gains. As indicated by Cambier[1], the average thrust increases with an increasing fraction of energy extracted from the flow, and with reduction in the filling time. It is noted that, when blow-down and filling processes are allowed to overlap via appropriate application of the magnetic field, filling time is effectively reduced, leading to a large increase in average thrust. The magnetic piston concept, separately as well as in concert with the PDRIME with bypass flow, will be explored here.

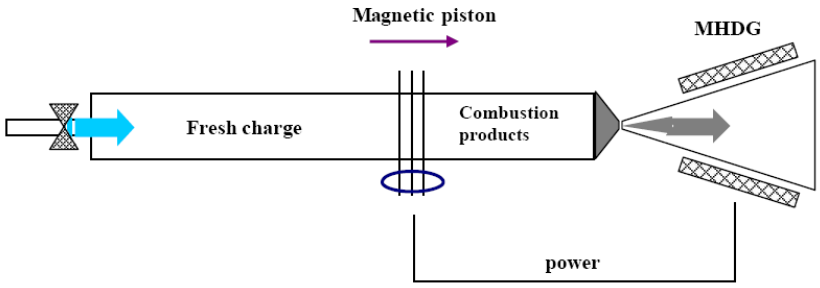

Figure 3: Schematic of the PDRE concept with MHD augmentation via a generator in the nozzle and a magnetic piston in the chamber (from Cambier[1]).

The goal of the present research involves use of a simplified model for the blow-down portion of the PDRE, coupled to a more detailed simulation of the relevant MHD processes in the nozzle and/or adjacent bypass sections, as a means of predicting overall PDRIME and magnetic piston phenomena and performance parameters. The model is validated using detailed numerical simulations of PDRE processes, so that projections for optimal performance and operating conditions may be made.

Description of the PDRIME Model and Simulation Procedure

Model Framework

Due to the large number of available system parameters in the PDRIME, a rapid simulation technique is required, one that is simpler than a detailed numerical simulation of flow and reactive processes in the PDRE and adjacent flow sections. Detonations constitute a major computational cost. The sharp gradients and large sound speeds present in the PDE greatly reduce the time-step and require finer spatial resolution[16,17]. After the shock waves have subsided in the combustion chamber, the properties of the fluid within the combustion chamber are mostly uniform, resembling the products of a constant volume reaction. For these reasons a blow-down model was developed by Cambier[18] to predict chamber properties as a function of time after a constant volume reaction. This blow-down model is in a single cell which represents the entire PDE combustion chamber. The converging section of the nozzle is also represented by a single cell approximation. An adiabatic solution for the throat conditions for every time-step is determined based on the combustion chamber properties and the assumption that the throat is choked. The divergent section, throat to exit, is fully discretized, as is the entire bypass-tube. In order to validate certain aspects of the engine cycle and flow processes, comparisons with full 2D transient numerical simulations are also made.

Description of Blowdown Model

The PDE cycle begins when the combustion chamber is full of reactants. An external spark then sends a detonation wave through the combustion chamber, raising the pressure of the propellants. The pressure difference between the combustion chamber and the ambient air drives the propellants out of the combustion chamber, representing the blow-down process. The presence of a nozzle changes the blow-down profile. Intuitively, a smaller throat, which restricts the mass flow of propellants out of the chamber, will lead to a slower decay, increasing the blow-down period. With small enough throat areas, the constant pressure period following the PDE's detonation becomes negligible and only blow-down needs to be considered for thrust calculations. Here the reaction is approximated as a constant volume reaction.

To predict this pressure decay inside the combustion chamber a simple model developed by Cambier is used. This model starts with the combustion chamber filled with post-constant volume reaction products at high pressure

and temperature. The mass and energy flow rate of the products through the throat are then calculated based on current conditions:

$$\frac{dM}{dt} = -\dot{m} = -\Gamma \rho_o c_o A^* \tag{10a}$$

$$\frac{dE}{dt} = -\dot{m} \cdot h_o = -\dot{m} \cdot C_p T_o \tag{10b}$$

where

$$\Gamma = \left(\frac{2}{\gamma + 1} \right)^{\frac{\gamma+1}{2(\gamma-1)}} \tag{11}$$

and ρ_o is the density of the products, A* is the area of the choked throat, c_o is the sound speed, h_o is the total enthalpy, and C_p is the heat capacity at constant pressure. In (10a-b), $M = \rho_0 \mathsf{V}_c$ and $E = \rho_0 C_\mathrm{v} T_0 \mathsf{V}_c$. The chamber volume V_c is constant, thus the system of equations (10) reduces to a partial differential equation for the stagnation temperature, which can be easily integrated[1]. This blowdown process is assumed to be adiabatic and quasi-steady. For high temperature water vapor (products), γ ~ 1.2 and is held constant. In this approach the entire combustion chamber is represented with a single cell, greatly reducing computational time.

Discretization of Nozzle and Bypass Sections

The diverging section of the nozzle and the bypass-tube are divided into cells. The quasi-1D equations which govern this flow in conservative form are similar to those in He and Karagozian[11] but without the species terms and with the inclusion of momentum and energy source terms corresponding to MHD effects:

$$\frac{\partial (AU)}{\partial t} + \frac{\partial A F_x(U)}{\partial x} = \frac{dA}{dx} H + A S(U) \tag{12}$$

$$U = \begin{pmatrix} \rho \\ \rho u \\ \widehat{E} \end{pmatrix}, \; F_x(U) = \begin{pmatrix} \rho u \\ \rho u^2 + p \\ (\widehat{E} + p) u \end{pmatrix}, \; H = \begin{pmatrix} 0 \\ p \\ 0 \end{pmatrix}, \; S(U) = \begin{pmatrix} 0 \\ j_y B_z \\ j_y E_y \end{pmatrix} \tag{13}$$

$$\widehat{E} = \frac{p}{\gamma - 1} + \frac{\rho u^2}{2} \tag{14}$$

where A(x) is the cross-sectional area as a function of position, and $\widehat{E}$ is the total energy density . To further streamline this rapid simulation, the flow inside the diverging section of the nozzle is modeled using a quasi-steady solution to these equations. This is valid when the characteristic time scale of the flow in the nozzle with the small throat is much shorter than the blow-down time scale of the chamber. First the governing equations are rewritten in primitive form:

$$\frac{1}{\rho}\frac{d\rho}{dx} + \frac{1}{u}\frac{du}{dx} + \frac{1}{A}\frac{dA}{dx} = 0 \tag{15}$$

$$\frac{dp}{dx} + \rho u \frac{du}{dx} = j_y B_z \tag{16}$$

$$\frac{\gamma}{\gamma - 1} \rho u \frac{d}{dx}\left(\frac{p}{\rho} \right) + \rho u^2 \frac{du}{dx} = j_y E_y \tag{17}$$

These equations are then normalized and solved with a forward marching scheme, starting with the throat conditions and marching to the exit. The flow is supersonic everywhere in the diverging section of the nozzle, which allows for the quasi-steady forward-marching scheme to be employed. Since this model is quasi-steady, there is no numerical time integration, though the time-step between applications of the model is still limited by the speed of sound in the combustion chamber.

When the pressure at the exit drops to sufficiently low levels, a shock will propagate into the nozzle. The forward-marching scheme has no way to detect this condition, hence a separate check of the conditions at the exit is performed. When a shock enters the nozzle, it reduces the local exit velocity and raises the pressure at the exit to become equal to the ambient fluid just outside the nozzle.

Transient flow in the bypass-tube involves a shock created by the nozzle exhaust, traveling into the bypass exit and propagating to the left into a high speed right-moving flow. Quasi-steady forward-marching methods are thus not adequate for these regimes, especially since this method has a singularity when the flow Mach number is equal to one. For these reasons, a fully transient numerical scheme must be used to simulate flow in the bypass-tube.

In simulating flow in the bypass-tube, the WENO method[13] is used to approximate spatial derivatives, with a stencil including upstream and downstream cells. WENO is an adaptation of the Essentially Non-Oscillatory (ENO) method[12,,19] which uses the conservation laws for high order accuracy with shock capturing capabilities. Artificial viscosity is added via the Local Lax Friedrich (LLF) scheme to avoid entropy violation and reduce dispersion. Temporal integration is performed by a 3rd order Runge-Kutta method, which uses an internally iterative process to achieve fairly large time-steps without loss of high order accuracy. The time-step is regulated by the Courant-Friedrichs-Levy (CFL) condition, which ensures stability by limiting the time-step to a ratio of the cell lengths and sound speeds.

Integration of PDRIME Model Components

The **c**omputation of flow in the combustion chamber and nozzle constituting the PDE is decoupled from that in the bypass-tube. The PDE system simulation does not require input from the bypass-tube simulation and will be discussed first. No components of the engine system have dependence on past time-steps using Cambier's blow-down model. This cycle starts with the initiation of blow-down and ends when combustion chamber pressure reaches a prescribed value (specified by the refill process). At a given time the combustion chamber properties are calculated by the blow-down model, which is only a function of time and system parameters. The conditions in the throat are then determined based on chamber properties. The flow in the diverging section of the nozzle is then found by marching forward from the throat, where the properties are known, to the exit. The maximum allowable time-step is then calculated; time is increased, and the blow-down model again calculates combustion chamber properties. The cycle continues until the chamber pressure is reduced far enough or until shock conditions are detected.

Each cycle may be simulated for specific ambient conditions dictated by altitude. For the engine system, altitude affects pressure downstream of the nozzle, and changes the thrust calculated by equation (1), via changes in P_a. The PDE code thus stores exit pressure and Mach number as a function of time, as well as total impulse and energy extracted for every altitude and engine system configuration. The bypass-tube is then employed and coupled with a specific engine system simulation. The bypass model is run using the specified altitude to determine inlet conditions. The exit pressure from the PDE system is used as a time dependent boundary condition for the downstream end of the bypass-tube. The energy applied in the bypass-tube to accelerate the air is limited to the energy extracted from the engine system at that time during the cycle. At the end, the net impulse arising from flow in both systems over one cycle is found. The speed at which the vehicle travels is the only independent variable in the bypass-tube and dictates the inlet velocity or Mach number.

Two-Dimensional Transient Simulations

As a means of validating many of the assumptions that enter in to the quasi-1D simulations of the PDRIME configuration, corresponding simulations of two-dimensional flow in the nozzle, bypass tube, and exterior region have been conducted by Zeineh[20]. These simulations employ a simplified representation of the blow-down process as done in the present modeling, but then employ a 5th order WENO scheme for spatial discretization and a 3rd -order Runge-Kutta scheme for time integration, as done in He and Karagozian[10,11], to resolve the detailed evolution of flow beyond the nozzle throat and exterior to the PDRIME. This allows assumptions pertaining to the transmission of the shock from the nozzle to the bypass tube, for example, to be validated.

Model Validation

This section shows the steps taken to ensure that, despite the many simplifications utilized in these simulations, the results reasonably accurately reflect the performance of a PDRIME system. Thrust estimation from flow properties may be derived from the momentum fluxes in the problem. For PDREs, the contributions of the transient term in the momentum conservation equation are observed to be negligible, a result of the blow-down approximation with a small throat area.

As noted previously, to reduce computational costs the present model represents the PDE cycle by a constant volume reaction followed by a blow-down period. The validity of this model depends on the throat cross-sectional area. A large throat area will allow propellants to leave the combustion chamber as the detonation wave propagates through it, hence this will not produce a constant volume reaction. A smaller throat area (compared with the cross-

sectional area of the chamber) can limit the amount of mass which escapes until the reflected waves have brought the products in the combustion chamber to conditions resembling the result of a constant volume reaction. Cambier[17] demonstrated that the aforementioned simple blow-down model (with a constant volume reaction) can produce nearly the same computed impulse for the actual pulse detonation reaction with a nozzle, with chamber-to-throat area ratio of 16. The comparison is accomplished by closing the throat in the PDE computation until the reaction has gone to completion and then allowing the reactants to escape. The full quasi-1D PDE cycle starts with reactants being ignited by a detonation wave, whose evolution is simulated numerically using a 4th order piecewise parabolic method (PPM) . These two different methods show good agreement and have consistent trends, hence the present exploration incorporates the Cambier blow-down model in its PDRIME simulations.

Comparison of the simple blow-down model and a quasi-1D, transient numerical simulation of blow-down is also conducted and also shows good agreement. The adiabatic calculation which approximates the conditions at the nozzle throat, based on the combustion chamber properties, can be validated using the quasi-1D numerical code. **Figure 4** shows consistency between the WENO simulation and the rapid blow-down model, but with a slight time lag. This provides us with confidence in replacing the entire numerical domain for the PDE, from combustion chamber to the nozzle throat, with the simplified blow-down model, which provides similar results at a fraction of the computational cost.

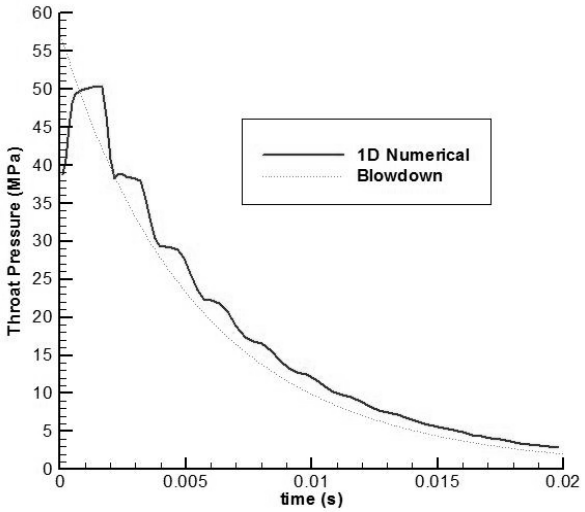

Figure 4: Throat pressure (MPa) as a function of time (s), derived using the numerical, quasi-1D spatially resolved model and the blow-down model.

We finally note that use of a quasi-1D simulation for flow processes associated with a PDE with a nozzle, as compared with results from a fully 2D transient code; yield very similar results for relatively low exit-to-throat nozzle ratios (He and Karagozian[11]). Hence both the blow-down model and quasi-1D portions of the simulation should represent the PDRIME concept quite well.

Results and Performance Evaluation

MHD Energy Generation/Extraction versus Thrust Lost

This section first focuses only on resolving phenomena for the PDE, that is, in the combustion chamber and nozzle. The results of this system are hence independent of the presence of bypass-tube. The impulse and thrust of this system are shown with and without MHD generation to compare the net result of MHD energy extraction from the nozzle on device performance. Extracted energy as well as nozzle exit pressure are quantified as a function of time, to be used as inputs to the bypass-tube computations.

As an example of conditions for PDE operation using the blow-down model, the cycle starts with water vapor products in the combustion chamber at a pressure and temperature of 100atm and 3000K, respectively. The chamber is 0.5m in length and 0.1257m^2 in cross-sectional area with a chamber-to-throat area ratio of 5. The cycle is first assumed to operate at an altitude of 10km and has an exit-to-throat ratio of 35. A magnetic field is uniformly applied (spatially) across the rear half of the diverging section. The strength of the magnetic field is varied with time to maximize energy extraction while keeping the flow at the exit supersonic, at a specified Mach number of 1.2. For this cycle the strength of the applied magnetic field, B as a function of time is shown in **Figure 5**.

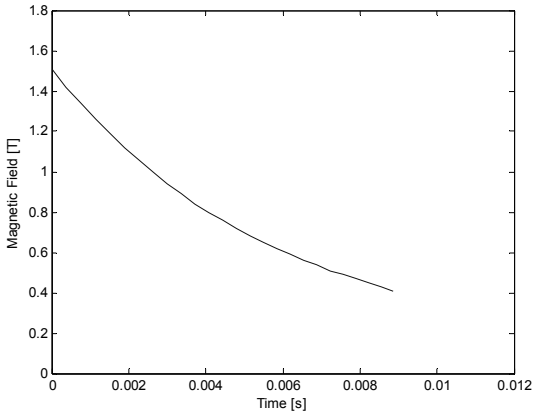

Figure 5: Magnetic field applied across the divergent section, in units of Tesla, as a function of time.

The applied magnetic field must be reduced in time as the chamber pressure decays in order to maintain a constant exit Mach number for the present computation. The applied magnetic field shown in **Figure 5** maximizes the energy extracted while avoiding decelerating the flow to subsonic speeds. **Figure 6** shows the actual Mach number obtained at the nozzle exit on the basis of the applied magnetic field shown in **Fig. 5**.

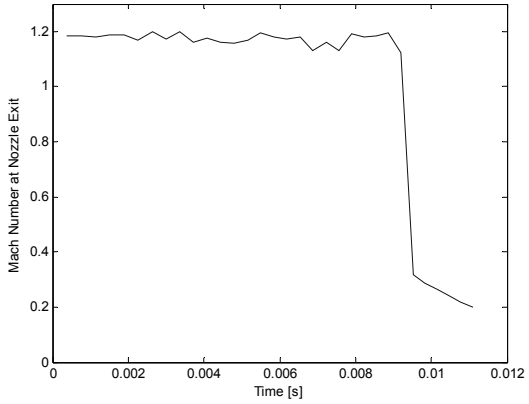

Figure 6: Nozzle exit Mach number as a function of time, computed from the blow-down model for the applied magnetic field shown in **Fig. 5**.

Note that at a time of about 9ms, a shock does enter the nozzle, indicated by the drop in the exit Mach number in **Fig. 6**. This shock is a result of a reduced dynamic pressure at the nozzle exit from the blow-down pressure decay and not a result of MHD application. The magnetic field is turned off when this shock occurs. This particular system operates at a relatively high ambient pressure and with a high exit-to-throat ratio. Both factors contribute to the formation of a shock. This will not occur with most other configurations.

The effect of the MHD generation/extraction on the Mach number within the nozzle flow is shown in **Figure 7**. At time t = 2.3ms, the plot shows Mach number, starting at the throat of the nozzle where the flow is sonic and ends at the nozzle exit. No MHD is applied in the first half of this section to allow the flow to be accelerated, since energy extraction at high velocities is beneficial. A spatially uniform magnetic field is applied to the downstream half of the diverging section, with temporal variation as shown in **Figure 5**. The energy extracted and drag created by the MHD generator lowers the Mach number. Without the MHD generator the flow would be accelerated to Mach ~ 4, but the flow is only Mach 1.2 (by design) with the generation at the nozzle exit. This greatly reduces the impulse for the PDE, as momentum flux is the main component of thrust for this type of configuration. The Lorentz force and joule heating do raise the pressure in this divergent section, and at the exit at the time shown in **Fig. 7**, the exit pressure with MHD generation is 6 times higher than without the MHD. A lower exit Mach number increases the shock angle of the exhaust and increases the PDE's ability to have a shock travel into the bypass-tube.

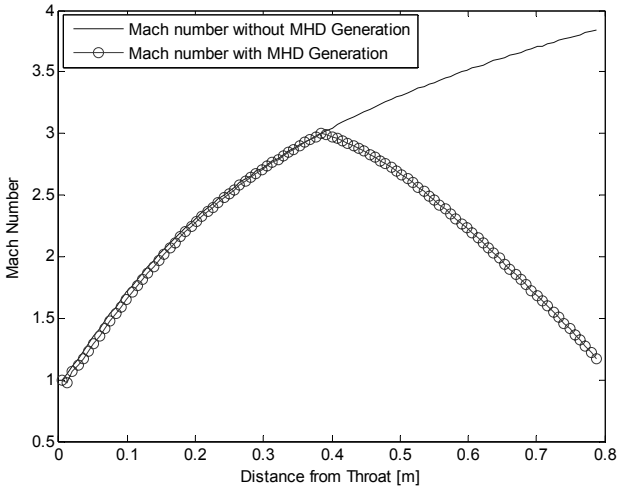

Figure 7: Mach number spatial evolution in the divergent section of the nozzle as a function of distance from the nozzle throat, at time 2.3ms. Results are shown for the PDE (blow-down model) with and without MHD generation in the region between 0.4 and 0.8m from the throat.

The six-fold exit pressure increase due to MHD generation is not enough to overcome the drag imparted on the system by the Lorentz force. **Figure 8** plots the overall impulse versus time with and without the MHD generation, as well as energy extracted (generated). There is a 40% loss of impulse due to the MHD generation in the nozzle for these conditions, but over 3 MJ may be extracted from this process for operation of the PDRIME.

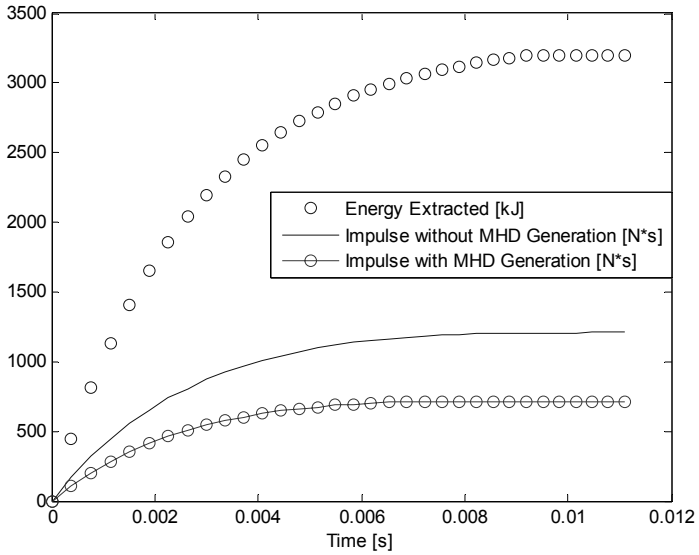

Figure 8: Energy extracted and impulse with and without MHD generation, plotted as a function of time, for the PDE (blow-down model).

The results of the PDE/blow-down model are then input into the bypass-tube model. There it can be determined whether this generated energy can be used to improve the net impulse of the system. This performance will be explored in a later section. At 6.8ms into blow-down, the chamber pressure is $1/10^{th}$ of its initial value. By this time, as seen in **Fig. 8**, nearly 100% of the impulse of this cycle has been produced and 95% of the energy has been generated. This is potentially a time at which the combustion chamber can start to be refilled with reactants.

The chamber pressure after a constant volume reaction is dependent on the pre-reaction pressure and temperature, assuming a fixed mass and volume. To achieve a ten-fold pressure increase during combustion, the initial temperature of the reactants must be 300K. Higher pressure increases are created by lowering the initial

temperature proportionally. The design trade-off is then average thrust versus required filling pressure. The total impulse of each cycle is relatively independent of the filling choice. However, filling at higher chamber pressures allows the filling process to start sooner, increasing the average thrust but requiring more elaborate pumping, something the basic PDE itself is supposed to avoid. At 10.8 ms, the chamber pressure is reduced to $1/30^{th}$ of the initial value. A 30-fold pressure increase can be achieved with reactants filled at 100K. Depending on the application, this 4ms increase in blow-down time may be beneficial.

For every PDE configuration there are four important results to examine in the PDRIME concept. First, the impulse per cycle without MHD augmentation is recorded as a baseline. Next, both impulse per cycle with the MHD generation in the nozzle, as well as the energy generated, are also quantified. Lastly, the pressure at the exit of the nozzle is saved as a function of time.

The effect of the exit-to-throat area ratio and the altitude of operation for the PDRIME system may thus be explored for the PDE itself with a fixed combustion chamber geometry and an initial chamber pressure of 100atm. Cases with alternative initial chamber pressure conditions were run, as were cases with different chamber volumes while holding the initial chamber pressure constant. This latter instance increases the total mass of propellants used per cycle, but it makes little difference in specific impulse results. Initial combustion chamber pressure does have an impact on performance which is not fully explained by the proportional increase in propellant mass per cycle required to achieve it. This will be discussed further below. For the results in this section, the initial chamber pressure is held constant. Chamber pressure does proportionally change the nozzle exit pressure, of course.

Figure 9 plots the impulse per cycle of the PDE itself (via the blow-down model) for different values of the exit-to-throat area ratio and for different altitudes, without MHD generation and without the presence of the bypass tube. It should be noted that the ambient pressure is approximately halved with an altitude increase of 5km. At roughly ground level, where the ambient pressure is highest, the impulse is lowest due to the high drag ($P_a >> P_e$ in equation 1). The optimal exit-to-area ratio for this altitude is five. Similar to constant-pressure rockets, as the ambient pressure is decreased, higher exit-to-throat area ratios are preferred, as the flow can be further expanded so as to equal the ambient pressure. At altitudes in excess of 15km, no maximum is achieved within this area ratio range. Due to the quasi 1-D approximation, momentum losses due to non-streamwise velocities are not accounted for. At large area ratios this will significantly reduce impulse. In addition, heavier nozzles required to achieve larger area ratios will counteract gains. These cycles all use 0.46kg of propellants. Here an impulse I of 1,000N*s corresponds to a specific impulse Isp of 221s.

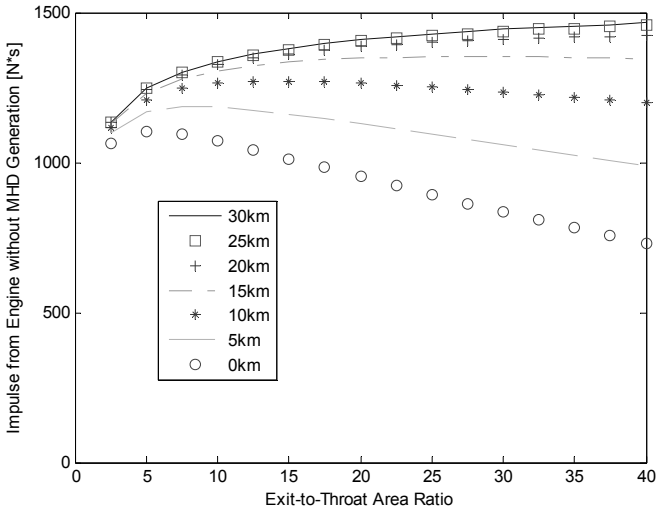

Figure 9: Total impulse as a function of exit-to-throat area ratio for various altitudes, for a single cycle PDE without MHD generation or augmentation.

MHD generation via a Lorentz force exerted on the propellant in the nozzle during energy extraction reduces the impulse of the engine system. **Figure 10** plots the impulse per cycle of the PDE, as a function of exit-to-throat ratio, with MHD generation in the nozzle's divergent section but without accounting for flow in the bypass tube. As seen in the figure, the greatest impulse reductions occur with the larger area ratios, due to the higher velocities and larger areas over which MHD is applied. These factors also lead to a larger amount of energy being extracted from the flow.

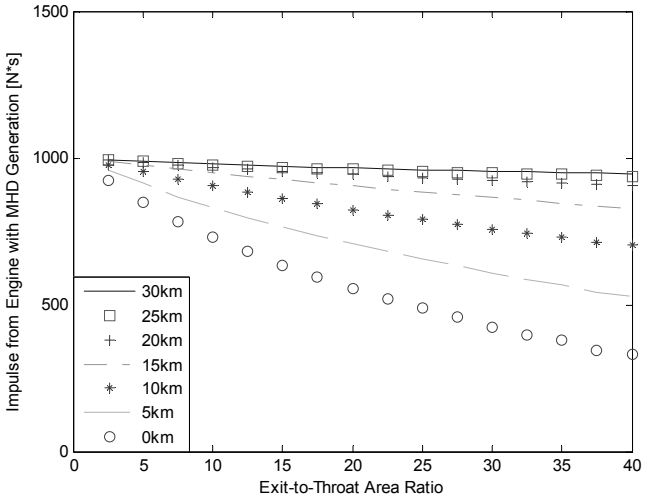

Figure 10: Impulse as a function of exit-to-throat area ratio for various altitudes for a PDE with MHD generation in the nozzle.

Figure 11 plots the energy generated by MHD in the nozzle as a function of nozzle exit-to-throat area ratio. The energy extracted in the nozzle strongly increases with increase exit-to-throat area ratio. Above 5km these are fairly independent of altitude. At lower altitudes the formation of shocks in the nozzle at high area ratios prematurely ends the energy extraction process. A comparison of energy generated per impulse lost, measured as the difference between impulse without and with MHD generation, yields approximately 6.3 [kJ/N*s] for all area ratios and altitudes.

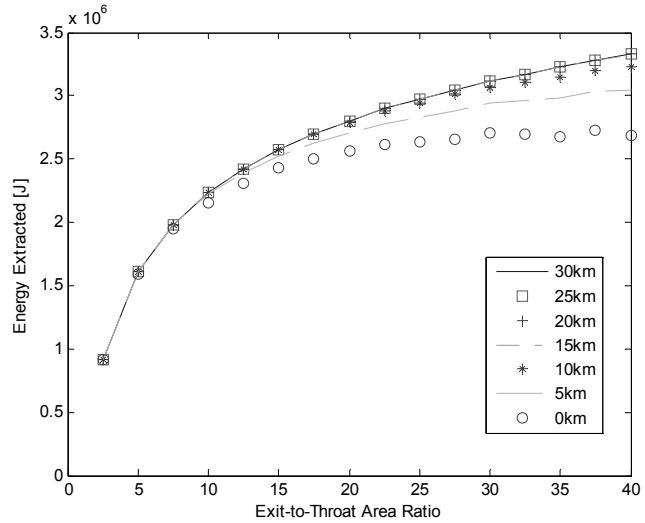

Figure 11: MHD energy generated in the nozzle as a function of exit-to-throat area ratio at different altitudes

At higher altitudes (20 km and above), **Figure 10** shows the impulse per cycle is nearly constant versus given area ratio. More energy is extracted at higher area ratios and this would appear to be the favorable configuration. However, this extra energy cannot be applied because of lower PDE nozzle exit pressures. **Figure 12** plots nozzle exit pressure versus time for different exit-to-throat area ratios at an altitude of 20km. The initial exit pressure for an area ratio of 2.5 is 9 times larger than for the area ratio 22.5 and 5 times greater than for the area ratio 12.5. In order to apply this extracted energy to the bypass-tube section, a shock must be produced to slow the flow in the bypass-tube. Low PDE nozzle exit pressures will not create strong enough (or any) shocks. All altitudes higher than 20km will have identical exit pressure profiles, as the ambient pressure is too low to allow formation of a shock

in the nozzle, which would disrupt blow-down. The results in **Fig. 13** suggest that lower nozzle area ratios could be more appropriate for PDRIME performance improvements.

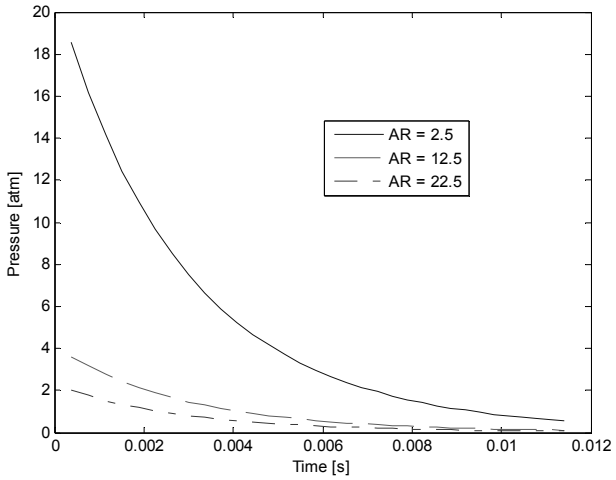

Figure 12. PDE nozzle exit pressure as a function of time for different exit-to-throat area ratios, with MHD generation in the nozzle.

For a given area ratio, the exit pressure can be proportionally increased by increasing the initial chamber pressure. Holding the post-reaction temperature in the chamber constant at 3000K dictates that an increase in initial chamber pressure also increases density proportionally. For all initial chamber pressures where nozzle shocks do not occur, energy extracted behaves identically as a function of area ratio when normalized by initial mass. While PDE impulse per cycle per mass does not behave the same for different initial chamber pressures at the same altitude, the values of specific impulse per cycle, for equal initial chamber to ambient pressure ratios, are equivalent. **Figure 13** plots the specific impulse, Isp, per cycle for initial chamber pressures of 100 and 200 atm at several different altitudes, thus producing different chamber-to-ambient pressure ratios. This result allows quick estimates of extracted energy, impulse per cycle and exit pressure versus time to be obtained for different initial chamber pressures, information that allows computation of PDE impulse.

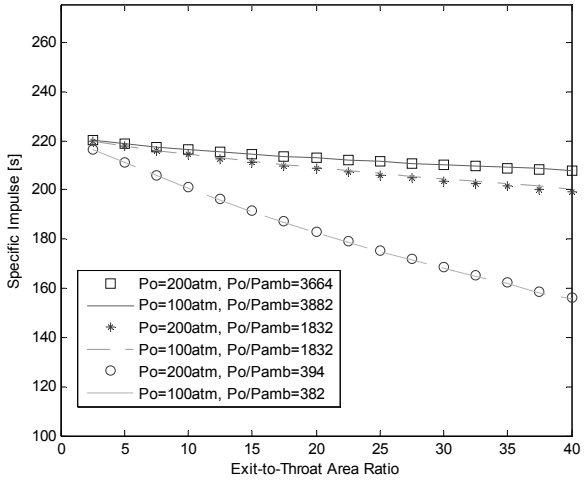

Figure 13. Specific impulse (Isp) per cycle for different initial PDE chamber to ambient pressure ratios.

PDRIME Behavior

To study the overall PDRIME concept, the PDE model results may be used as input for bypass-tube computations. The energy extracted from the PDE is used to power an MHD accelerator in the bypass-tube to create additional thrust. The performance of the whole system is analyzed.

As a 0^{th}-order approximation to this process, the pressure at the downstream end of the bypass-tube is set equal to the recorded PDE exit pressure. In reality the exhaust expands as it exits the PDE nozzle, reducing pressure, thus this 0^{th} order approximation is clearly an over-estimation. The actual phenomena associated with shock transfer from the nozzle to the bypass section are explored separately using 2D transient WENO simulations, discussed later. For now, the best case scenario is assumed. This allows for the validity of this method of augmentation to be shown and important trends to be identified.

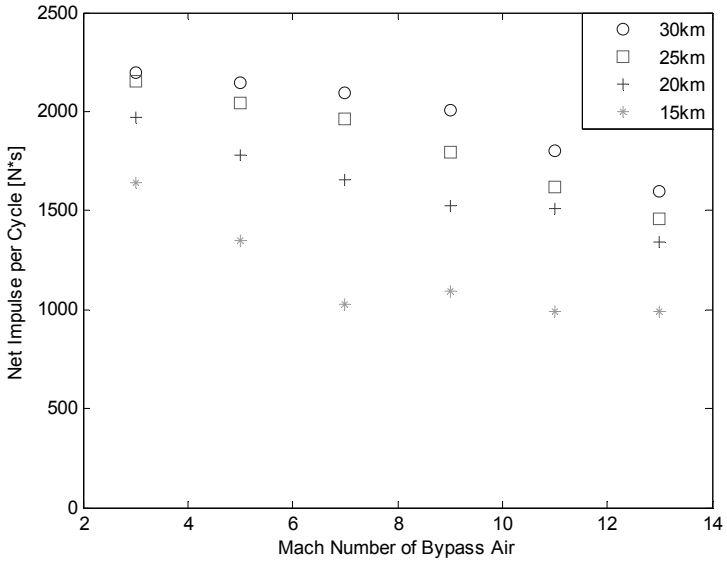

Figure 14: Net impulse of the PDRIME cycle as a function of bypass air Mach number at different altitudes for an exit-to-throat area ratio of 2.5 with a bypass-tube area of $0.09m^2$.

Figure 14 plots the net impulse per cycle of the PDRIME system with an exit-to-throat area ratio of 2.5. Each set of similar marks represent a single PDRIME operating at a fixed altitude at different flight Mach numbers. A net impulse of 2,200N*s is achieved at two different altitudes. One set of operating conditions where this is achieved is at an altitude of 25km where the vehicle is traveling at Mach 3 (the inlet Mach number for the bypass tube). This corresponds to a specific impulse of 489s, more than a 60% increase in impulse over any non-augmented PDE configuration with the same geometry, and shows potential for the PDRIME concept.

There are several factors which contribute to the range of inlet Mach numbers and altitudes for which the PDRIME can be effective. At low flight Mach, the shock in the by-pass tube may not be strong enough to raise the temperature of the air above 3000K in order to be able to achieve thermal ionization of the injected Cesium seed. Yet at large flight Mach numbers (and sufficiently low altitudes) the total pressure of the air stream can become too large, and no shock can enter the bypass-tube. Low altitudes are specially challenging, due to both pressure and temperature jump constraints; at altitudes below 15km the PDRIME system does not appear to be viable, at least for peak PDE chamber pressures of the order of 100 atm.

If the exit pressure of the PDE nozzle is too low, no combination of altitude and Mach number can be successful. Even if a shock can be formed in the bypass section, it will not generate the require temperature gain. **Figure 15,** for example**,** plots the net impulse per cycle of the PDRIME system for only the PDE portion with an exit-to-throat area ratio of 7.5, producing a high Mach number and relatively low pressure at the nozzle exhaust; the resulting impulse is over a factor of two below that for the nozzle with area ratio 2.5, shown in **Fig. 14**. This illustrates the principal difficulty of this system and its need for high nozzle exit pressure. Even when assuming no pressure loss or expansion as the shock travels from the nozzle exit to the downstream end of the bypass section, the net impulse is relatively low; the system is in fact ineffective for exit-to-throat areas exceeding 5.

Weak exit pressures reduce total net impulse in three ways. First, the lower pressures fail to keep the shock in the bypass-tube at higher Mach numbers. Second, the lowered pressure ratio results in less of a temperature jump across the shock entering the bypass section, making seeding difficult. Third, the velocity of the air behind the bypass-tube shock is higher for lower pressures across the entering shock. These higher velocities in the tube require more energy to be applied to produce the same addition impulse.

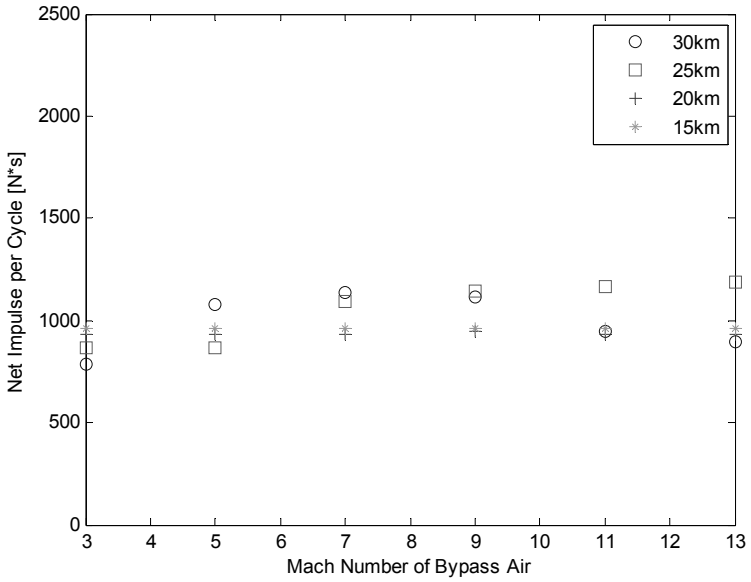

Figure 15: Net impulse of the PDRIME cycle as a function of bypass air Mach number at different altitudes for an exit-to-throat area ratio of 7.5 with a bypass-tube area of 0.09m^2.

The effect of the cross-sectional area of the bypass-tube is now considered. First this will be examined while maintaining the pressure match between the exit of the PDE nozzle and the exit of the bypass-tube. **Figure 16** plots the net impulse of the PDRIME cycles at an altitude of 25km for different cross-sectional areas of the bypass-tube. There is a clear trend indicating that the higher the bypass-tube area, the greater the net impulse of the cycle. Recall that the energy applied is proportional to velocity squared. When MHD acceleration is applied, a Lorentz force is exerted on the air in the nozzle as an equal and opposite force to that which acts on the bypass-tube magnets providing thrust. If the bypass-tube area is large, most of the energy can be applied before the air is accelerated to very high velocities where MHD acceleration becomes inefficient.

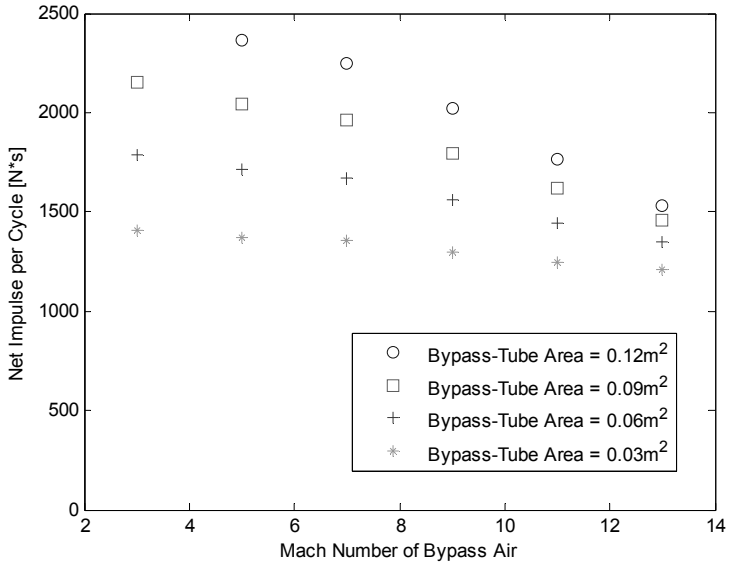

Figure 16: Net impulse of the PDRIME cycle as a function of bypass air Mach number at different bypass-tube areas for an exit-to-throat area ratio of 2.5 at an altitude of 25km, assuming no shock pressure losses associated with flow from the nozzle exit to the bypass exit.

The exit area of the PDE used in **Figure 17** is 0.06m^2. The ability of the nozzle exhaust to send a shock into the bypass-tube will surely be a function of the bypass-tube cross-sectional area. To put a theoretical limit on the bypass-tube area, the energy of the exhaust flow may be quantified. The exit pressure for the quasi-1D simulation represents the entire pressure across the nozzle exit. If this is viewed as a type of energy density, when the exhaust leaves the nozzle and expands vertically across the bypass-tube exit, the maximum pressure that can be present at the bypass-tube exit could be considered to be the "new" energy density, which accounts for this expansion via the relation:

$$p_{by} = \left(\frac{A_e}{A_e + A_{by}} \right) \cdot p_e \tag{18}$$

where p_{by} is the pressure applied to the exit of the bypass-tube accounting for the bypass section's cross-sectional area, A_{by}, and the nozzle exhaust area, A_e. This expression is still an over-estimation of the pressure at the bypass tube exit because it assumes uniform pressure in the transition from the center of the nozzle exit to the top of the bypass-tube. **Figure 17** shows the variation in net impulse for the PDRIME as a function of flight Mach number for different bypass tube cross-sectional areas. In comparison with the more idealized performance shown by the results in **Figure 16**, there is a considerable drop in impulse, in some cases by a factor of two. It is clear that the benefits of larger bypass-tube areas are canceled by the more realistically low average pressure across the tube's exit.

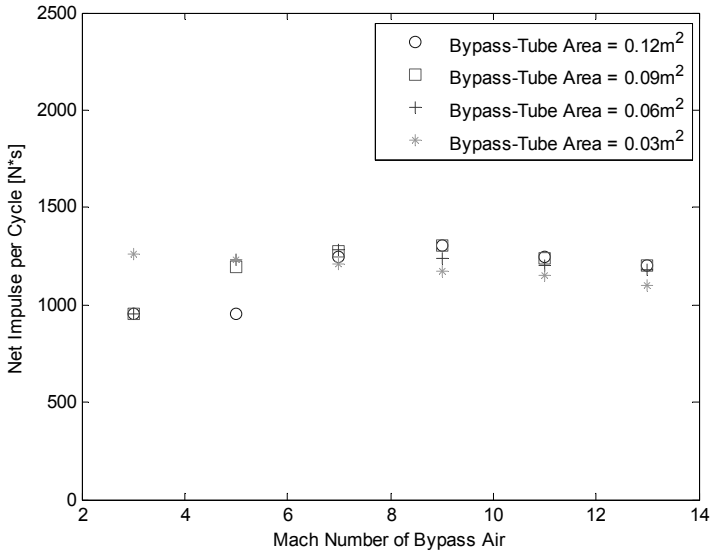

Figure 17: Net impulse of the PDRIME cycle as a function of bypass air Mach number at different bypass-tube areas for an exit-to-throat area ratio of 2.5 at an altitude of 25km, accounting for expansion pressure losses via (18).

As noted previously, a comparison of results from the present simplified blow-down model and quasi-1D nozzle and bypass tube simulations to represent the PDRIME configuration may be made with a more realistic, 2D transient simulation of nozzle, external flow, and bypass tube flow and MHD processes. The transmission of the shock from the nozzle exit to the end of the bypass tube is one obvious phenomenon to explore, given the approximations leading to the differing results in **Figures 16 and 17**. For example, using the 2D transient simulation, it is observed that, for the PDRIME configuration with a nozzle area ratio of 2.5 operating at Mach 10 and at an altitude of 30 km, the shock exiting the nozzle does propagate into the bypass tube and travel upstream. But it is observed in this case that the temperature in the bypass section does not exceed 3000K, a requirement for ionizing seeded Cesium in the tube. Hence a slightly altered PDRIME geometry, one where the upper wall is extended by 0.4 m, is considered in these simulations. This altered system allows the shock to be directed and captured more fully into the bypass tube, and correspondingly allows the temperature there to increase, exceeding 3000K. A comparison of the temperature fields at the same time for both configurations is shown in **Figure 18**. Since the presence of the upper wall would not have an effect in the idealized, inviscid quasi-1D model results, the configuration with the extended upper wall will be used in the 2D simulations for further comparisons.

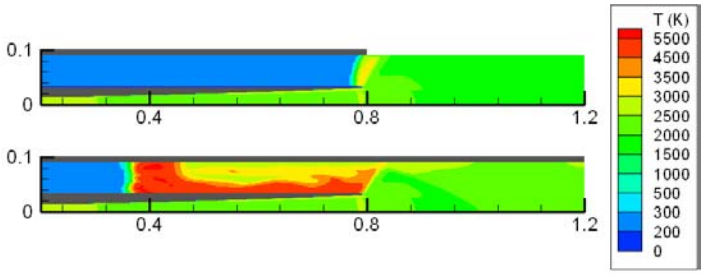

Figure 18: 2D temperature field contours for the upper part of the PDE section and the bypass section, at a time t = 0.6 ms after the start of the blowdown process. Both images show a PDRIME geometry with MHD generation in the nozzle but without energy application in the bypass section, but the lower image has a 0.4 m extension to the upper wall of the bypass section; the upper image does not. The flight Mach number is 10 at altitude 30 km, the nozzle area ratio is 2.5 and the bypass section cross-sectional area is 0.06 m^2.

Figures 19 and 20 show the predicted evolution of the pressure and temperature fields, respectively, for the PDRIME with MHD generation in the nozzle and with energy application in the bypass tube, for a geometry that includes the bypass upper wall extension. A shock structure is observed to transition from the nozzle to the bypass tube before being forced back downstream under the influence of both the Mach 10 inlet flow and the MHD accelerator.

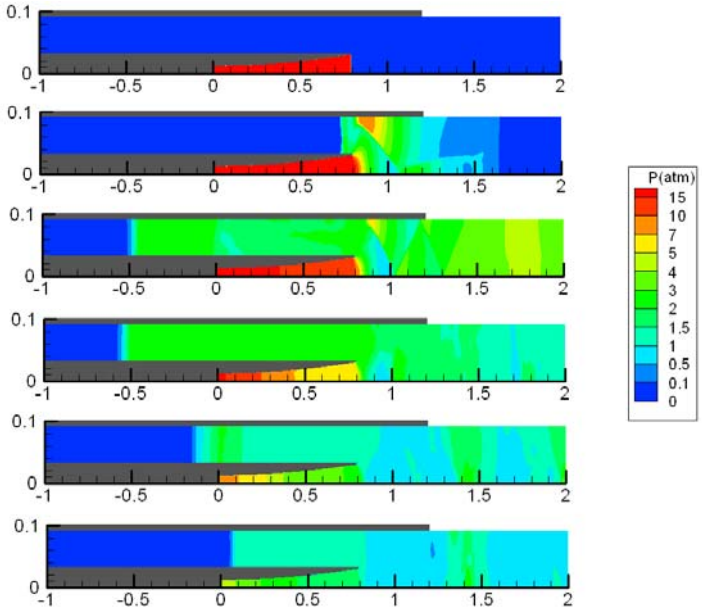

Figure 19: 2D pressure (in atm) field contours for the upper part of the PDE section and the bypass section, at different times after the start of the blowdown process (top to bottom, t = 0.0 ms, 0.2 ms, 2.0 ms, 4.0 ms, 6.0ms, and 8.0 ms). Results are for a PDRIME geometry with MHD generation in the nozzle and with energy application in the bypass section. The flight Mach number is 10 at altitude 30 km, the nozzle area ratio is 2.5 and the bypass section cross-sectional area is 0.06 m^2.

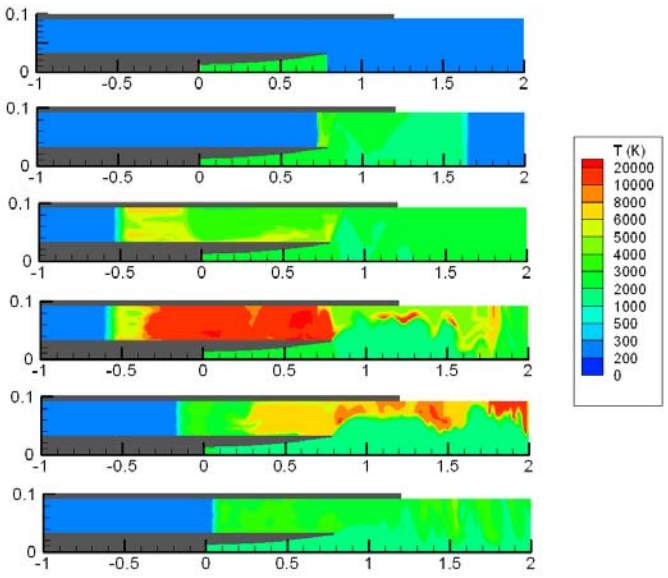

Figure 20: 2D temperature (in K) field contours for the upper part of the PDE section and the bypass section, at different times after the start of the blowdown process (top to bottom, t = 0.0 ms, 0.2 ms, 2.0 ms, 4.0 ms, 6.0ms, and 8.0 ms). Results are for a PDRIME geometry with MHD generation in the nozzle and with energy application in the bypass section. The flight Mach number is 10 at altitude 30 km, the nozzle area ratio is 2.5 and the bypass section cross-sectional area is 0.06 m^2.

The temperature plot in **Fig. 20** illustrates a few sectors of very high-temperature fluid appearing briefly within the bypass tube, a result of the vertical Lorentz forces accelerating the fluid upward and away from the wall, producing a small very low-density region. In reality, viscous forces would likely prevent these regions from forming, while the artificial dissipation inherent to the WENO numerical scheme is likely over-estimating the associated temperature. Since this is an inviscid simulation and since artificial dissipation is necessary for properly capturing shocks, we prevent the temperature from rising to unrealistic degrees by setting the accelerator to induce force on a fluid cell only if its temperature lies below 15000K. The nozzle/bypass exit pressure evolution indicates that after the bypass has begun pushing back the shock, the bypass tube exit pressure p_{by} is roughly half of the nozzle exit pressure, which is consistent with the approximation in eqn. (18). Yet at the earlier stages of the cycle, this loss factor is below the value predicted by eqn. (18).

Magnetic Piston Effects

The Magnetic Piston MHD augmentation concept (see **Fig. 3**) extracts energy in the divergent section of the nozzle and applies a portion of this energy in the combustion chamber to effectively reduce the chamber volume and keep the chamber pressure constant. This avoids the decay in chamber pressure during the blowdown portion of the cycle and thus increases the PDE nozzle exit pressure. This is desired in the PDRIME concept to help keep a shock in the bypass-tube. **Figure 21** plots the PDE nozzle exit pressure as a function of time for a nozzle of area ratio 2.5 operating at an altitude of 25km and compares this exit pressure with that for a PDE operating at similar conditions with a magnetic piston in the chamber. This shows that the PDE exit pressure can be maintained at a constant level instead of decaying. The magnetic piston does shorten the length of the cycle, however (from about 5.5 msec to 3 msec). The higher chamber pressure forces the propellants through the throat faster, and once they are exhausted, the pressure at the exit will rapidly drop to ambient.

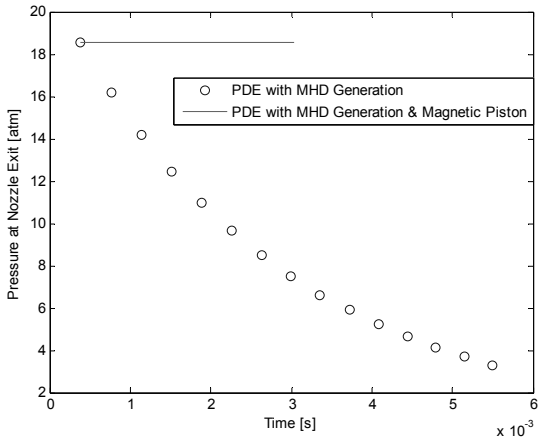

Figure 21 PDE nozzle exit pressure versus time for a with and without magnetic piston operating in the combustion chamber for PDEs with a exit-to-throat area ratio of 2.5.

Figure 22 plots the impulse per cycle of the PDE for a range of exit-to-throat area ratios for several alternative configurations. The square symbols show the results for the PDE itself without bypass and with no MHD generation. The star symbols represent impulse for the PDE with MHD generation in the nozzle but without application of the extracted energy in the bypass tube or for a Magnetic Piston. The solid line shows impulse for the PDE with MHD generation in the nozzle and with partial energy application toward the Magnetic Piston (the remainder is available for application in the bypass tube).

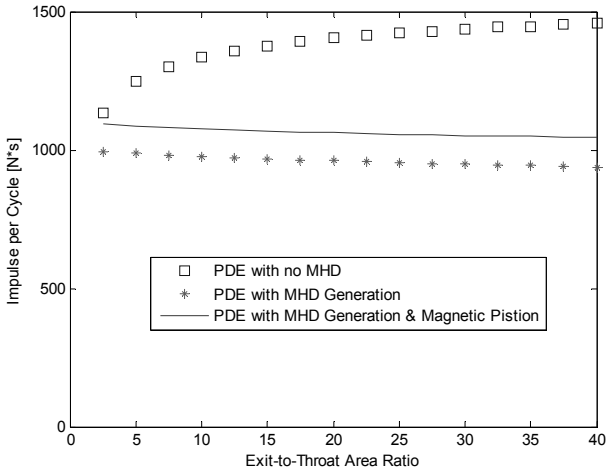

Figure 22: Impulse per cycle at an altitude of 25km of PDEs for a range of exit-to-throat area ratios. Results are shown for the configurations of the PDE with no MHD generation in the nozzle (square symbols), the PDE with MHD generation but without application of the extracted energy in the chamber (star symbols), and MHD generation in the nozzle with partial energy application in the chamber (solid line).

It can be seen from **Figure 22** that in addition to increasing the PDE nozzle exit pressure, the Magnetic Piston does moderately increase the impulse per cycle via energy application in the chamber. When used alone, not in conjunction with a bypass-tube (the PDRIME concept), the Magnetic Piston's main advantage is its shortening the cycle time, thus increasing the PDE's frequency and average thrust. It should be noted that the energy extracted by the MHD generator in the PDE nozzle is affected by application of energy in the Magnetic Piston. At a nozzle to throat area ratio of 2.5, half of the energy extracted in the PDE nozzle is required to power the Magnetic Piston, although less than 10% of the energy extracted is required for an area ratio of 10. While under these conditions the magnetic piston will improve the ability of the PDE nozzle exhaust to shock the bypass-tube air for the PDRIME

concept, the reduction in available energy to accelerate this air reduces the effectiveness of this combined augmentation strategy.

Overall Performance

Although there are clearly differences between the more realistic flow evolution predicted by the 2D PDRIME simulation and the flow predicted the quasi-1D idealized model, the ultimate difference in PDRIME total impulse is not very large. For the PDRIME configuration with MHD generation and acceleration in the bypass section, the differences between the 2D and quasi-1D computed impulses achieved by the end of the cycle are on the order of 10% or lower. The favorable comparisons between relatively inexpensive, quasi-1D simulation results and the more detailed, computationally expensive 2D results suggest that the former model may be quite suitable for quick performance estimates for various PDRIME configurations.

With the more "realistic" 2D flow simulation, there is actually an overall reduction in impulse seen between the case without MHD thrust augmentation and with MHD in the generator/single bypass system, in contrast to the improvement in impulse observed by the quasi-1D simulation. On the other hand, when a second bypass tube is employed in the 2D simulations (not shown here), below the PDE (thus creating a symmetric configuration), there is an approximate 10% improvement in overall impulse observed. Splitting the energy extracted from the PDE nozzle between bypass-tubes above and below the PDE allows the energy to be applied at low velocities, effectively doubling the bypass-tube area without reducing the pressure by its exit. Additional 2D computations described by Zeineh[20] suggest that the added effect of the "magnetic piston" in the chamber, in addition to the PDRIME bypass configuration, can yield further increases in impulse, that is, when energy extraction from the nozzle is used to accelerate flow in the bypass section as well as to accelerate products out of the combustion chamber. Further exploration of these alternative MHD thrust augmentation concepts is ongoing.

Discussion and Conclusions

The present simulations do suggest that the PDRIME system may have some potential for an increase in both impulse and specific impulse, but serious difficulties remain to be resolved . Under idealized, optimal conditions, a possible 60% increase in these performance parameters is observed, but only under the assumption of matching pressure in the nozzle exit and the bypass-tube exit. Under the still idealized energy density conditions assumed via eqn (18) for the area difference between the nozzle exit and the bypass tube, the net improvement is greatly decreased, but comparisons with full 2D simulations suggest that this reduced performance may be a reasonable approximation for actual performance.

The potential benefits of the PDRIME system are mainly seen for low exit-to-throat area ratios, 2.5, due to the reduction in exit pressure from further expansion. Yet the impulse gained by the PDRIME system is strongly dependent on the area of the bypass-tube and the exit pressure applied to its exit. With the idealization of the nozzle exit pressure boundary condition applied to the bypass-tube held constant, larger areas lead to larger impulse improvements, due to the larger amount of energy which can be applied before this acceleration brings the bypass air to high velocities. The bypass-tube area is limited by the decrease in average pressure which occurs as its cross-sectional area is increased. This relationship between average pressure and area makes this concept seem unlikely to create great improvement in net impulse over standard PDEs with larger area ratios. On the other hand, this concept may be able to provide modest impulse gains at high altitudes. At low altitudes the MHD energy transfer mechanisms can be disengaged. Due the low area ratio required for the PDRIME, drag as a result of high ambient pressure could be mitigated. The PDRIME system would thus be best suited for low and high altitude flight.

The PDRIME concept may achieve more of its high potential by inventive methods for increasing the pressure at the exit of the bypass-tube. One method is a extending the top wall of the bypass-tube to trap the exhaust from the nozzle exit, as shown in **Fig. 18** and subsequent images, or by employing a second bypass tube, or by also employing a magnetic piston with the PDRIME, all of which are being explored in greater detail by Zeineh[19]. There are thus a range of alternative configurations to explore in assessing the benefits of MHD thrust augmentation for propulsive devices.

Acknowledgments

The authors wish to acknowledge the technical assistance of Dr. Xing He of the UCLA Department of Radiological Sciences in performing the 2D transient simulations, and by Mr. Lord Cole of the UCLA MAE Department in performing the quasi-1D simulations described in this work. This research has been supported at UCLA by the Air Force Office of Scientific Research under the space power and propulsion program managed by Dr. Mitat Birkan

(Grants FA9550-07-1-0156 and FA9550-07-1-0368). Grant management by Dr. Andrew Ketsdever of the Air Force Research Laboratory at Edwards, CA (AFRL/RZSA) is also gratefully acknowledged.

References

[1] J.-L. Cambier, "MHD Augmentation of Pulse Detonation Rocket Engines", 10th Intl. Space Planes Conf., Kyoto, Japan, April 2001, AIAA paper 2001-1782.
[2] Hill, P. and Peterson, C., **Mechanics and Thermodynamics of Propulsion**, 2nd Edition, Addison-Wesley publishing company, 1992.
[3] Kailasanath, K., and Patnaik, G., "Performance Estimates of Pulse Detonation Engines," ***Proceedings of the Combustion Institute***, Vol. 28, 2000, pp. 595–602.
[4] Cooper, M., and Shepherd, J. E., "The Effect of Nozzles and Extensions on Detonation Tube Performance", AIAA paper 02-3628, 38th AIAA/ASME/SAE/ASEE Joint Propulsion Conference, July, 2002.
[5] Cooper, M. and Shepherd, J. E., "Single Cycle Impulse from Detonation Tubes with Nozzles", ***Journal of Propulsion and Power,*** Vol.24 no.1, 2008, pp. 81-87.
[6] Eidelman, S., Grossmann, W., and Lottati, I., "Review of Propulsion Applications and Numerical Simulations of the Pulse Detonation Engine Concept," ***Journal of Propulsion and Power***, Vol. 7, No. 6, 1991, pp. 857–865.
[7] Wintenberger, E., Austin, J. M., Cooper, M., Jackson, S., and Shepherd, J. E., "An Analytical Model for the Impulse of a Single Cycle Pulse Detonation Engine," ***Journal of Propulsion and Power***, Vol. 19, No. 4, 2003, pp. 22–38; also ***Journal of Propulsion and Power***, Vol. 20, No. 4, 2004, pp. 765–767.
[8] Li, C., and Kailasanath, K., "Partial Fuel Filling in Pulse Detonation Engines," ***Journal of Propulsion and Power***, Vol. 19, No. 5, 2003, pp. 908–916.
[9] Warwick, G., "U.S. AFRL proves pulse-detonation engine can power aircraft", Flight Magazine, March 5, 2008 (online at http://www.flightglobal.com/articles/2008/03/05/222008/us-afrl-proves-pulse-detonation-engine-can-power-aircraft.html).
[10] He, X. and Karagozian, A. R., "Numerical Simulation of Pulse Detonation Engine Phenomena", ***Journal of Scientific Computing***, Vol. 19, Nos. 1-3, pp.201-224, December, 2003.
[11] He, X. and Karagozian, A. R., "Pulse Detonation Engine Simulations with Alternative Geometries and Reaction Kinetics", ***Journal of Propulsion and Power***, Vol. 22, No. 4, pp. 852-861, 2006.
[12] Harten, A., Osher S. J., Engquist, B. E., and Chakravarthy, S. R., "Some Results on Uniformly High-Order Accurate Essentially Nonoscillatory Schemes", ***J. Appl. Numer. Math.***, Vol. 2, pp. 347-377, 1986.
[13] Jiang, G. S. and Shu, C. W., "Efficient Implementation of Weighted ENO Schemes", ***Journal of Computational Physics***, Vol. 126, pp. 202-228, 1996.
[14] Cole, J., Campbell J., Robertson A., "Rocket-Induced Magnetohydrodynamic Ejector – A Single-Stage to Orbit advanced propulsion concept", AIAA Space Programs and Technology Conference, Huntsville, Sept. 1995: AIAA paper 1995-4079.
[15] Cambier, J.-L., "A Thermodynamic Study of MHD Ejectors", 34th AIAA/ASME/SAE/ASEE Joint Propulsion Conference, 1998, AIAA 98-2827.
[16] Hwang, P., Fedkiw, R. P., Merriman, B., Aslam, T. D., Karagozian, A. R., and Osher, S. J., "Numerical Resolution of Pulsating Detonation Waves", ***Combustion Theory and Modelling***, Vol. 4, No. 3, pp. 217-240, September, 2000.
[17] Henrick, A. K., Aslam, T. D., and Powers, J. M., "Mapped Weighted Essentially Non-oscillatory Schemes: Achieving Optimal Order near Critical Points," ***Journal of Computational Physics***, Vol. 207, No. 2, 2005, pp. 542–567.
[18] J.-L. Cambier, "Preliminary Model of Pulse Detonation Rocket Engines", 35th AIAA/ASME/SAE/ASEE Joint Propulsion Conference, Los Angeles, June 1999, AIAA paper 1999-2659.
[19] Shu, C. W., and Osher, S., "Efficient Implementation of Essentially Non-Oscillatory Shock Capturing Schemes II", ***Journal of Computational Physics***, Vol. 83, pp. 32-78, 1989.
[20] Zeineh, C., "Numerical Simulation of Magnetohydrodynamic Thrust Augmentation for Pulse Detonation Rocket Engines", Ph.D. prospectus, UCLA Department of Mechanical and Aerospace Engineering, 2008.

JOURNAL OF PROPULSION AND POWER
Vol. 28, No. 1, January–February 2012

Appendix B

Magnetohydrodynamic Augmentation of Pulse Detonation Rocket Engines

Christopher F. Zeineh,* Lord K. Cole,† Timothy Roth,‡ and Ann R. Karagozian§
University of California, Los Angeles, Los Angeles, California 90095-1597
and
Jean-Luc Cambier¶
U.S. Air Force Research Laboratory, Edwards Air Force Base, California 93524

DOI: 10.2514/1.B34146

Pulse detonation engines are the focus of increasing attention due to their potentially superior performance over constant-pressure cycle engines. Yet, due to its unsteady chamber pressure, the pulse detonation engine system will either be over- or underexpanded for the majority of the cycle, with energy being used without maximum gain. Magnetohydrodynamic augmentation offers the opportunity to extract energy and apply it to a separate stream where the net thrust can be increased. With magnetohydrodynamic augmentation, such as in the pulse detonation rocket-induced magnetohydrodynamic ejector concept, energy could be extracted from the high-speed portion of the system (e.g., through a magnetohydrodynamic generator in the nozzle) and then applied directly to another flow or portion of the flow as a body force. This paper explores flow processes and the potential performance of such propulsion systems via high-resolution numerical simulations. In the pulse detonation rocket-induced magnetohydrodynamic ejector, at the appropriate point in the pulse detonation engine cycle, the magnetohydrodynamic energy extracted from the nozzle is applied in a separate bypass tube by a magnetohydrodynamic accelerator, which acts to accelerate the bypass air and potentially impart an overall net positive thrust to the system. An additional magnetic piston applying energy in the pulse detonation engine chamber can also act in concert with the pulse detonation rocket-induced magnetohydrodynamic ejector for separate or additional thrust augmentation. Results show potential performance gains under many flight and operating conditions (as high as a 6% increase in total impulse per cycle) but with some challenges associated with achieving these gains, suggesting further analysis and optimization are required.

Nomenclature

A	=	cross-sectional area
$\mathbf{B}$	=	magnetic field
c	=	speed of sound
$\mathbf{E}$	=	electric field
E	=	energy
$\mathbf{F}_{\text{body}}$	=	body force
F_L	=	Lorentz force
I	=	impulse
$\mathbf{J}$	=	current density
K_x	=	loading factor (x component)
K_y	=	loading factor (y component)
$\dot{m}$	=	mass flux
p	=	pressure
R_m	=	magnetic Reynolds number
T	=	thrust
$\mathbf{u}$	=	velocity vector
x, y, z	=	streamwise, transverse, and axial coordinates
β	=	Hall parameter
γ	=	ratio of specific heats
ρ	=	density
σ	=	electrical conductivity
$\dot{\Omega}_{Cs}$	=	cesium atom reaction source term
$\dot{\Omega}_{Cs^+}$	=	cesium ion reaction source term

Superscript

$*$	=	throat value

Subscripts

byp	=	bypass
cham	=	chamber value
conv	=	converging section
div	=	diverging section
e	=	exit value
open	=	open area downstream of nozzle exit
uwall	=	upper wall downstream of nozzle exit
0	=	initial value

Received 9 October 2010; revision received 20 April 2011; accepted for publication 23 May 2011.

*Graduate Student Researcher, Department of Mechanical and Aerospace Engineering; currently Technical Staff Member, The Aerospace Corporation, El Segundo, California 90245-4609.
†Graduate Student Researcher.
‡Graduate Student Researcher; currently Technical Staff Member, Northrop Grumman Electronic Systems, Azusa, California 91702.
§Professor; ark@seas.ucla.edu. Fellow AIAA (Corresponding Author).
¶Senior Scientist, Aerophysics Branch.

I. Introduction

ROBUST propulsion systems for advanced high-speed airbreathing and rocket vehicles are critical to the future of military missions, including those for global/responsive strike and assured access to space. A novel combined cycle propulsive concept, the pulse detonation rocket-induced magnetohydrodynamic ejector (PDRIME) proposed by Cambier et al. [1], is one of a number of alternative magnetohydrodynamic (MHD) thrust augmentation ideas that could have promise for application to a wide range of advanced propulsion systems. Taking advantage of the periodic engine cycle associated with the pulse detonation rocket engine (PDRE), the PDRIME involves periodic temporal energy bypass to a seeded airstream, with MHD acceleration of the airstream for thrust enhancement and control. The range of alternative MHD-augmented propulsion configurations that could be employed suggests that the

PDRIME type of concept could be applied to supersonic or hypersonic airbreathing systems, space power production for remote sensing systems, and other potential military systems for the mid- to far terms. This paper explores the fundamental flow processes associated with the PDRIME and modifications thereof via numerical simulation.

Liquid rocket engines typically employ a constant pressure reaction, where reactants are continually fed at high pressure into the combustion chamber and a nozzle expands and exhausts the flow, generating thrust for the vehicle. The general expression for the force or thrust acting on an object takes the form

$$\mathbf{F}_{\text{body}} = \frac{\partial}{\partial t}\iiint_V \rho\mathbf{u}\,\mathrm{d}V + \iint_S (\rho\mathbf{u}\cdot\mathrm{d}\mathbf{S})V + \iint_S p\,\mathrm{d}\mathbf{S} \qquad (1)$$

where ρ is the local density, $\mathbf{u}$ is the local velocity vector, and $\mathbf{F}_{\text{body}}$ is the sum of the thrust and any forces acting from outside the control volume over which the integrals are calculated; in the case of the present studies, $\mathbf{F}_{\text{body}}$ includes MHD forces. The control volume can be constructed either around the rocket's interior walls or around the nozzle exit, encapsulating all fluid therein. The former method calculates MHD forces as body forces, while the latter calculates the changes in momentum resulting from these forces. Both methods, which we call the pressure flux and momentum flux methods, produce the same results [2], and we choose to use the pressure in the present study. For a steady flow rocket engine with a solid back wall, Eq. (1) reduces to the standard expression for rocket thrust:

$$T = \dot{m}u_e + (p_e - p_a)A_e \qquad (2)$$

where $\dot{m}$ is the mass flux of gas exiting the nozzle, u_e is the exhaust velocity, A_e is the nozzle exit cross-sectional area, p_a is the ambient pressure, and p_e is the pressure at the exit plane of the nozzle. The total impulse I over the course of an engine cycle is calculated by integrating thrust over time t. The maximum thrust [3] for an engine occurs when the exhaust gases are expanded to the point where the pressure at the exit of the nozzle is equal to the ambient pressure in Eq. (2). Further expansion of the gas in the nozzle will reduce the thrust, as the ambient pressure will then exceed the exhaust pressure, creating pressure drag. This added drag can outweigh momentum gains arising from the further acceleration of the flow from the nozzle, i.e., the increase in exhaust velocity. Underexpansion in the nozzle will result in lower than optimal thrust as the maximum momentum gains are not realized. MHD augmentation is in part designed to recapture some of these losses through modification of the exhaust pressure.

One alternative and theoretically more efficient configuration to the traditional rocket engine is the pulse detonation engine (PDE), a subset of which is the PDRE. The PDE operates in a cycle wherein reactants are mixed into the combustion chamber at low pressure, the mixture is ignited, and a detonation wave propagates across the chamber, raising the pressure and temperature and creating a constant-volume reaction, which is more efficient than a constant pressure reaction [4]. After the detonation wave (or shock wave, after reactants have been consumed) exits the nozzle, a reflected expansion wave propagates into the chamber, lowering the overall pressure throughout the chamber and, upon reflection at the thrust wall, allows reactants to be drawn into the chamber. The reflection of the expansion wave at the nozzle exit results in a compression wave, which can be strengthened to become a shock, igniting reactants in the chamber as a detonation and starting the process once again. A number of studies have explored the reactive flow and performance characteristics of PDEs of various geometries [4–8]. The PDE was recently tested for the first time in flight on a Scaled Composites Long-EZ aircraft [9], with four PDE tubes operating at a cycle frequency of 20 Hz.

In the past, our group at the University of California, Los Angeles [10,11], has explored the influence of PDE geometry, reaction kinetics, and flow processes using high-order numerical methods. A fifth-order weighted essentially nonoscillatory (WENO) scheme [12,13] is used for spatial integration of the reactive Euler equations, with a third-order Runge–Kutta time integration in the case of simplified reaction kinetics; a stiff ordinary differential equation solver was used for temporal integration in complex kinetics simulations. While the simulations using complex kinetics provide useful quantitative data, the simulations with reduced kinetics (a single-step reaction) can in fact provide very similar quantitative performance results.

In general, two different methods could be used to generate thrust for the PDRE. The first involves a straight or slightly contoured nozzle, as examined for the PDE. The main goal of this configuration is to exploit the thrust generation from the reflection of the wave, the ignition of the detonation near the thrust wall, and its propagation through the device, as described above. The second approach is more similar to a constant-pressure rocket. Here, the nozzle throat area A_t is very small: small enough to prevent the main detonation wave from escaping the chamber. This creates multiple reflected compressive waves in the chamber that homogenize the chamber pressurization, resulting in an approximately constant-volume reaction. During the blowdown period, the reactants are driven out from the chamber and through the nozzle. Similar to the constant-pressure rocket, the exhaust gases are expanded, increasing the velocity and reducing the pressure. The difference between this type of PDRE and a constant-pressure rocket is that in the PDRE, the chamber pressure is decreasing throughout the blowdown period as mass is ejected from the chamber, with no immediate replacement. New reactants are added to the combustion chamber once the pressure has been reduced to a specified value, and then the cycle is repeated.

Because of the unsteady nature of the chamber pressure, however, a PDRE nozzle can only be perfectly expanded briefly within a blowdown period. This implies suboptimal use of energy to attain this condition for most of the cycle. At low altitudes, nozzles with large area ratios are subject to large drag forces [$p_a > p_e$ in Eq. (2)], while nozzles with relatively smaller exit areas will be underexpanded for the majority of blowdown. Whether or not the configuration includes a converging section, the lack of perfect matching conditions essentially negates the benefits of a constant-volume combustion [14].

Ejectors are often used to transfer energy from one stream to another stream, providing an additional source of thrust, especially for an airbreathing engine. Ejectors have been shown to produce overall thrust gains when energy is taken from a high-velocity flow and transferred to a low energy stream (in the ejector) that has a high mass flow rate. In the present application for the PDRE, energy can be extracted from the nozzle when the marginal decreases in thrust are small and added to a bypass airflow that acts as an ejector to assist in augmentation of the thrust. Ejectors typically transfer energy between streams through shear stress between separate flow streams, where a portion of the main flow is diverted into a channel to mix with the lower velocity flow. The drawback of this method is that the ability to transfer energy is limited by the contact area and the slow rate of viscous transport between the two streams. At large velocities, shear layer thicknesses are small, leading to the necessity for large channels and/or large interfacial surfaces such as lobed shapes [15] for mixing, which add weight to the vehicle.

In contrast, if MHD forces are applied as body forces to the ejector flow, affecting the entire flowfield immediately, there can be benefits. This could reduce the length of the bypass tube and time necessary for complete energy transfer as well as providing the flexibility of energy extraction and application, since the applied fields can be varied [16]. One possible configuration attaches a converging–diverging nozzle to the combustion chamber of a PDRE with a bypass tube. Just as the AJAX concept [17] proposes to divert energy from an inlet flow by an MHD generator before reapplying it after the combustor via an MHD accelerator, this energy bypass concept could also be applied to the PDRE [16].

A generic configuration for this concept, the PRDIME, is shown in Figs. 1a and 1b , where the interaction between a magnetic field and an electrically conducting fluid flow (MHD) takes place. For the present applications, magnetic and electric fields are both applied normal to each other in the z and y directions, respectively, and

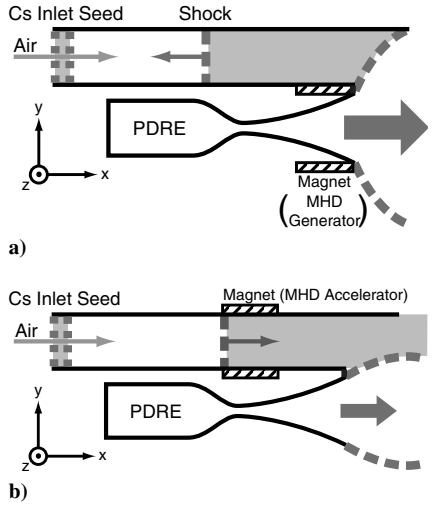

Fig. 1 Schematics of the PDRIME concept: a) During the initial portion of the cycle. Overpressure at the nozzle exit allows an upstream propagating shock (dashed line) to enter the bypass section. This shock slows and raises the temperature of the seeded air in the bypass channel, shown in the shaded portion of the figure. A magnet adjacent to the nozzle extracts energy from the flow. b) In the latter part of the cycle, during blowdown. As the pressure at the nozzle exit drops, exhaust of the compressed and heated air from the bypass channel takes place. Power is applied via the magnets shown, resulting in the MHD acceleration of the air slug in the bypass channel.

normal to the fluid velocities (which are, in the nozzle and bypass tube, in the x direction). In the expanding (divergent) section of the nozzle, magnetic and electric fields are applied to extract energy from this portion of the flow. A bypass tube sits adjacent to the engine. Ambient air enters this tube and is accelerated by an MHD accelerator powered by the energy extracted from the nozzle. A gain in thrust is realized by extracting energy from the nozzle, which would otherwise be used inefficiently, and by applying the energy to the air in the bypass tube. A planar design is used here to achieve a spatially uniform magnetic field, only in the z direction, by placement of magnets above and below each region.

The evolution of the flow cycle for the PDRIME is shown in Figs. 1a and 1b. Because a PDRE can be designed to have a converging–diverging nozzle such that the initial peak pressure in the combustion chamber results in pressure at the nozzle exit plane that is well above ambient, a contact surface originates at the nozzle lip and extends to the upper wall of the bypass tube, creating conditions for an unsteady shock with propagates into the bypass channel, as shown in Fig. 1a. If the air in the bypass channel is initially at high Mach number, this traveling shock brings the air to a high temperature. If a species such as cesium can be added to the flow, high conductivity can be attained by thermal ionization. The cesium seeded into the nozzle is assumed to be premixed with the reactants in the chamber, while the cesium for the bypass is assumed to be seeded uniformly across the width of the tube. The ionization potential of cesium is approximately 3.6 eV, which is low enough to provide sufficient conductivity to operate the MHD components operating within the 2000 K range. Hence, the shock generates a slowly moving slug of high-temperature air, shown as the shaded section in Fig. 1a, that can be more easily ionized. This approach eliminates the need for nonequilibrium ionization, as in the AJAX concept.

As the pressure at the nozzle exit drops during blowdown, the shock then slows down, and eventually, the ionized air in the bypass section starts to move downstream. At this point, electrical power can be applied via an MHD accelerator to eject the air slug from the bypass tube, and thus generate thrust (Fig. 1b). In the present simulations, approximately 3000 J are required to accelerate each gram of air trapped within the bypass section. The procedure can then be repeated at each cycle. One only needs to design the nozzle such that the flow is underexpanded during the initial part of the blowdown phase. In fact, there may be a self-adjusting process at work, depending on PDRE nozzle design and altitude, as outlined by Cambier [14]. While at launch, the nozzle exit pressure is equal to ambient and there is no interaction with the bypass air; as the vehicle accelerates and gains altitude, the nozzle becomes progressively underexpanded, so that eventually a strong shock can be generated for the bypass channel to ionize the seeded air, and the ejector operates. This is one of several configurations in which the PDRIME concept could be used for thrust augmentation in advanced propulsion systems.

As noted above, the MHD generator is located in the diverging section of the nozzle where the velocity is largest, so that the expansion of the fluid counteracts some of the velocity reduction arising from the Lorentz (drag) force acting in the generator. The Lorentz force acts on the conducting fluid carrying a current of density $\mathbf{J}$ in a magnetic field of strength $\mathbf{B}$. This force is given in general by

$$\mathbf{F}_L = \mathbf{J} \times \mathbf{B} \tag{3a}$$

or for the orientation of vectors in Fig. 1 by

$$F_{L,x} = J_y B_z \tag{3b}$$

The current density $\mathbf{J}$ is an important property of the MHD flow system that is related to electric and magnetic fields, $\mathbf{E}$ and $\mathbf{B}$, respectively, and the velocity vector $\mathbf{u}$ via Ohm's law:

$$\mathbf{J} = \sigma(\mathbf{E} + \mathbf{u} \times \mathbf{B}) \tag{4}$$

where σ is the electrical conductivity (with units of reciprocal ohms per meter). For the PDRIME orientation described in Fig. 1, this reduces to a current density with a component in the y direction only:

$$J_y = \sigma(E_y - uB_z) \tag{5}$$

where E_y is the electric field acting in the y direction, and B_z is the magnetic field acting in the z direction. The magnetic field is assumed constant, which implies a low rate of field convection compared with field diffusion. As an analogy to hydrodynamics, the ratio of these two rates is given by the magnetic Reynolds number R_m:

$$R_m = \mu\sigma uL \tag{6}$$

where μ is the permeability of free space (units of newtons per squared cross-sectional area), u is the velocity magnitude, and L is a characteristic length scale. The motion of the electrically conducting fluid induces an additional magnetic field, but for low magnetic Reynolds numbers, this is negligible and the magnetic field may be considered constant. A low magnetic Reynolds number approximation is assumed for our MHD applications. The maximum R_m for the PDRIME configuration is in the vicinity of the nozzle exit, where the fluid velocity is largest in the presence of active magnetic fields; in this region, we estimate R_m to be approximately 0.16.

Note that, with a constant and positive magnetic field, the direction of the current density, and thus of the Lorentz force, depends on the relative magnitudes of E_y and uB_z from Eq. (5). We employ Cambier's definition of a loading factor K to compare these strengths [14]:

$$K_x = \frac{E_x}{\beta u B_z} \qquad K_y = \frac{E_y}{uB_z} \tag{7}$$

where β is the Hall parameter, defined as the ratio of the cyclotron frequency to the total elastic collision frequency of the electrons. When $K_x = 0$, the generator is of the Faraday type, and when $K_y = 0$, it is of the Hall type. For the present study, we consider only Faraday generators; thus, we set E_x and, in turn, K_x to zero. We likewise assume no induced electromagnetic fields are present and no magnetization, so the Hall effect is absent.

For a Faraday configuration, $\mathbf{E}$ and $\mathbf{u} \times \mathbf{B}$ are defined such that they are antiparallel and that K_y is always positive. In all cases

presented in this study, B_z is assumed positive in the z direction throughout all MHD component domains, if not necessarily uniform. Presuming $u > 0$, then E_y and K_y are both positive. If $u < 0$, as can occur within the bypass flow, then $\mathbf{u} \times \mathbf{B} = -uB_y > 0$, so E_y becomes negative while K_y remains positive.

If $u > 0$ and $0 < K_y < 1$, then the current density in the y direction is negative. According to Eq. (3b), this results in a Lorentz force opposing the fluid motion, reflecting the behavior we expect of the nozzle generator. If $u > 0$ and $K_y > 1$, then the current density is positive and the resulting Lorentz force accelerates the fluid, which we require in the bypass accelerator. However, if the shock-induced stagnation of the bypass flow results in local velocities flowing upstream, we would prefer to locally decelerate rather than accelerate this flow. Thus, within these limited domains where $u < 0$, we define $0 < K_y < 1$ such that the local bypass MHD components temporarily act as generators.

For all MHD application, energy effects are governed by the current density multiplied by the electric field. This energy source term can be decomposed as follows:

$$\mathbf{J} \cdot \mathbf{E} = \frac{\mathbf{J}^2}{\sigma} + \mathbf{u} \cdot (\mathbf{J} \times \mathbf{B}) \tag{8}$$

where the terms on the right-hand side represent the dissipative heating and mechanical power, respectively. When $u > 0$ and $0 < K_y < 1$, the mechanical power is negative because energy is being extracted from the fluid. Thus, in the PDRIME configuration, for MHD generation in the nozzle operating under such parameters, energy is extracted from the fluid with a negative Lorentz force. In the accelerator (bypass section), a positive Lorentz force and application of energy takes place (Fig. 1a), with $K_y > 1$. Regardless of the loading factor, the ohmic heating will always be a positive term, representing a loss in both cases. Ignoring dissipative effects, we see that the Lorentz force scales with velocity, while the energy associated with both generation and acceleration scales with velocity squared. For this reason, maximum thrust gain is achieved when energy is extracted from high-velocity flows, as in the nozzle, and applied to low-velocity flows [16].

For $0 < K_y < 1$, the goal is to extract maximum power (K_y) with minimal dissipation (K_y^2). The optimal loading factor magnitude K_y for MHD generation has been demonstrated [14] to be 0.5. The energy generated in the nozzle is then applied in the bypass tube by an MHD accelerator. Any value $K_y > 1$ will accelerate the flow. We arbitrarily choose $K_y = 1.5$ to balance efficiency and effectiveness. However, if a negative flow is detected in that location in the course of the cycle, $K_y = 0.5$ in the accelerator mode, is assumed in the present study in order to help decelerate it.

Another alternative configuration by which MHD can be used to augment thrust generated by a PDRE is one in which energy extracted by MHD from the high-velocity flow in the expansion portion of the nozzle can be applied to the combustion chamber in order to accelerate combustion products from the chamber while allowing a fresh mixture of reactants to fill the available volume. Creation of this magnetic piston in the chamber, as outlined in Cambier [14], can be used to push combustion products from the chamber while allowing a fresh mixture of reactants to fill the available volume. Such a configuration is shown in Fig. 2. As noted above, extraction of energy from a high-velocity stream and delivered to a low-velocity stream is one mechanism for thrust augmentation; hence, a configuration such as that in Fig. 2 can theoretically lead to performance gains. As indicated by Cambier [14], thrust increases with an increasing fraction of energy extracted from the flow and with reduction in the filling time. When blowdown and filling processes are allowed to overlap via appropriate application of the magnetic field, filling time is effectively reduced, leading to a large increase in average thrust. The magnetic piston concept, separately as well as in concert with the PDRIME with bypass flow, will be explored here.

The goal of the present research involves use of a simplified model for the blowdown portion of the PDRE, coupled to a more detailed simulation of the relevant MHD processes in the nozzle and/or adjacent bypass sections, as a means of predicting overall PDRIME and magnetic piston phenomena and performance parameters. The model has been validated using detailed numerical simulations of PDRE processes [2,11] so that projections for optimal performance and operating conditions may be made.

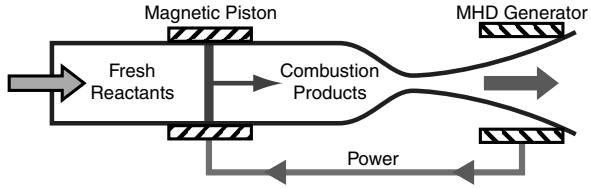

Fig. 2 Schematic of the magnetic piston concept. The piston accelerates the combustion products out of the chamber in such a way that constant pressure and temperature are maintained at the throat. Fresh reactants are simultaneously drawn in to replace the evacuated products.

II. Description of the Pulse Detonation Rocket-Induced Magnetohydrodynamic Ejector Model and Simulation Procedure

A. Framework and Blowdown Model

Because of the large number of available system parameters in the PDRIME, a rapid simulation technique is required: one that is simpler than a detailed numerical simulation of flow and reactive processes in the PDRE and adjacent flow sections. Resolution of detonations constitutes a major computational cost; the sharp gradients and large sound speeds present in the PDE greatly reduce the time step and require finer spatial resolution [18,19]. For the PDRE configuration, after the shock waves have subsided in the chamber, the properties of the fluid within the combustion chamber are mostly uniform, resembling the products of a constant-volume reaction. For these reasons, a blowdown model was developed by Cambier [20] to predict chamber properties as a function of time after a constant-volume reaction. Intuitively, a small throat also restricts the mass flow of propellants out of the chamber, which leads to a slow decay of chamber pressure, increasing the blowdown period.

Cambier's model [20] uses a single computational cell to represent a combustion chamber filled with postconstant volume reaction products at high pressure and temperature. The converging section of the nozzle is also represented by a single-cell approximation. An adiabatic solution for the throat conditions for every time step is determined based on the combustion chamber properties and the assumption that the throat is choked. The divergent section, throat to exit, is fully discretized to account for the MHD coupling, as is the entire bypass tube. To validate certain aspects of the engine cycle and flow processes, comparisons between the blowdown model and full two-dimensional (2-D) transient numerical simulations are made.

The blowdown evolutions of the stagnation variables in the chamber are calculated as functions of specific heat ratio and time [14]:

$$p_0 = \hat{p}_0[f(t)]^{\gamma/(\gamma-1)} \tag{9a}$$

$$\rho_0 = \hat{\rho}_0[f(t)]^{1/(\gamma-1)} \tag{9b}$$

$$T_0 = \hat{T}_0[f(t)] \tag{9c}$$

where the caret (^) indicates the value at time $t = 0$, and the subscript 0 indicates chamber stagnation conditions. The function $f(t)$ has an analytic solution which takes the form

$$f(t) = \frac{1}{(1 + \nu t)^2} \tag{10a}$$

where

$$\nu = \frac{(\gamma-1)\Gamma c_0}{2L_{\text{cham}}}\frac{A^*}{A_{\text{cham}}} \tag{10b}$$

and

$$\Gamma = \left(\frac{2}{\gamma+1}\right)^{(\gamma+1)/[2(\gamma-1)]} \tag{10c}$$

and where c_0 is the chamber fluid's speed of sound, γ is the specific heat ratio, L_{cham} is the chamber length, A^* is the cross-sectional area at the nozzle throat, and A_{cham} is the cross-sectional area of the chamber. All simulations in the present study use sufficiently small time steps such that, within a given time step, we assume the values of γ and Γ in the chamber to be constant, in accordance with the Cambier blowdown model [20]. Between time steps, γ and Γ are updated as new chamber properties are calculated to account for variation over the extended temperature range observed throughout the engine cycle. The caret variables in Eqs. (9a), (9c), and (9c) become the values at current time level t^n, and t becomes the time step at the next time level $\mathrm{d}t = t^{n+1} - t^n$.

B. Discretization of Nozzle and Bypass Sections

The diverging section of the nozzle and the bypass tube are divided into cells. The 2-D transient equations that govern this flow in conservative form are similar to those in He and Karagozian [10,11] but with additional species terms (to simulate air, water vapor exhaust, cesium atoms, and cesium ions), an ionization/recombination source term $S(\mathbf{U})$ when we simulate the injection of cesium, and an MHD source term $M(\mathbf{U})$ denoting related momentum and energy effects:

$$\mathbf{U}_t + \mathbf{F}(\mathbf{U})_x + \mathbf{G}(\mathbf{U})_y = \mathbf{S}(\mathbf{U}) + \mathbf{M}(\mathbf{U}) \tag{11}$$

$$\mathbf{U} = \begin{pmatrix} \rho \\ \rho u \\ \rho v \\ E \\ \rho Y_{Cs} \\ \rho Y_{Cs^+} \\ \rho Y_{\mathrm{H_2O}} \end{pmatrix} \qquad \mathbf{F}(\mathbf{U}) = \begin{pmatrix} \rho u \\ \rho u^2 + p \\ \rho uv \\ (E+p)u \\ \rho u Y_{Cs} \\ \rho u Y_{Cs^+} \\ \rho u Y_{\mathrm{H_2O}} \end{pmatrix}$$

$$\mathbf{G}(\mathbf{U}) = \begin{pmatrix} \rho v \\ \rho uv \\ \rho v^2 + p \\ (E+p)v \\ \rho v Y_{Cs} \\ \rho v Y_{Cs^+} \\ \rho v Y_{\mathrm{H_2O}} \end{pmatrix} \tag{12}$$

$$S(\mathbf{U}) = \begin{pmatrix} 0 \\ 0 \\ 0 \\ 0 \\ \dot{\Omega}_{Cs} \\ \dot{\Omega}_{Cs^+} \\ 0 \end{pmatrix} \qquad M(\mathbf{U}) = \begin{pmatrix} 0 \\ (\mathbf{J}\times\mathbf{B})_x \\ (\mathbf{J}\times\mathbf{B})_y \\ \mathbf{J}\cdot\mathbf{E} \\ 0 \\ 0 \\ 0 \end{pmatrix} \tag{13}$$

where $\dot{\Omega}_{Cs}$ and $\dot{\Omega}_{Cs^+}$ are the cesium reaction source terms for cesium atoms and ions, respectively, which take the Arrhenius form

$$\begin{pmatrix} \dot{\Omega}_{Cs} \\ \dot{\Omega}_{Cs^+} \end{pmatrix} = \frac{\mathrm{d}}{\mathrm{d}t}\begin{pmatrix} [Cs] \\ [Cs^+] \end{pmatrix} = \begin{pmatrix} -k_f[Cs][M] + k_r[Cs^+][M][e^-] \\ k_f[Cs][M] - k_r[Cs^+][M][e^-] \end{pmatrix} \tag{14}$$

where k_f and k_r are the forward the reverse reaction rates; and $[Cs]$, $[Cs^+]$, $[Cs^+]$, $[M]$, and $[e^-]$ are the molar concentrations of cesium atoms, cesium ions, third bodies, and electrons, respectively. Since this is a weakly ionized flow, we also assume that $[e^-] \approx [Cs^+]$. The total energy term E is given by

$$E = \frac{p}{\gamma-1} + \frac{\rho(u^2+v^2)}{2} + \rho q Y_{Cs^+} \tag{15}$$

where the heat release per unit mass $q = 2.827 \times 10^6$ J/k (or 375.7 kJ/mol, the first ionization energy of cesium) and is affixed to the mass fraction of cesium ions since ionization is endothermic and no other reactions take place. As in previous studies, the current simulations assume inviscid flow; at the high-speed conditions at which the PDRIME operates, boundary layers are very thin compared with the dimensions of the PDRIME. For MHD flows, the inviscid assumption is somewhat more approximate, especially for accelerator operation, in that joule heating in the boundary layers is a key contributor to poor MHD accelerator efficiency. Nevertheless, given that the boundary layers are of the order of 3% of the bypass tube width, the inviscid approximation is reasonable for the present performance calculations.

Transient flow in the bypass tube involves a shock created by the nozzle exhaust, traveling into the bypass exit and propagating upstream into a high-speed flow (see Fig. 1a). Quasi-steady forward-marching methods are thus not adequate for these regimes, especially since this method has a singularity when the flow Mach number is equal to 1. For these reasons, a fully transient numerical scheme must be used to simulate flow in the bypass tube.

In simulating flow in the bypass tube, the WENO method [12] is used to approximate spatial derivatives, with a stencil including upstream and downstream cells. WENO is an adaptation of the essentially nonoscillatory method [13] that uses the conservation laws for high-order accuracy with shock capturing capabilities. Artificial viscosity is added via the local Lax–Friedrichs scheme [10] to avoid entropy violation and reduce dispersion while introducing dissipation. Temporal integration is performed by a third-order Runge–Kutta method, which uses a multistep process to achieve fairly large time steps without loss of high-order accuracy. The time step is regulated by the Courant–Friedrichs–Levy condition, which ensures stability in temporal integration by ensuring that information does not propagate completely through any one computational cell in a given time step.

The ionization/recombination source terms in Eq. (13) are discretized using an implicit scheme via operator splitting, and this can introduce some stiffness in nonequilibrium regions such as those exhibiting shocks or large amounts of applied joule heating. We test the degree to which the scheme affects accuracy via single-cell simulations, wherein a molar mixture of 96% water vapor and 4% cesium ions at $P = 10$ atm and $T = 2000$ K is allowed to reach equilibrium over the course of 10^{-2} s, roughly the timescale of the PDRIME cycle in the current study. The size of the time steps for the implicit simulation varies from 10^{-2} s (i.e., a single step) to 10^{-8} s, and the results are compared with the analytical solution. We see in Fig. 3 that, for all time-step magnitudes at or below 10^{-4} s, the results are extremely precise. Since the experiments conducted in this study use time steps below 10^{-6} s within similar pressure and temperature domains, we determine that no significant errors result from the source terms.

C. Geometries and Grid Generation

In quasi-one-dimensional (quasi-1-D) simulations of a PDRIME configuration, as described in recent studies [1,21,22], the computation of quasi-1-D flow in the supersonic nozzle flow must be decoupled from that in the bypass tube, with no resolution

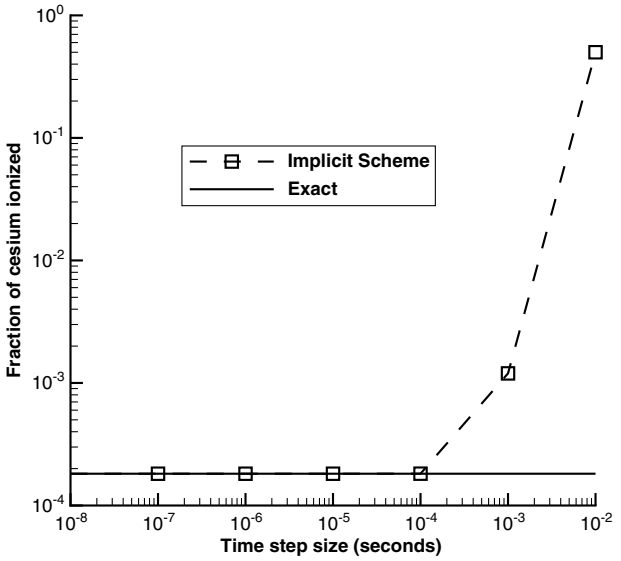

Fig. 3 Single computational cell results for a mixture of water vapor and cesium ions, the latter consisting of 4% of the mixture by moles. Pressure is initialized at 10 atm, temperature to 2000 K, and the mixture is allowed 10 ms to reach equilibrium. Time-step sizes below 0.1 ms are shown to result in sufficient accuracy.

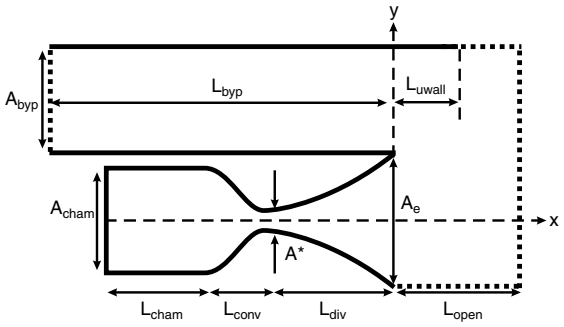

Fig. 4 General configuration of a planar PDRIME of unit depth. The parabolic contour of the nozzle wall and the extension of the upper bypass wall assist in the transfer of high-pressure products from the nozzle exit to the bypass exit.

of the transfer of fluid from the nozzle to the bypass section. These quasi-1-D models thus prescribed the bypass exit boundary conditions as a function of the nozzle exit conditions, which themselves are a function of time. The 2-D simulations conducted in the present study will explore the full 2-D flowfield and will mimic the conditions under which the quasi-1-D tests operated to determine whether the quasi-1-D boundary condition functions accurately reflect 2-D PDRIME behavior.

In the present study, the 2-D configuration for the general form of the planar PDRIME is shown in Fig. 4. A_{cham}, A^*, A_e, and A_{byp} are the areas of the chamber, throat, nozzle exit, and bypass, respectively, and L_{cham}, L_{conv}, L_{div}, L_{byp}, L_{uwall}, and L_{open} indicate the lengths of the chamber, converging nozzle, diverging nozzle, bypass tube, upper wall of the bypass extending beyond the nozzle lip, and outflow area from the nozzle lip, respectively. The expanding nozzle between the throat and the exit is parabolic so that the curved lip of the nozzle allows shocks to more easily follow the contour of the wall to enter the bypass.

The bypass tube runs straight along the top of the PDE, and although the lower bypass wall ends at the tip of the nozzle, the upper wall can extend further. This extension can help maximize impulse by "catching" the outgoing shock from the nozzle and diverting into the bypass tube to be used by the MHD accelerator. The bypass tube should not be excessively wide or else the shock migrating into the tube ceases to be uniform, creating inefficiencies in the MHD accelerator. It must also not be too narrow, lest not enough fluid becomes available to accelerate. The geometrical parameters used in the present calculations are given in Table 1.

The grid used for the present 2-D calculations consists of a grid of cells measuring n_x cells horizontally by n_y cells vertically, flanked on all four sides by a layer of three ghost cells for spatial interpolation (i.e., boundary conditions) along both axes. The grid for these simulations is shown in Fig. 5, representing the PDRIME as well as a downstream area where one can observe the region where the flow from the nozzle into the bypass takes place. Symmetry across the nozzle's centerline enables the 2-D grid to simulate only the upper half of the cross section of the PDRE, and the centerline is treated as a solid wall boundary. The top of the grid indicates the top of the bypass tube, and thus uses a reflective boundary condition along the length of the bypass upper wall. An open-air outflow boundary condition is used for the remaining section downstream of the PDRIME. To minimize the thickness of the nozzle wall, we use a block grid, in which our larger grid is effectively split into two regions: the nozzle with its exhaust downstream and the bypass with its outflow downstream, as illustrated in Fig. 5. This way, the upper nozzle wall and lower bypass wall can meet at a point of zero thickness while the ghost cells needed to simulate either side can be prescribed without hindering each other in a single grid. The nozzle section has as its left boundary condition at the nozzle throat the inlet prescribed by the Cambier blowdown model [20], as described in Sec. II.A.

Since the simulations in this study will use the blowdown model prescribed by Cambier [14], resolution requirements would depend upon the numerical scheme's ability to handle only shocks rather than more tasking detonation waves. The most significant shocks we will observe will be those within the PDRE chamber at the beginning of the blowdown cycle, when the chamber is filled with high-pressure products. We set up a straight 1.0 m shock tube filled with water vapor (i.e., H_2-O_2 reaction products) and initialize the 0.1 m section nearest the wall to $P_0 = 100$ atm, $T_0 = 3000$ K, while the rest of the tube is initialized to $P_0 = 1$ atm, $T_0 = 300$ K. When one simulates this with the quasi-1-D WENO code for which the pressure profiles are shown in Fig. 6a, we see that a horizontal resolution of 100 cells/m sufficiently captures the peak pressure of the shock.

When we conduct 2-D simulations of the PDRIME, we will observe shocks not only through a single species but also across multiple species, as between the water vapor in the nozzle exhaust and the air in the bypass tube. We set up another quasi-1-D shock test using a straight tube, this time measuring 0.6 m and filled with two different species initialized to temperatures and pressures we expect to observe near the nozzle and bypass exits during the PDRIME's operation. The left side is filled with stagnant water vapor at $P_0 = 10$ atm and $T_0 = 3000$ K, while the right side is filled with stagnant air at conditions observed at 25 km: $P_0 = 0.02573$ atm and $T_0 = 216$ K. The resulting waves at $t = 0.1$ ms, as shown in Fig. 6b, illustrate that a resolution of 100 cells per meter (cpm) once again sufficiently captures the peak pressure of the shock, while further resolution produces only marginally improved results.

Table 1 Dimensions of the PDRIME in meters and meters squared for lengths and areas, respectively

Parameter	Value
A_{cham}	0.1256
A^*	0.02513
A_e	0.06283
A_{byp}	0.06
L_{cham}	0.50
L_{conv}	0.02
L_{div}	0.80
L_{byp}	3.00
L_{uwall}	0.40
L_{open}	1.60

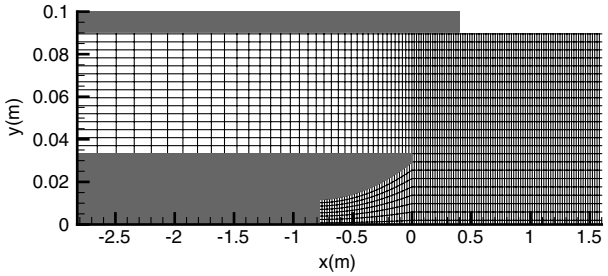

Fig. 5 2-D planar PDRIME domain of real cells.

Thus, our quasi-1-D simulations will use a resolution of 100 cells/m, while the 2-D simulations will use this resolution in both the x and y axes. This is the resolution shown in Fig. 5 in order to accurately capture shocks being transferred from the nozzle into the bypass section.

D. Magnetohydrodynamic Application

The MHD generator in the PDRIME configuration should be active only at the divergent section of the nozzle, where it will most benefit performance during the blowdown phase of the cycle. Thus, the generator source terms will be added to the governing equations for only those grid cells lying in the PDRIME between the nozzle throat and the exit, in particular, the downstream half of the diverging region where they use a loading factor of K_y will be 0.5. In the bypass section, the MHD components must act as a generator in places where the average flow travels upstream and as an accelerator when the local flow travels downstream, thus further accelerating the fluid. When acting as a generator, the loading factor K_y is 0.5, and when acting as an accelerator, K_y is 1.5, as noted previously. This can be accomplished by assuming that the capacitors imposing the electric fields are segmented such that they can be independently and simultaneously activated: some as generators and others as accelerators (obviously an idealized configuration).

A magnetic piston modeled in the chamber operates in the same manner as an MHD accelerator, except that the magnitude of the magnetic field changes in time such that the throat pressure remains constant until the chamber is emptied of products. If we instead model only the diverging nozzle and assign values to the throat inlet based off a blowdown model, we can alternatively use the numerical magnetic piston model to determine its rate of energy consumption while maintaining constant inlet conditions at the throat. Both approaches are explored here.

In all of these cases, the ability of the MHD components to manipulate the flow depends upon the fluid's conductivity, which in turn depends upon the density of cesium ions. Introducing such ions will be accomplished by seeding both the chamber and bypass flows with cesium atoms, which have a low enough ionization energy to be practical for this purpose. The current study simulates the flow of cesium atoms and ions within the PDRIME, calculating conductivity directly, but it also examines an approximation used in earlier research by Roth [21], whereby any fluid in the bypass for which the temperature exceeds 3000 K is assumed to be ionized while any fluid below this threshold is not. The nozzle flow is under no such restriction since the chamber fluid is assumed to be ionized to equilibrium after the initial detonation has left the PDRE and the convection timescale is much less than the chemical timescale, allowing us to assume frozen flow conditions.

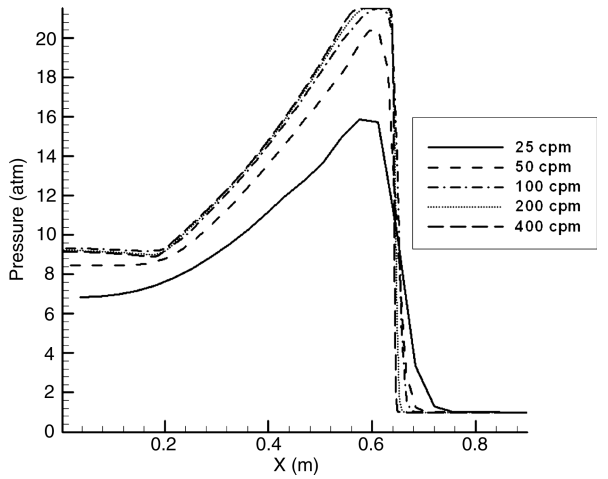

a) Nozzle blowdown resolution test

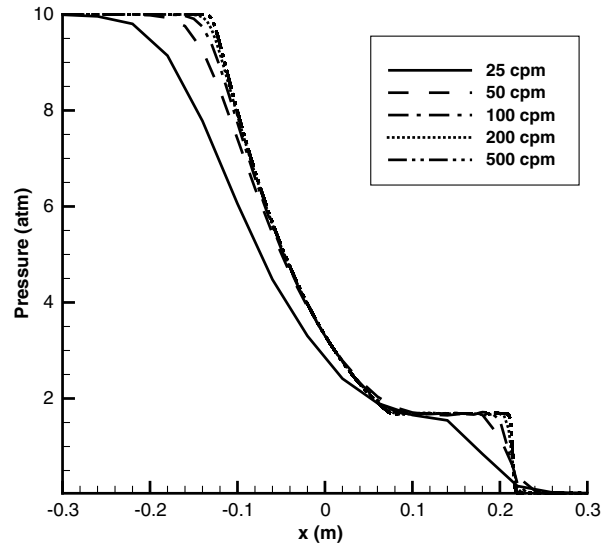

b) Dual species resolution test

Fig. 6 Quasi-1-D shock tube tests with different resolutions in cells per meter: initialized as a) $P_0 = 100$ atm, $T_0 = 3000$ K (left) and $P_0 = 1$ atm, $T_0 = 300$ K (right); and b) water vapor at $P_0 = 10$ atm, $T_0 = 3000$ K (left); $P_0 = 0.02573$ atm, $T_0 = 216$ K (right). All pressure profiles shown at $t = 0.1$ ms.

III. Results and Performance Evaluation

A. Blowdown Validation

Validity of the blowdown model in representing detonation and shock reflections in a PDRE combustion chamber may be ascertained by comparing the behavior of the modeled blowdown process with actual PDRE blowdown as represented via a detailed quasi-1-D or 2-D WENO simulation. The starting conditions of the Cambier model [20] assume that the detonation wave has already left the combustion chamber and that the remaining compression wave has reflected within the chamber sufficiently for the fluid within to become more or less stagnant. Since the chamber pressure and temperature in the wake of the repeatedly reflecting compression wave depend directly upon the reactants' pressure and temperature before the detonation, we must establish a set of assumptions to correspond to a set of initial conditions.

For the purposes of this study, we assume the reactants to be a stoichiometric mixture of hydrogen and oxygen, leaving behind pure water vapor in the chamber, and that the water vapor at the start of the blowdown cycle is pressurized to 100 atm and heated to either 3000 or 4000 K. The fluid in the nozzle is filled with products such that the fluid at the throat is sonic and the fluid in the converging and diverging sections corresponds to a quasi-steady isentropic compression and expansion. Both quasi-1-D and 2-D simulations of this blowdown process will be explored in this validation. For 2-D simulations, the fluid directly downstream of the nozzle will match the fluid at the nozzle exit, while all fluid outside of the nozzle and above the nozzle exhaust will consist of air at the appropriate altitude. The results will be compared with the ignition and propagation of a detonation and relevant reflection of shocks computed for a quasi-1-D PDRE configuration.

The flow and performance characteristics of the quasi-1-D PDRE chamber simulation and the quasi-1-D and 2-D blowdown models

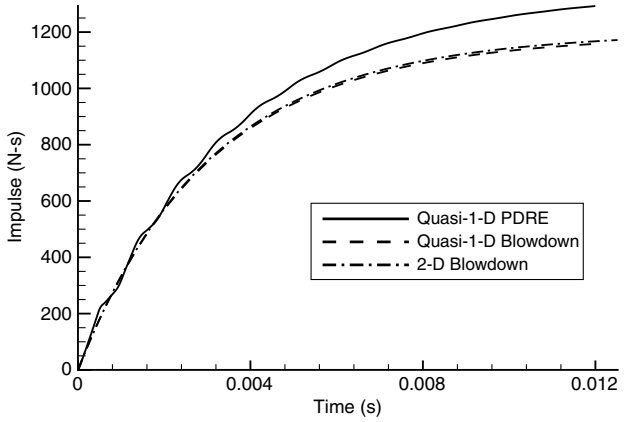

a)Total impulse (N-s)

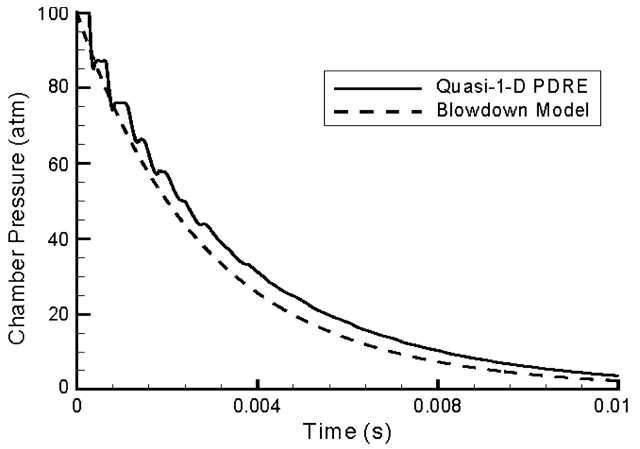

b) Chamber pressure (atm)

Fig. 7 Comparisons among the quasi-1-D PDRE simulation, the quasi-1-D blowdown nozzle simulation, and the 2-D blowdown nozzle simulation, showing a) impulse and b) chamber pressure as a function of time. The chamber pressure blowdown model in Fig. 7b is identical in both quasi-1-D and 2-D simulations.

are shown in Figs. 7a and 7b. We examine the impulse and chamber pressure using the same base case among the alternative cases. The impulse and pressure plots match up very closely with one another, aside from the fact that we assume the initial flow to be stagnant in the PDRE case. The reflecting shock waves observed in the PDRE chamber also expectedly make the corresponding results less smooth than those from the blowdown method, but any oscillations are also shown to become smooth with time, indicating that our substitution of throat model inlet conditions in place of the combustion chamber is appropriate. On this basis, in order to reduce computational costs in performing PDRIME and other MHD-augmentation concepts, we will use Cambier's blowdown model [20] to provide "input" to a detailed simulation of transient flow processes beyond the nozzle throat and, if present, within the PDRIME bypass section.

B. Baseline Pulse Detonation Rocket Engine with and Without Nozzle Generator

The first simulations will use the baseline PDRE geometry with only the diverging nozzle and no bypass tube or active MHD components therein. Cambier's blowdown model [20] is used for the throat inlet conditions. Initial chamber pressure is set to 100 atm, and simulations will be conducted for the initial chamber temperatures set to both 3000 and 4000 K. In both cases, we assume that the blowdown phase of the PDRE cycle ends when the chamber pressure reaches 2% of its original value (i.e., 2 atm). When we keep the initial chamber pressure constant but increase the temperature by 1000 K, the impulse per cycle drops from 1150 to 1025 $\mathrm{N}\cdot\mathrm{s}$ because the initial chamber density has been reduced, thus also reducing the mass available to be expelled from the nozzle.

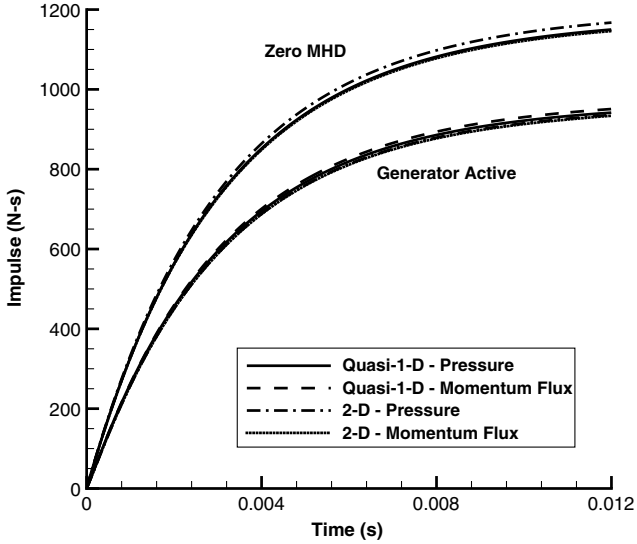

Fig. 8 Impulse calculation test comparing quasi-1-D and 2-D simulations of a PDRE with $AR = 2.5$. Pressure- and momentum-based methods employ wall pressure and momentum flux integrations. Results with and without the MHD generator active in the nozzle are shown for both quasi-1-D and 2-D simulations.

This calculation is compared with the same PDRE but with the nozzle generator activated, indicated in Fig. 8. Quasi-1-D quasi-steady simulations by Roth [21] using the same PDRE design iteratively calculated the magnetic field strength B at each time step such that the nozzle exit Mach number would be 1.2 throughout the blowdown cycle [14]. These data were used to produce a curve fit for the evolution of the magnetic field strength with time that is used in the transient quasi-1-D and 2-D simulations with the nozzle generator. The generator's domain of operation runs between the midpoint and exit of the diverging nozzle section, and it activates as soon as the blowdown commences. The electrical conductivity σ in this entire region is assumed to hold constant at 1000 $\mathrm{mho/m}$.

Both the quasi-1-D and 2-D results for these simulations illustrate how activating the nozzle generator produces energy but at a cost of reduced impulse due to drag. Figure 8 shows that, for a chamber temperature of $T_{0,\mathrm{cham}} = 3000$ K, the reduction in impulse for the PDRE with the nozzle generator is about 120 $\mathrm{N}\cdot\mathrm{s}$ at the end of the cycle. About 420 kJ in available energy is generated during this process; this can be used either in the bypass section or in the magnetic chamber piston, as described previously. As expected, calculating impulse using either the pressure method or momentum flux method produces the similar results; subsequent calculation of impulse uses the pressure method. No substantive differences are observed between quasi-1-D and 2-D results.

The benefits of the nozzle generator in affecting flow from the nozzle to the bypass section may also be explored. The presence of the nozzle generator alone can affect how much of the bypass fluid is blocked by the nozzle exhaust and whether a shock traverses upstream to heat the flow. Figure 9 shows temperature contours for the PDRIME geometry, both for the cases without MHD at all and with only the MHD nozzle generator operating for an altitude of 25 km and at flight Mach numbers 7, 9, and 11. This is the altitude and flow regime in which MHD augmentation would have the most benefit according to earlier quasi-1-D simulations [21,22]. We observe that much greater heating occurs in the bypass section when we activate the nozzle generator because the higher pressure at the nozzle exit allows a stronger shock, traveling at a higher speed, to enter the bypass section. Increasing the nozzle exit pressure through extraction of the flow's kinetic energy is vital to the heating and ionization of the bypass fluid, which in turn is vital to MHD acceleration for the PDRIME.

Unlike in an idealized quasi-1-D simulation of the bypass tube, however, the high-pressure nozzle exhaust does not block the bypass air in such a way that it is brought to a complete halt or even simply

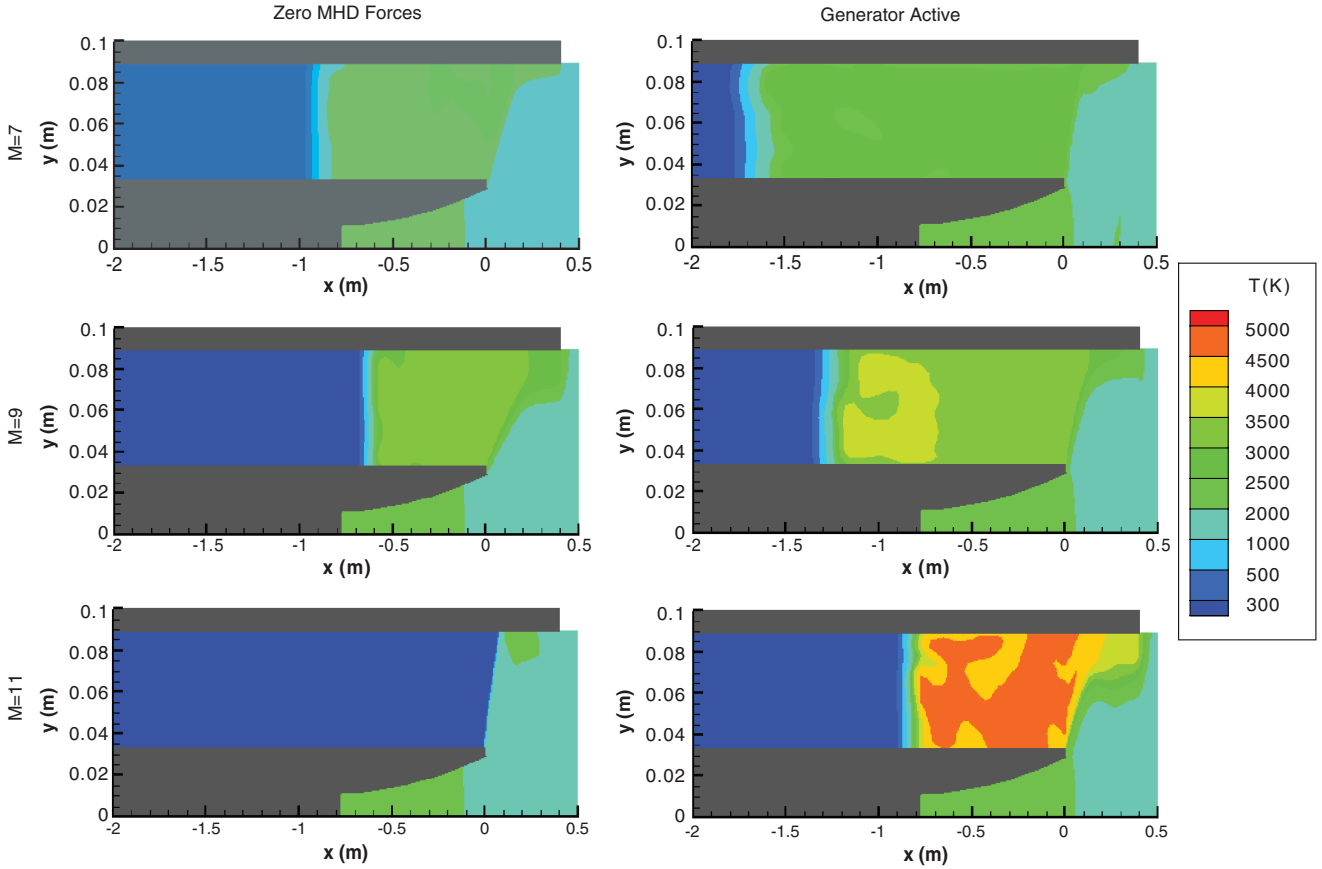

Fig. 9 Temperature contours of the PDRIME, with and without the nozzle generator running, at time $t = 3$ ms. The altitude of operation is 25 km, with an initial chamber temperature of 3000 K.

decelerates. The contact surface between nozzle exhaust and bypass outflow is not always a vertical wall but lies at an angle that grows more shallow as the Mach number increases [1]. Some air creeps over this contact surface, but the rest circulates back and upstream into the bypass tube, partially inducing numerical mixing with the water vapor from the nozzle and creating exit conditions considerably different from those assumed for quasi-1-D PDRIME simulations in earlier research by Roth [21] and Cole [22].

C. Pulse Detonation Rocket-Induced Magnetohydrodynamic Ejector with Nozzle Generator and Chamber Piston

As noted above, energy generated from the nozzle can be reintroduced within the PDRE's chamber, allowing operation of a magnetic chamber piston. Running the piston and the generator at the same time would be counterproductive, so we activate them in series, where the nozzle generator runs until the chamber pressure reaches a fixed percentage of its initial value (called either the generator shutoff pressure or the chamber activation pressure). Immediately after this point, the magnetic chamber piston uses this energy to blow down the remainder of the products. In some cases, not enough energy is available to evacuate all of the remaining products with the piston, in which case normal blowdown resumes after the piston runs out of energy to complete the cycle. Activation pressures that bring about this scenario are said to fall into the "mass-rich" domain. In other cases, the piston is able to evacuate all of the products and still have energy to spare; we call this the "energy-rich" domain. We define the critical pressure to be the activation pressure for which the piston finishes evacuating the chamber with exactly no energy remaining.

Figure 10 shows the effects of varying the activation pressure on the PDRE with the nozzle generator and magnetic chamber piston operating, in contrast to the same configuration but with zero MHD (no generator or chamber piston operational). Results are shown for the impulse at the end of a cycle (Fig. 10a) and the amount of energy that can be generated and consumed for different chamber temperatures (Fig. 10b). The activation pressure at which the energy generated is equal to that consumed by the chamber piston is the critical pressure, which is shown here to be approximately 45 atm.

We note that all of the results for the MHD generator and piston operation shown in Fig. 10a produce impulse per cycle totals that are below those using no MHD application at all. This is expected for the energy-rich simulations where kinetic energy is extracted from the flow and not completely reallocated (i.e., activation pressure is below the critical pressure), but we also see it in the mass-rich simulations where all available extracted energy is completely reallocated (i.e., activation pressure is greater than the critical pressure). This tells us that, while the generator/piston combination can reduce the cycle time, and thus possibly improve impulse per unit time at the cost of extra fuel, it does not improve impulse or operative efficiency. Since our goal is to improve efficiency, the piston should be used only in conjunction with the bypass accelerator. Ideally, this would mean that energy should not be redirected toward the chamber piston unless the bypass accelerator is unable to use all of the energy provided by the generator. If the generator must extract more energy than the bypass accelerator can consume in order to ensure sufficient bypass heating, then the chamber piston can consume the remainder and perhaps be used efficiently. This operation is explored in the PDRIME simulations below.

D. Pulse Detonation Rocket-Induced Magnetohydrodynamic Ejector Simulations with Constant Conductivity

While the results at flight Mach 7 (Fig. 9) produced some heating in the bypass, tests [2] with the 2-D PDRIME simulation reveal that not enough of the flow can be maintained at a temperature above 3000 K to facilitate nonnegligible MHD acceleration. In contrast, our simulations at Mach 9 and 11 heat up just enough of the bypass fluid to be considered useful, so further 2-D simulations with the full PDRIME are conducted only at Mach 9 and Mach 11. Any higher flight speeds at altitudes of 25 or 30 km cause the heated bypass fluid

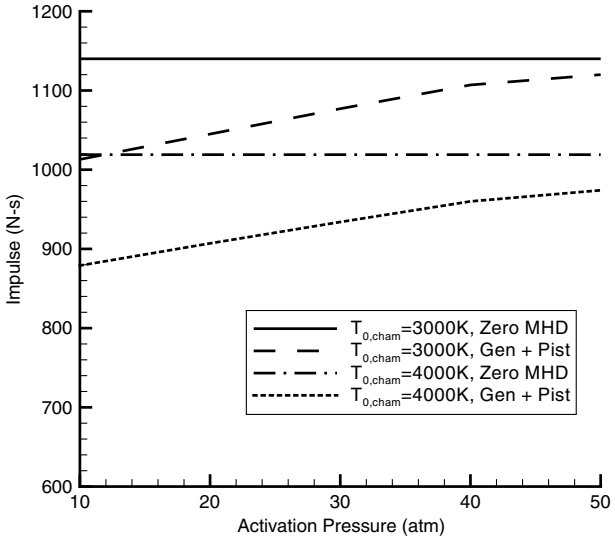

a) Shutdown/activation pressure test - impulse

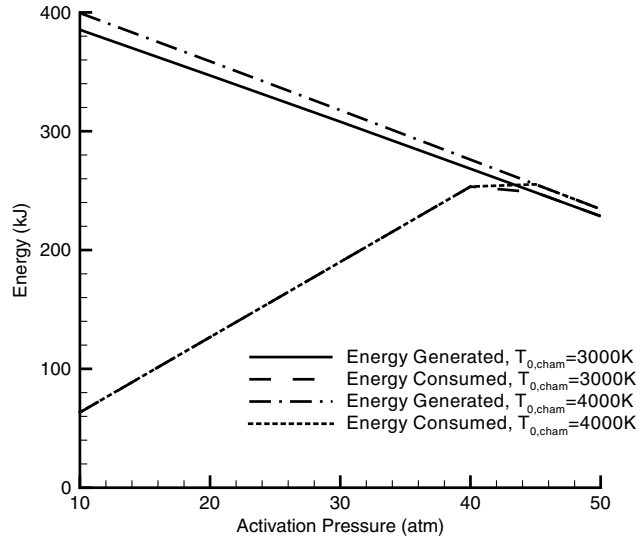

b) Shutdown/activation pressure test - energy

Fig. 10 PDRE operation using the MHD generator in series with the magnetic chamber piston. The MHD generator operates from the beginning of the cycle, and the time at which the generator deactivates and the piston activates is determined by the chamber activation pressure. Simulations are run for initial chamber temperatures of 3000 and 4000 K. (Gen denotes generator; Pist denotes piston.)

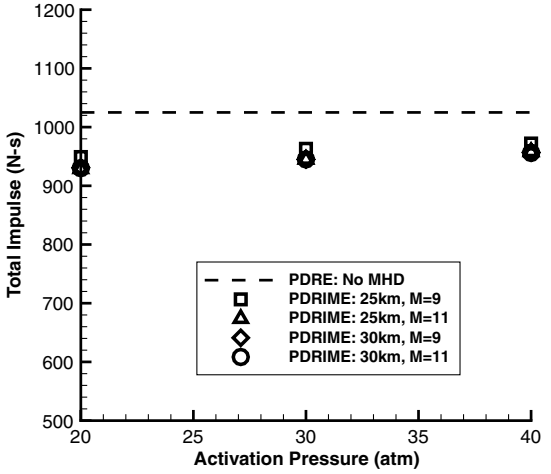

Fig. 11 Total impulse for several constant-conductivity PDRE simulations in which initial chamber temperature is set to 4000 K. The dashed line indicates the minimum impulse that the bypass must contribute in order to outperform the PDRE without any MHD components.

to be too small to use the accelerator. Any slower, and the fluid that is heated will not be hot enough for ionization. First, we calculate flow evolution and performance assuming a constant electric conductivity in the flow.

At altitudes of both 25 and 30 km, and for both flight Mach numbers 9 and 11, the MHD generator heats up the bypass flow enough that the bypass accelerators can reintroduce all available energy into the bypass section at higher activation pressures, meaning that the chamber piston is not actually needed at times. Results for the total impulse as a function of activation pressure for a chamber temperature of 4000 K, for example, are shown in Fig. 11 for different flight Mach numbers and altitudes. In these cases, we activate only the nozzle generator and the bypass accelerator, leaving the chamber piston inactive. The bypass accelerator, however, does not activate until 3.5 ms after the blowdown cycle commences so as to give the nozzle-driven shock sufficient time to propagate and heat the bypass flow. For these simulations in Fig. 11, the conductivity in the nozzle is set to 1000 mho/m, and the conductivity in the bypass is set arbitrarily to 500 mho/m in regions where the average temperature across a given cross section exceeds 3000 K; σ is equal to 0 mho/m elsewhere. The magnetic field strength in the nozzle varies according to the quasi-1-D quasi-steady evolutions determined earlier, while the magnetic field strength in the bypass section is uniformly 3 T, which is used throughout this study unless otherwise noted. While electromagnets in the 2–3 T range introduce considerable weight, such components are still compact enough for large flight vehicles. The simulations are for activation pressures of 20, 30, and 40 atm, as these were deemed the most promising from the chamber piston tests for their residing in the energy-rich domain.

What we discover in Fig. 11 is that, no matter which activation pressure we use for the generator, we are never able to produce enough impulse in the bypass to replace the impulse lost by the nozzle generator. Furthermore, the bypass accelerator is able to provide more impulse at an altitude of 25 km than at 30 km, despite the latter case resulting in greater heating of the bypass tube. At both altitudes, worse performance results are observed when more energy is made available to the bypass accelerator, which evidently cannot use it as efficiently as it was generated.

These results lie in contrast to those observed in quasi-1-D simulations, where at Mach 9 conditions the bypass was able to fully use all available energy to positive effect without either shutting off the generator early or activating the chamber piston. Such results are shown, for example, in Fig. 12. Comparisons between this quasi-1-D simulation and the 2-D simulation are difficult due to the varying nature of the MHD component operation (i.e., the 2-D results correspond to the nozzle generator being shut off at a chamber pressure of 30 atm, while no such shutoff occurs in the quasi-1-D simulations). Moreover, the quasi-1-D results use constant specific heat ratios, while the 2-D results use variable specific heat ratios. As a consequence, even the baseline PDRE results vary between the two simulations, shown in Fig. 13. Despite such differences, it is apparent that the quasi-1-D PDRIME simulations predict performance enhancement, while the 2-D simulations do not, as seen in the figure.

The disparity between MHD effects in Fig. 13 is largely explained by the significant 2-D effects occurring at the contact surface between the bypass outflow and nozzle exhaust. A sample of the 2-D time evolution of temperature for the Mach 9 condition at 25 km, including streamlines, is shown in Fig. 14. Vortical structures are observed to arise due to baroclinic vorticity generation as the shock migrates about the lip of the nozzle into the bypass section. While the quasi-1-D simulation assumes a bypass exit boundary condition consisting of a vertical wall of stagnant high-pressure fluid, in reality, the contact surface between the bypass and nozzle outflows is at a variable angle. The bypass flow travels up the contact surface before circling back along the extended bypass upper wall, creating significant vortical structures that the quasi-1-D simulations cannot resolve, leading to different conditions under which the bypass

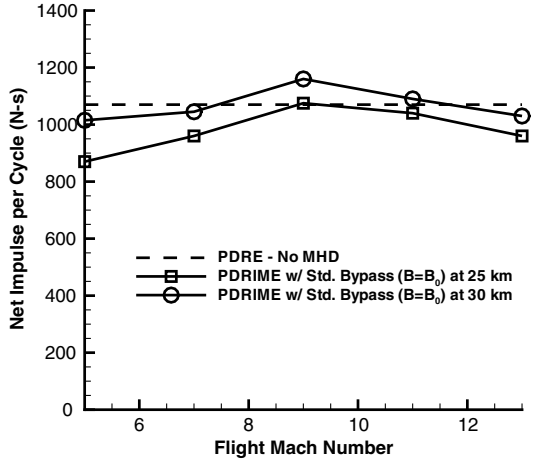

Fig. 12 Total impulse for quasi-1-D constant-conductivity PDRIME simulations in which initial chamber temperature is set to 3000 K. The dashed line indicates the minimum impulse that the bypass must contribute in order to outperform the PDRE without any MHD components.

accelerator operates. While the temperature field appears to be roughly 1-D in the bypass section, the substantial vorticity generation alters the flow from that assumed in quasi-1-D simulations.

E. Pulse Detonation Rocket-Induced Magnetohydrodynamic Ejector Simulations with Cesium Ionization

We now represent the more realistic effects of the seeding, ionization, recombination, and transport of cesium in the nozzle and bypass in the 2-D simulations and calculate the conductivity directly to see how this influences performance. The initial conditions, flight conditions, magnetic field strengths, and PDRIME dimensions are the same. To the chamber, we add a mixture of cesium atoms and ions at equilibrium, amounting to 0.5% of chamber's initial contents on a molar basis. We assume the converging section of the nozzle to be short enough that the level of recombination occurring between the chamber and the nozzle is negligible. To the bypass inlet, we add 0.1% cesium atoms on a molar basis. Overall, cesium amounts to roughly 4% of the propellant weight in the most optimized case studied.

PDRE simulations of cesium ionization with the nozzle generator active can produce conductivity in the nozzle at 1000 mho/m, as prescribed in the simplified simulations, but only if the initial

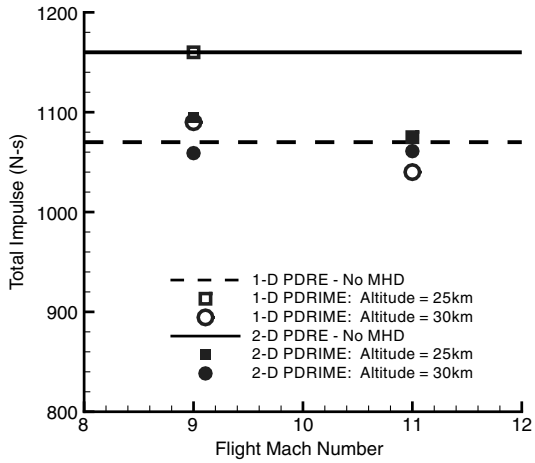

Fig. 13 Comparisons between quasi-1-D and 2-D simulations of the PDRIME in which initial chamber temperature is set to 3000 K and conductivity is constant. Dashed and solid lines indicate the minimum impulse that the bypass must contribute in order to outperform the PDRE without any MHD components for the quasi-1-D and 2-D simulations, respectively.

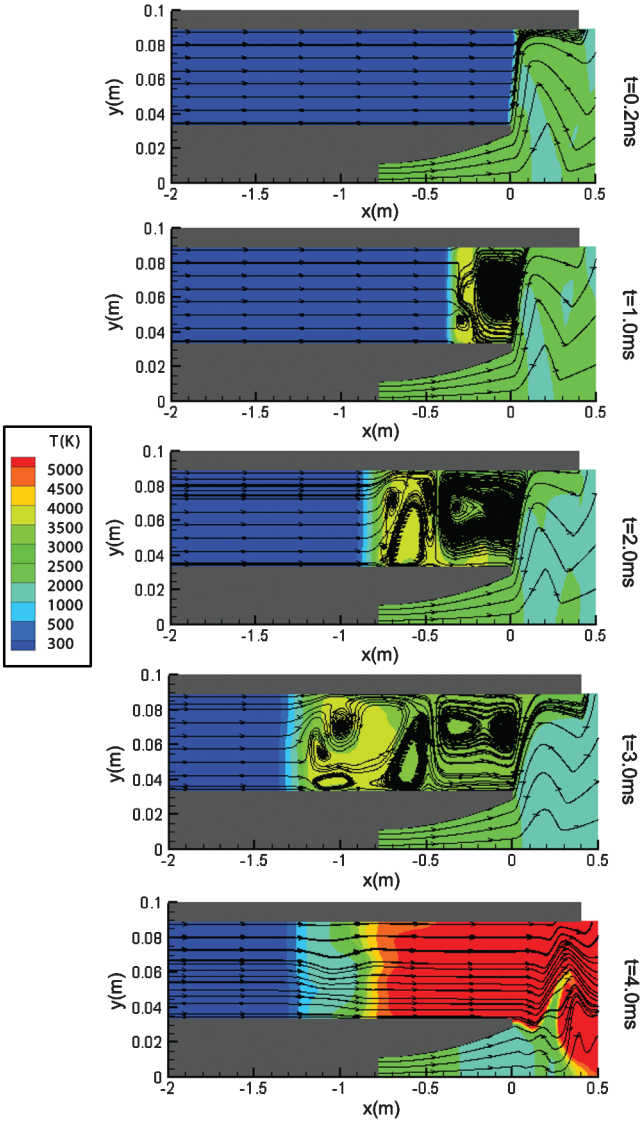

Fig. 14 Temperature contours of the PDRIME with the nozzle generator, superimposed with streamlines to illustrate fragmented vortical structures. Altitude is 25 km, initial chamber temperature is 3000 K, and Mach number is 9.

chamber temperature is set to 4000 K rather than 3000 K. Thus, for this next set of simulations, only a 4000 K chamber pressure initialization will be used. Matching conductivity levels for the 3000 K initialization would require increasing the molar percentage of cesium in the nozzle inlet to 2% of the fluid by moles, or 14% by mass, at which point any performance benefits from MHD augmentation are dwarfed by the momentum imparted by the mass addition of cesium, rendering the MHD components moot.

Running similar test cases as before, with results in Fig. 15, reveals that we are once again unable to obtain significant impulse improvements over the baseline total of 1000 N · s per cycle. Variances between the results in Fig. 11 and those in Fig. 15 arise from the fact that the nozzle fluid conductivity profiles in the former are constant at 1000 mho/m, while those in the latter are transient, despite staying near 1000 mho/m for the majority of the cycle. Furthermore, while the bypass fluid conductivity had previously been assumed to hold constant at 500 mho/m, results with cesium ionization result in conductivities within the bypass varying between 500 and 2500 mho/m.

F. Optimization of Engine Operation

In the foregoing PDRIME configuration, the bypass accelerator is able to use only a small fraction of the energy provided by the nozzle

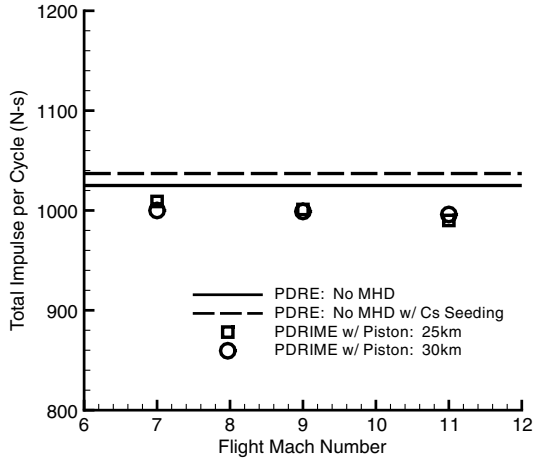

Fig. 15 Maximum total impulse for several 2-D simulations with cesium ionization and recombination. Chamber temperature is initialized to 4000 K. The solid line indicates the total impulse of the PDRE without any MHD components or seeding of cesium. The dashed line indicates the total PDRE impulse with no MHD components but with the additional mass of cesium added. The dashed line also indicates the minimum impulse that the bypass must contribute in order to outperform the PDRE without any MHD components.

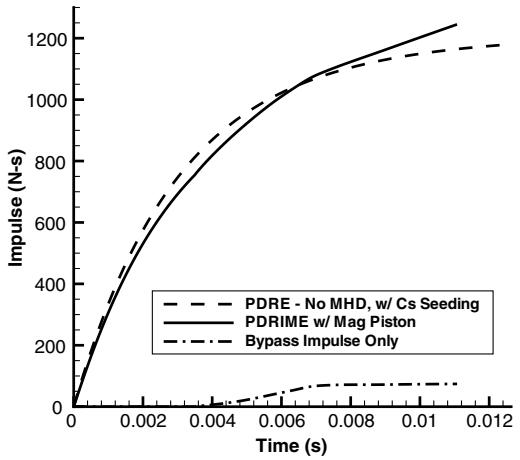

Fig. 16 PDRIME performance at 20 km and flight Mach 2 with initial chamber temperature of 3000 K. Impulse evolution is plotted for both a baseline PDRE seeded with cesium but with no MHD activation and a PDRIME with the nozzle generator, bypass accelerator, and magnetic (Mag) piston activated. An additional impulse plot illustrates the contribution from the bypass accelerator during the PDRIME simulation. Chamber-to-throat $AR = 5.0$, exit-to-throat $AR = 2.5$, and bypass width = 15 cm. Chamber is initially seeded with 0.5% cesium by moles, and the width of the bypass is seeded with 0.1% cesium by moles.

generator, per the results shown in Fig. 10. To prevent unnecessary drag, the remainder of this energy is sent to the chamber piston for consumption (e.g., as in Fig. 11), but this not only introduces significant impulse losses (due to alteration of nozzle exit conditions) but also hastens the end of the cycle and thus allows even less time for the bypass section to conduct its work.

One solution is to generate less energy in the first place by reducing either the nozzle flow conductivity or the MHD generator magnetic field strength. This approach would result in a reduced nozzle exit pressure, higher exit Mach number, and reduced heating in the bypass section; but here, the bypass accelerator would not eject the fluid as quickly as before, and it might be able to consume a greater percent of the total available energy, leaving less for the magnetic piston and lowered impulse losses.

Hence, rather than focus on heating the bypass fluid to as high a temperature as possible, an alternative objective is to provide the bypass with as much ionized low-velocity fluid as possible, even if the fluid is relatively weakly ionized. The air mass in the bypass can be increased by either reducing the altitude to increase its density or by widening the bypass tube to increase its volume. Both of these methods have the drawback of inhibiting propagation of the nozzle-driven shock upstream in the bypass tube, but this can be compensated by reducing the flight Mach number. All of these changes will result in a weaker shock, and thus reduced conductivity, on the order of 300–400 mho/m in the nozzle and 100–200 mho/m in the bypass, so ejecting the increased shock will take more time. If the piston is activated too early, it might consume energy that the bypass accelerator would have used had the cycle been allowed to run longer. Thus, this change to the PDRIME operating conditions will be to desynchronize the generator from the chamber piston, setting the latter to activate at some time after the former shuts off and allowing more time for the bypass accelerator to function.

The next set of results uses all of these suggested improvements at once. The PDRE chamber is initially set to 100 atm and 3000 K, the bypass width is increased to 15 cm, the flight Mach number is reduced to 2, and the altitude is reduced to 20 km so that the bypass inlet pressure and temperature are 5529 Pa and 216 K, respectively. The bypass accelerator continues to run with a uniform magnetic field of 3 T and activates only on fluids that travel slower than 1000 m/s and temperatures above 300 K so that the simulation does not mistake the trace ionization in the unheated bypass fluid as viable ejection material. The bypass length remains at 3 m, and the nozzle dimensions remain the same as in previous tests.

The results in Fig. 16 show that this new PDRIME configuration is much more effective than prior configurations. In contrast with the baseline PDRE (but with cesium seeding to replicate PDRIME mass addition), the PDRIME with the bypass alone has an increase in cycle impulse of 80 N · s, and since the chamber piston uses very little energy, it also costs very little in impulse losses, netting the PDRIME a 60 N · s impulse improvement over the baseline. Figure 17 illustrates how the energy consumption by the magnetic piston and the bypass accelerator is slow and steady, occurring right up until the end of the cycle at roughly 0.012 s.

We run similar tests for a variety of flight Mach numbers and bypass widths, in all of which the generator shuts off when the chamber pressure reaches 30 atm. The time at which the piston activates varies according to that which produces the most efficient performance under the flight conditions. In these cases, the chamber pressure at which the piston activates lies between 8 atm for the lower flight Mach numbers and 18 atm for the higher Mach numbers. Figure 18 demonstrates that, for these calculations, there is

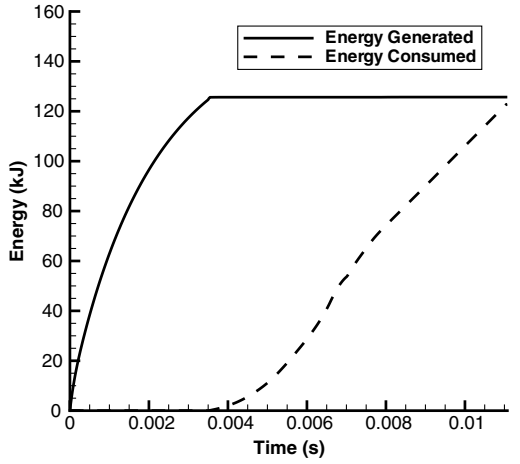

Fig. 17 PDRIME energy generation and consumption at 20 km and flight Mach 2 with initial chamber temperature of 3000 K. The solid line illustrates the initial activation of the nozzle generator and its shutoff at roughly 0.0035 s. At this time, the dashed line illustrates the chamber piston activating, followed by a gradual consumption of energy from the bypass accelerator. Chamber-to-throat $AR = 5.0$, exit-to-throat $AR = 2.5$, and bypass width = 15 cm. Chamber is initially seeded with 0.5% cesium by moles, and the width of the bypass is seeded with 0.1% cesium by moles.

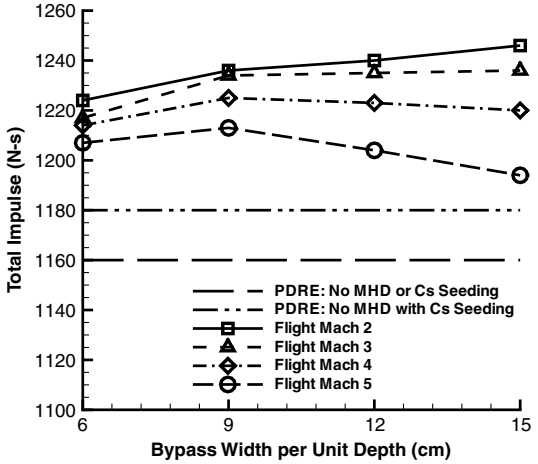

Fig. 18 PDRIME total impulse per cycle at 20 km varying with flight Mach number and bypass area per unit depth. Initial chamber temperature of 3000 K. Bypass length = 3 m. Chamber is initially seeded with 0.5% cesium by moles, and the width of the bypass is seeded with 0.1% cesium by moles.

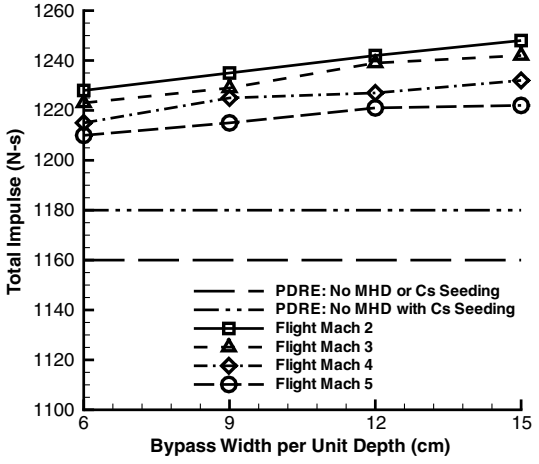

Fig. 20 PDRIME total impulse per cycle at 30 km varying with flight Mach number and bypass area per unit depth. Initial chamber temperature of 3000 K, and bypass length = 6 m. Chamber is initially seeded with 0.5% cesium by moles, and the width of the bypass is seeded with 0.1% cesium by moles.

increasing impulse improvement with a reduced flight Mach number. At lower Mach numbers, increasing the bypass width also increases performance by facilitating the ionization of additional fluid, but as the flight Mach number increases, increasing bypass width produces diminishing returns as the extra inlet mass starts expelling the upstream shock before the bypass accelerator has a chance to operate effectively on the ionized gas. Less energy is redirected into the bypass flow this way, thus necessitating earlier chamber piston activation to make certain that all stored energy is reintroduced. Accounting for cesium seeding in the baseline and PDRIME configurations, Fig. 18 shows up to a 70 N · s increase in impulse for Mach 2 operation.

Running the same experiments at altitudes of 25 and 30 km requires an adjustment to the PDRIME, since in some cases the reduced inlet bypass pressure results in the upstream shock's escaping the tube and taking useful heat energy with it. Thus, at 25 and 30 km, we run the same tests with a bypass of length 4 and 6 m, respectively. Figures 19 and 20 illustrate how we are able to obtain similar results at these altitudes as we did at 20 km (Fig. 18) for the same ranges of flight Mach numbers and bypass widths. In these cases, the shock waves propagate further up the bypass tube and heat the air to higher temperatures, but these are compensated by the reduced air density and greater distances over which the fluid must be accelerated.

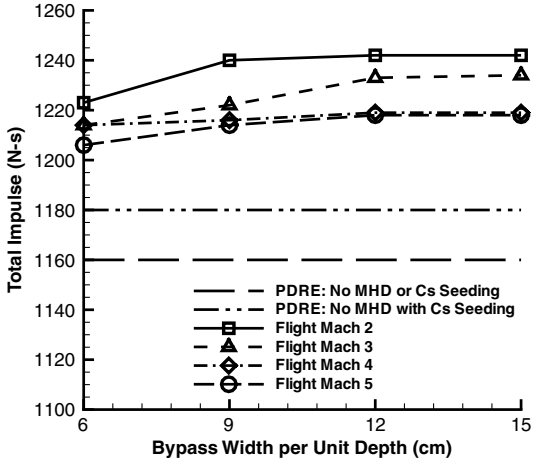

Fig. 19 PDRIME total impulse per cycle at 25 km varying with flight Mach number and bypass area per unit depth. Initial chamber temperature of 3000 K, and bypass length = 4 m. Chamber is initially seeded with 0.5% cesium by moles, and the width of the bypass is seeded with 0.1% cesium by moles.

Despite the similar impulse results per cycle, one significant drawback to operating at higher altitudes is that longer bypass tubes are required to accelerate the extra volume of less dense air, necessitating a heavier PDRIME device with additional electromagnetic components such as magnets. Bypass lengths in excess of 3 m are not required for the higher flight Mach numbers tested, but the best impulse improvement is observed at the lowest flight Mach numbers, thereby rendering 20 km to be the optimal altitude at which to operate this PDRIME configuration.

IV. Conclusions

A range of alternative PDRIME configurations and operating conditions have been explored in the present studies. It has been observed that performance enhancement under the given simulations conditions can be accomplished mainly by the bypass accelerator, and even then only under the condition that it be prevented from accelerating fluid that is already above a given velocity. While the magnetic chamber piston can be used early in the cycle to maintain higher nozzle exit pressure and can aid in causing the shock to propagate up the bypass tube, the piston can also hasten the end of the cycle too quickly for the accelerator to completely eject the heated fluid. This suggests that the piston should be activated later, only as a measure of consuming any energy that would otherwise go unused.

The primary method of performance improvement observed in this study is configuring the PDRIME to heat and ionize a large mass of low-velocity bypass flow just enough for the accelerator to efficiently reintroduce as much available energy as possible before the end of the cycle. This configuration is observed to function most efficiently at low flight Mach numbers and at low altitudes, where the inlet air is slow enough to be efficiently accelerated and dense enough to consume sufficient amounts of energy during acceleration. Improved performance can also be observed at higher altitudes, provided that the bypass tube is extended to prevent the nozzle-driven shock from escaping, but the additional weight of the tube and of the electromagnetic components affixed to it would increase the performance requirements of the PDRIME.

Further studies into the breadth of application of the PDRIME could include alternate chamber and nozzle configurations and determining the corresponding optimal operating and flight conditions. Although the present studies were conducted with a low magnetic Reynolds number approximation, future computations would have to account for induced fields. Future simulations might also operate the bypass ejector in such a way that its cycle period is much longer than that of the chamber detonations, a configuration which cannot be simulated using only the blowdown model, as done in the present studies. All of these simulations eventually require full

coupling of the electric and magnetic fields as well as more detailed analysis of cesium ionization, beyond a single reversible reaction, to determine the complete feasibility.

Acknowledgments

This research has been supported at University of California, Los Angeles, by the U.S. Air Force Office of Scientific Research under the Space Power and Propulsion program managed by Mitat Birkan (grants FA9550-07-1-0156 and FA9550-07-1-0368). The authors wish to acknowledge the technical assistance of Xing He of HyperComp, Inc., in the early stages of this work.

References

[1] Cambier, J.-L., Roth, T., Zeineh, C., and Karagozian, A. R., "The Pulse Detonation Rocket Induced MHD Ejector (PDRIME) Concept," 44th AIAA/ASME/SAE/ASEE Joint Propulsion Conference, AIAA Paper 2008-4688, July 2008.

[2] Zeineh, C., "Numerical Simulation of Magnetohydrodynamic Thrust Augmentation for Pulse Detonation Rocket Engines," Ph.D. Thesis, Dept. of Mechanical and Aerospace Engineering, Univ. of California, Los Angeles, 2010.

[3] Hill, P., and Peterson, C., "Mechanics and Thermodynamics of Propulsion," 2nd ed., Addison Wesley, Reading, MA, 1992.

[4] Eidelman, S., Grossmann, W., and Lottati, I., "Review of Propulsion Applications and Numerical Simulations of the Pulse Detonation Engine Concept," *Journal of Propulsion and Power*, Vol. 7, No. 6, 1991, pp. 857–865. doi:10.2514/3.23402

[5] Kailasanath, K., and Patnaik, G., "Performance Estimates of Pulse Detonation Engines," *Proceedings of the Combustion Institute*, Vol. 28, 2000, pp. 595–602. doi:10.1016/S0082-0784(00)80259-3

[6] Cooper, M., and Shepherd, J. E., "Single Cycle Impulse from Detonation Tubes with Nozzles," *Journal of Propulsion and Power*, Vol. 24, No. 1, 2008, pp. 81–87. doi:10.2514/1.30192

[7] Wintenberger, E., Austin, J. M., Cooper, M., Jackson, S., and Shepherd, J. E., "Analytical Model for the Impulse of a Single Cycle Pulse Detonation Engine," *Journal of Propulsion and Power*, Vol. 19, No. 1, 2003, pp. 22–38. doi:10.2514/2.6099; also erratum, Vol. 20, No. 4, 2004, pp. 765–767. doi:10.2514/1.9442

[8] Li, C., and Kailasanath, K., "Partial Fuel Filling in Pulse Detonation Engines," *Journal of Propulsion and Power*, Vol. 19, No. 5, 2003, pp. 908–916. doi:10.2514/2.6183

[9] Warwick, G., "U.S. AFRL Proves Pulse-Detonation Engine Can Power Aircraft," *Flight Magazine*, March 2008 [online] http://www.flightglobal.com/articles/2008/03/05/222008/us-afrl-proves-pulse-detonation-engine-can-power-aircraft.html [retrieved 2011].

[10] He, X., and Karagozian, A. R., "Numerical Simulation of Pulse Detonation Engine Phenomena," *Journal of Scientific Computing*, Vol. 19, Nos. 1–3, Dec. 2003, pp. 201–224. doi:10.1023/A:1025351924837

[11] He, X., and Karagozian, A. R., "Pulse Detonation Engine Simulations with Alternative Geometries and Reaction Kinetics," *Journal of Propulsion and Power*, Vol. 22, No. 4, 2006, pp. 852–861. doi:10.2514/1.17847

[12] Harten, A., Osher, S. J., Engquist, B. E., and Chakravarthy, S. R., "Some Results on Uniformly High-Order Accurate Essentially Nonoscillatory Schemes," *Applied Numerical Mathematics*, Vol. 2, 1986, pp. 347–377. doi:10.1016/0168-9274(86)90039-5

[13] Jiang, G. S., and Shu, C. W., "Ecient Implementation of Weighted ENO Schemes," *Journal of Computational Physics*, Vol. 126, 1996, pp. 202–228. doi:10.1006/jcph.1996.0130

[14] Cambier, J.-L., "MHD Augmentation of Pulse Detonation Rocket Engines," 10th International Space Planes Conference, Kyoto, Japan, AIAA Paper 2001-1782, April 2001.

[15] O'Sullivan, M. N., Krasnodebski, J. K., Waitz, I. A., Gretizer, E. M., and Tan, C. S., "Computational Study of Viscous Effects on Lobed Mixer Flow Features and Performance," *Journal of Propulsion and Power*, Vol. 12, No. 3, 1996, pp. 449–456. doi:10.2514/3.24056

[16] Cambier, J.-L., "A Thermodynamic Study of MHD Ejectors," 34th AIAA/ASME/SAE/ASEE Joint Propulsion Conference, AIAA Paper 1998-2827, July 1998.

[17] Gurijanov, E. P., and Harsha, P. T., "AJAX: New directions in hypersonic technology," 7th International Space Planes Conference, AIAA Paper 1996-4609, 1996.

[18] Hwang, P., Fedkiw, R. P., Merriman, B., Aslam, T. D., Karagozian, A. R., and Osher, S. J., "Numerical Resolution of Pulsating Detonation Waves," *Combustion Theory and Modelling*, Vol. 4, No. 3, Sept. 2000, pp. 217–240. doi:10.1088/1364-7830/4/3/301

[19] Henrick, A. K., Aslam, T. D., and Powers, J. M., "Mapped Weighted Essentially Non-Oscillatory Schemes: Achieving Optimal Order Near Critical Points," *Journal of Computational Physics*, Vol. 207, No. 2, 2005, pp. 542–567. doi:10.1016/j.jcp.2005.01.023

[20] Cambier, J.-L., "Preliminary Model of Pulse Detonation Rocket Engines," 35th AIAA/ASME/SAE/ASEE Joint Propulsion Conference, AIAA Paper 1999-2659, June 1999.

[21] Roth, T., "Modeling and Numerical Simulations of Pulse Detonation Engines with MHD Thrust Augmentation," M.S. Thesis, Department of Mechanical and Aerospace Engineering, Univ. of California, Los Angeles, 2007.

[22] Cole, L., "Combustion and Magnetohydrodynamic Processes in Advanced Pulse Detonation Rocket Engines," Ph.D. Prospectus, Department of Mechanical and Aerospace Engineering, Univ. of California, Los Angeles, 2010.

J. Powers
Associate Editor